Dental Applications of Computerized Tomography

Surgical Planning for Implant Placement

Stephen L. G. Rothman, MD



quintessence books

Dentsply Sirona Inc. – Exhibit 1016

To Melvin Schwarz, DDS, my dental mentor;
and to Michael Rhodes, PhD, and his computer science group,
who created the original dental reformation program

Library of Congress Cataloging-in-Publication Data

Rothman, Stephen L. G., 1942–
Dental applications of computerized tomography : surgical planning for implant placement / Stephen L. G. Rothman.
p. cm.
Includes bibliographical references and index.
ISBN 0-86715-338-5
1. Dental implants. 2. Jaws—Tomography. I. Title.
[DNLM: 1. Dental Implantation—methods. 2. Tomography, X-Ray Computed—methods. 3. Jaw—radiography. 4. Jaw—surgery. WU 640 R846d 1998]
RK667.I45R67 1998
617.5'22—dc21
DNLM/DLC
for Library of Congress 97-37997
CIP

quintessence books

© 1998 Quintessence Publishing Co, Inc

Quintessence Publishing Co, Inc
551 North Kimberly Drive
Carol Stream, Illinois 60188

Some of the product names, patents, and registered designs referred to in this book are registered trademarks or proprietary names even though specific reference to this fact is not always made in text. Therefore, the appearance of a name without designation as proprietary is not to be construed as a representation by the publishers that the product is in the public domain.

All rights reserved. This book or any part thereof may not be reproduced, stored in a retrieval system, or transmitted in any form or by any means, electronic, mechanical, photocopying, or otherwise, without prior written permission of the publisher.

Editor: Cheryl Anderson-Wiedenbeck
Production: Timothy M. Robbins and Michael Shanahan
Cover design: Michael Shanahan

Printed in Hong Kong

Contents

Contributors viii

Acknowledgments ix



Introduction 1

Historical Perspective 1
Diagnostic Modalities in Dental Implantology 3
Why Computerized Tomography? 7



Technique for Computerized Tomography of the Jaws 9

Historical Perspective 9
Choice of Scanners 10
Direct Coronal CT Scans of the Jaw 11
The Reformatted Axial CT Examination 13
Conclusion 38



Computerized Tomography of the Mandible 39

Definition of Terms 39
The Edentulous Mandible 39
Normal Anatomy of the Mandible 40
Computerized Tomography Evaluation of the Mandible 49



Computerized Tomography of the Maxilla 65

Normal Anatomy of the Maxilla 65
Postnatal Development 67
Computerized Tomography Evaluation of the Maxilla 67
Conclusion 86



Computerized Tomography of the Enhanced Alveolar Ridge 87

Ridge Maintenance Procedures 87
Ridge Augmentation Techniques 90
Conclusion 111



Computerized Tomography in Patients with Implants and Other Metal in the Jaw 113

Evaluation of the Osseointegrated Implant 114
Evaluation of the Failed Implant 123
Evaluation of the Symptomatic Implant 125
Evaluation of Blade Implants 129
Evaluation of Subperiosteal Implants 133
Evaluation of the Surgically Enhanced Jaw 134
Evaluation of Other Metallic Surgical Hardware 134
Conclusion 138



Interactive Implant Surgical Planning with SIM/Plant 139

Historical Development 139
Use of SIM/Plant Software 145
Future Directions 152



Nonimplant Uses for Dental Computerized Tomography 153

James W. Borrow, MD / Justin P. Smith, MD

Evaluation of Unerupted and Displaced Teeth 153
Evaluation of Cysts 155
Evaluation of Nonodontogenic Cysts 159
Evaluation of Lingual Mandibular Bony Defects 162
Differentiation of Intra-antral and Extra-antral Cystic Masses of the Maxillary Sinus 164
Evaluation of Fibrous Dysplasia and Ossifying Fibroma 165
Evaluation of Carcinomas of the Mandible and Maxilla 170
Evaluation of Osteomyelitis 172
Conclusion 174



Use of Prosthesis-Generated Computerized Tomographic Information for Diagnosis and Surgical Treatment Planning 177

Richard A. Mecall, DDS, MSD / Alan L. Rosenfeld, DDS

Facial Esthetics 177
Normal Anatomy of the Maxilla and Mandible 180
Impact of Pathologic Changes on the Alveolar Process or Residual Ridge 185
Classification of Residual Ridge Deformity 186
Determination of the Optimal Final Tooth Position 192
Analyses for Implant Placement 193
Analyses for Residual Ridge Augmentation 206
Problem Resolution and Execution Planning Analysis (PREP) 213
Prosthetic Designs 225
Clinical Cases 228
Conclusion 236

Index 241



Introduction

In the last decade, computerized tomography (CT) has become one of the most frequently used imaging modalities for the preoperative evaluation of the jaw for dental implants. Numerous scientific papers and posters have been presented defining the utility of the technique. There is, however, no comprehensive single reference available that can be used as a "how to" manual for the performance and interpretation of dental CT. In certain respects, dental CT is an overlooked examination. Computerized tomography scanners are, for the most part, operated by radiologists with no particular interest or training in dental radiology or pathology. These radiologists rarely interact with periodontists or oral surgeons. Consequently, there is no natural rapport between these two groups; they do not share a common jargon. Dental radiologists, who are expert in the anatomy of the jaws and are sensitive to the needs of the periodontist and oral surgeons, generally do not have access to CT scanners.

It is the goal of this monograph to become the bridge between the radiologist who is faced with an uninterpretable dental CT examination and the surgeon who needs expert advice to evaluate implant sites in difficult cases. Because the anticipated audience for this book comes from such different backgrounds, the discussion of the imaging techniques will be geared to the radiologist but somewhat detailed for the benefit of the dental surgeon. Similarly, some of the dental aspects will be presented in detail to aid the radiologist. It is hoped that a happy medium will be found on most topics.

Historical Perspective

A Honduran skull from pre-Colombian times is said to be the earliest known example of a successful dental implant. A black stone was implanted in place of one of the incisors. The stone was covered with a large amount of calculus, indicating that it had been present for a long time.[1] Implant surgery has come a long way since that time.

Over the last century, various techniques have been tried to anchor implants permanently in bone. The two most successful types have been subperiosteal and endosteal implants. Subperiosteal implants were originally conceived by Muller in 1937, and they have been used in one form or another for nearly 50 years with moderate success. Modern endosteal

implantation of various metals was performed near the beginning of the century. The technique of root-form implantation was brought into general acceptance by Brånemark and his associates[2] and blade implants were introduced by Linkow.[3]

Following the publication of a series of successful long-term endosteal implants,[4] the Brånemark technique became the standard for dental implantation. Many similar systems and techniques have appeared throughout the world and implantations are now routinely performed by many periodontists and oral surgeons.

In early 1987, Dr Melvin Schwarz, an experienced periodontist, wandered into my office at Multiplanar Diagnostic Imaging Co with a problem. He had recently returned from Sweden, where he had received training in the placement of Brånemark implants. He was rightfully concerned that there was no accurate way for the preoperative determination of the exact position for optimal implant placement. He wondered if our computer science group could produce CT images that would display mandibular and maxillary anatomy to optimize site selection for implantation. Multiplanar Diagnostic Imaging Co combined a clinical CT scanning practice and a computer science group, led by Dr Michael Rhodes, consisting of three PhDs in computer science and engineering and nine programmers. Their achievements had included, among many others, the perfection of state-of-the-art computer software for reformatting CT images of the spine into precisely sized sagittal and curved coronal images. Reformation is a technique whereby the digital data that make up the axial cross-sectional images produced by the CT scanner are rearranged so that they are displayed in alternative planes.

Computerized tomographic evaluation of the jaw for endosteal implantation requires images perpendicular to the curve of the alveolar ridge. To produce these reformatted images, Dr Rhodes and his associates set about to write a program to produce a set of "dentist-friendly" images. Our group designed, produced, and patented the first dental reformation package, called *DentaScan*. It has been copied many times, and similar products are now available for most commercially available CT scanners and many stand-alone imaging workstations. The DentaScan examination is unique in radiology. It was the first and perhaps only radiologic procedure specifically designed and produced to solve a specific clinical problem for a single surgical procedure.

Unlike most radiographic examinations, the dental CT exam is not primarily a diagnostic test. The diagnosis of periodontal disease has already been made, and a decision to perform endosteal implantation has been finalized. The CT study is primarily a map-making exercise. The pictures produced are used as a surgical guide to allow the performance of a safe procedure with the greatest likelihood for successful osseointegration of the fixtures. The careful choice of implant sites will also produce the most esthetic cosmetic results.

Diagnostic Modalities in Dental Implantology

A variety of diagnostic imaging techniques are available for the preoperative and postoperative analysis of the jaw for dental implants. They include conventional intraoral radiographs, extraoral routine films, panoramic tomograms, digital radiographic images, and CT scans. No single radiographic procedure produces ideal images for all steps along the diagnostic and therapeutic pathway. Consequently, most patients will undergo a series of imaging studies, each providing unique and vital pieces of information leading to successful implant surgery.[5]

Intraoral radiographs

Intraoral radiographs of most patients are taken at the initial evaluation. They are inexpensive and readily available. They are the highest-resolution images produced by radiographic procedures. The presence of localized pathosis can be defined, and the anatomy the maxillary sinus and often the inferior alveolar canal can be determined. There are, however, several problems with intraoral films. Because it is impossible to precisely orient the film parallel to the alveolar ridge, and the focus-film distance cannot be standardized, it is impossible to make precise measurements of the vertical height of the alveolar process. The most important deficiency is the inability to evaluate the buccolingual dimension of the alveolar process (Fig 1-1).

According to Klinge et al,[6] the inferior alveolar nerve canal could not be identified at the proposed implant sites in 25% of periapical radiographs. Furthermore, even in the mandibular specimens in which it could be identified, the measurement of distance between the crest of the alveolar ridge and the inferior alveolar canal was not adequately



Fig 1-1 Dental radiograph of a mandibular specimen. It is impossible to evaluate the cross section of the mandibular ridge. (Courtesy Dr Stuart C. White, UCLA School of Dentistry.)

precise. In only 53% of radiographed anatomic specimens were the measurements made on the dental films within 1 mm of the actual distance. The alveolar canal was, however, definable on all of their mandibular CT scans. In 94% of the scans, the measurement obtained from the CT scan was within 1 mm of the measurement on the specimen.[6]

Occlusal radiographs

Intraoral occlusal films are capable of demonstrating both the mandibular and maxillary arches. Views of the mandible are much more likely to be useful in implant planning in the anterior than the posterior portions of the bone. The internal structure of the implant site can be seen in detail. Occlusal views of the maxilla are much less useful, because the angle of inclination of the teeth precludes perfect positioning of the film parallel to the alveolar process.[7] Precise measurement of the buccolingual dimension cannot be made because the image is two-dimensional. The peripheral edges of the bone visible on these films represent the contour of the widest portion of the bone, which is at the base, rather than the apical portion, of the alveolar ridge (Figs 1-2a and 1-2b).

Panoramic tomograms

Panoramic tomograms (radiographs) are probably the most useful of the routine radiographic studies for the preoperative evaluation of the jaw. They are useful in identifying areas of periodontal erosion and other pathologic conditions of the alveolar bone. They are uniformly available and relatively inexpensive to perform.

Unfortunately, certain anatomic distortions inherent to the method make very accurate measurements impossible.[8-10] The magnification in the vertical plane is dependent on the focus-film distance, which is constant for each exposure. The magnification in the horizontal plane varies with the changing position of the film and the x-ray beam. Consequently, in only 17% of cases did measurements made from panoramic tomograms accurately represent the true osseous height on dried specimens.[6] Because of the linear distortion, especially in the anterior portion of the arch, measurements will be inconsistent even within the same bone. In an attempt to alleviate the problem of variable magnification, several authors[11,12] have advocated that radiopaque intraoral stents of known dimension be used to calculate the magnification at different locations along the jaw.

The main drawback of using panoramic radiographs for implant planning is that the images produced are two-dimensional. It is impossible to assess the buccolingual dimension of the jaw. In many instances, bone height appears to be adequate on the panoramic views, but cross-sectional images prove that there is inadequate bone to support an implant (Fig 1-3). Because of this major problem, some cross-sectional imaging should be performed to evaluate the cross-sectional dimensions of both the mandible and maxilla.

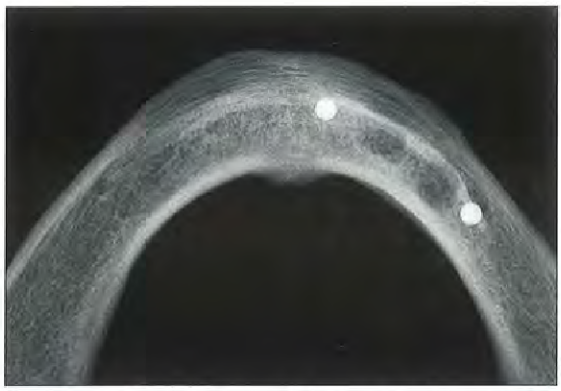


Fig 1-2a Occlusal radiograph of a mandibular specimen. The visible borders of the bone correlate with the most inferior, and therefore the broadest, portion of the bone rather than the alveolar process. (Courtesy Dr Stuart C. White, UCLA School of Dentistry.)



Fig 1-2b Photograph of the same specimen.

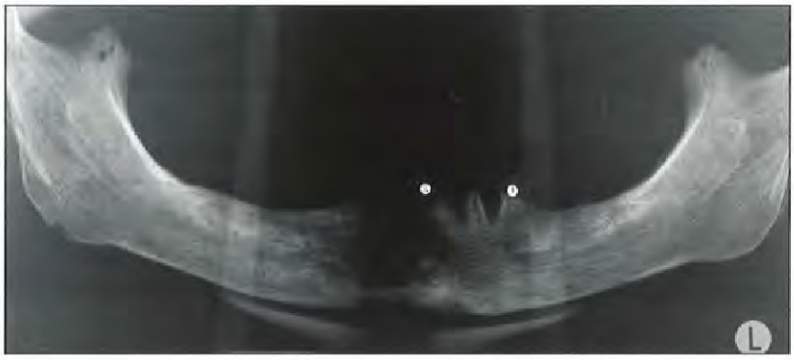


Fig 1-3 Panoramic view of the mandibular specimen in Figs 1-2a and 1-2b. (Courtesy of Dr Stuart C. White, UCLA School of Dentistry.)

Conventional tomograms

Conventional film tomography is a technique by which a series of thin, sectional images are produced in a way that only a single plane is in focus. All other parallel planes are purposely blurred so that they are not in focus. There are a wide variety of machines that produce tomographic images. They all operate on the same basic physical principle. The distance between the x-ray tube and the film is mechanically fixed. The tube and film are moved reciprocally so that the body part being imaged is viewed from multiple angles. The position of the plane of the fulcrum of motion between the tube and the film is the tomographic plane and will be the only portion of the patient to remain in focus.

The resolution of the tomogram and the sharpness of the image are dependent on the type of motion that the tube and film make. Linear tomography is the simplest to understand. The tube and film are fixed

to each other but move in opposite directions. Anatomic structures that are perpendicular to the focal plane are blurred maximally. Structures parallel to the plane are less well blurred. Complex motion tomography includes a variety of situations in which the tube and film undergo any of a series of motions, including circular, elliptical, hypocycloidal, and spiral. The more complex the motion, the thinner the focal plane and the higher the resolution.

Conventional linear tomograms produce images with a slice thickness of 3 to 5 mm. Hypocycloidal tomograms produce images approaching 1 mm in thickness. Tomographic images are always magnified because the focal plane is at a distance from the film. Because this distance is fixed, the magnification factor for each study is always the same. The magnification factor is calculated by comparing the apparent and actual sizes of a known object.

Tomography is ideal for the evaluation of a single implant site. It is relatively easy to identify the area of interest and position the patient in such a way that the tomographic plane is perpendicular to the edentulous area. This is easiest for anterior midline implants, which can be viewed in the lateral position, and posterior implants, which can be viewed in a frontal plane. The problem arises along those portions of the jaw that are the most curved. The patient must be oriented properly with respect to the x-ray beam. Most conventional tomographic devices found in hospital radiology departments are adequate for performing these images.

It is much more difficult to use conventional tomographic equipment to produce adequate images in patients who are to receive multiple implants. It is too time consuming to keep repositioning the patient for each slice so that each slice is perpendicular to the jaw. It is also very difficult to exactly localize the individual tomographic images. The use of intraoral stents with radiopaque markers during the tomographic examination eliminates this problem most of the time.[13,14]

Measurements are most precise when the bony borders are perpendicular to the tomographic plane. This is generally the case in the anterior portions of the alveolar arches. Measurements are least likely to be precise in the posterior maxilla, where the floor of the sinus is undulating. The sinus floor is therefore less likely to be perpendicular to the focal plane.

The Scanora multimodal imaging system (Orion/Sorodex)[15,16,17] is often used to produce conventional tomograms for dental implants. The system produces a series of four images, each 4 mm apart, on a single film. Measurements are most precise along relatively straight segments of bone and least precise through areas where the curvature of the bone is most prominent. The thick images are better than very thin scans for bone density measurements. An assessment of bone density can be made directly from the images.

Tomographic examination with a book cassette technique produces five simultaneous films. The cassette contains five pairs of intensifying screens separated by 3 mm. Each of the films in the cassette is at a different distance from the x-ray source. Consequently, the image plane of each film is 3 mm from its adjacent mates.[15]

Why Computerized Tomography?

Computerized tomograms are superior to conventional tomograms as a guide for implant placement for several reasons. First, CT scanners produce very high–resolution images. There are two types of resolution: geometric and contrast. *Geometric resolution* is defined as the ability to distinguish between closely spaced objects. It translates in nonscientific terms to sharpness, where edges and borders are distinct. *Contrast resolution* means the ability to distinguish between objects that are similar anatomically and chemically, such as neural tissue and fat. For most dental applications, it is the scanner's ability to produce clear, sharp images with very easily identifiable borders that is most important. Conventional tomographic images are produced by purposely blurring all nonfocal planes. These images are, by their very nature, blurry. Even spiral or hypocycloidal tomograms, which make the highest-resolution pictures, produce images with hazy borders (Figs 1-4a and 1-4b).

In addition, evaluation of the jaw with conventional tomography requires very precise patient positioning. Without specialized machines, it is necessary to reorient the patient for each series of images to keep the image plane perpendicular to the alveolar ridge. The reformatted CT examination, on the other hand, permits the production of all possible cross sections from a single data acquisition without moving the patient or reconfiguring the x-ray machine. Each of the pictures produced in this manner can be localized in three-dimensional space so that there is never a doubt as to which portion of the alveolar ridge is included in the image.

Moreover, with CT it is possible to generate three-dimensional images from the same data set. These images may be useful in conceptualizing complex anatomic relationships in unusual cases. They are certainly helpful in explaining the surgical procedure to patients. In rare



Fig 1-4a Tomogram of a mandibular specimen.



Fig 1-4b Computerized tomogram through the identical area. Note the difference between the images in edge sharpness. (Courtesy of Dr Stuart C. White, UCLA School of Dentistry.)

instances, life-sized three-dimensional plastic models can be produced. These models have been used to fabricate subperiosteal implants without the necessity of making intraoperative casts.

Finally, as previously mentioned, all conventional tomograms produce magnified images, while CT scans can be life-sized. Measurements are made directly from the CT films. Alternatively, the data obtained during the CT scan can be fed into a personal computer, and treatment planning can be performed on the computer (see Chapter 7).

References

1. Schroeder A. A brief history of implantology. In: Schroeder A, Sutter F, Krekeler G (eds). Oral Implantology. Stuttgart: Thieme, 1991:60.
2. Brånemark PI, Briene U, Adell R, Hansson BO, Lindstrom J, Ohlsson A. Intraosseous anchorage of dental prostheses. Scand J Plast Reconstr Surg 1969;3:81.
3. Linkow L. Maxillary and Mandibular Implants; A Dynamic Approach to Oral Implantology. New Haven, CT: Glarus, 1979:148–298.
4. Brånemark PI, Zarb G, Albrektsson T. Tissue-Integrated Prostheses: Osseointegration in Clinical Dentistry. Chicago: Quintessence, 1985:315.
5. Frederiksen NL. Diagnostic imaging in dental implantology. Oral Surg Oral Med Oral Pathol 1995;80:540–554.
6. Klinge B, Petersson A, Maly P. Localization of the mandibular canal: Comparison of macroscopic findings, conventional radiography, and computed tomography. Int J Oral Maxillofac Implants 1989;4:327–332.
7. Miles DA, Van Dis ML. Implant radiology. Dent Clin North Am 1993;4:645–668.
8. Truhlar RS, Morris HF, Ochi S. A review of panoramic radiography and its potential use in implant dentistry. Implant Dent 1993;2:122–130.
9. Glass BJ. Successful Panoramic Radiography, publication No. N-406 Rochester, NY: Eastman Kodak, 1991.
10. Schiff T, D'Ambrosio J, Glass BJ, Langlais RP, McDavid WD. Common positioning and technical errors in panoramoic radiography. J Am Dent Assoc 1986;113:422.
11. Hollender L. Radiographic examination of endosseous implants in the jaw. In: Worthington P, Brånemark PI. Advanced Osseointegration Surgery: Applications in the Maxillofacial Region. Chicago: Quintessence, 1992:80–93.
12. Buser D, Ewber HP, Bragger U. The treatment of partially edentulous patients with ITI hollow-screw implants: presurgical evaluation and surgical proceedures. Int J Oral Maxillofac Implants 1990;5:165–174.
13. Eckerdal O, Kvint S. Presurgical planning for osseointegrated implants in the maxilla: a tomographic evaluation of available alveolar bone and morphological relations in the maxilla. Int J Oral Maxillofac Surg 1986;15:722–726.
14. Stella JP, Tharanon W. A precise radiographic method to determine the location of the inferior alveolar canal in the posterior edentulous mandible: implications for dental implants. Part 1. Int J Oral Maxillofac Implants 1990;5:15–22.
15. Grondahl K, Ekestubbe A, Grondahl HG, Johnsson T. Reliability of hypocycloidal tomography for the evaluation of the distance from the alveolar crest to the mandibular canal. Dentomaxillofac Radiol 1991;19:200–204.
16. Tammisalo T, Luostarinen T, Vahatalo K, Rosberg J, Tommisalo EH. Radiographic detectability of periodontal disease. A comparison of perapical radiography with detailed zonagraphy. Dentomaxillofac Radiol 1995;24:185–190.
17. Molander B, Ahlquist M, Grondahl HG. Image quality in panoramic radiography. Dentomaxillofac Radiol 1995;1:17–22.



Technique for Computerized Tomography of the Jaws

Historical Perspective

The era of modern cross-sectional imaging began in 1972 with the advent of the computerized tomography (CT) scanner. Its inventor, Sir Godfrey Houndsfield, shared the Nobel Prize for medicine with Allen M. Cormack, who first computed the attenuation coefficient of a slice of an object from a series of projections.[1–3] This calculation was based on the theoretical mathematical model first described in 1917 by an Austrian named Radon,[4] who proved that the image of a three-dimensional object could be calculated from an infinite number of two-dimensional projections. The original scanner, by EMI, was designed to make cross-sectional images of the brain. It was made up of three basic components: a scanner gantry, a table for the patient, and a computer to perform the calculations.

The scanner gantry was a doughnut-shaped device that contained a movable x-ray tube focused on a pair of parallel scintillation crystal x-ray detectors. The tube and the detectors moved parallel from side to side across the gantry.

The patient reclined on a movable table with his or her head immobilized by a water bag. The patient's head was positioned within the center of the doughnut. The table could be advanced into the scanner in 1-cm increments, thereby allowing the operator to make cross-sectional images every centimeter.

A series of 80 radiation measurements were made by the detectors on each traverse across the patient. The tube and detectors would then rotate 1 degree and another traverse was begun. This would be continued for a total of 180 degrees. X-rays emitted by the tube were collimated to a beam 1 cm thick. X-rays striking the detectors would emit light proportionate to the quantity of x-ray getting through the patient. Photomultiplier tubes magnified the minute amount of light generated by the detectors to a useful electrical impulse, which was digitized. A total of 80 x 180 simultaneous equations were processed by a minicomputer.

The mathematical process, *back projection*, that was used on the first scanners was described at the beginning of the century. An attempt to create a primitive CT scanner in the 1940s failed because the mathematical calculations were too taxing for the technology of the day. By the mid-1970s, computer technology had progressed to the point that the



Fig 2-1 General Electric 9800 CT scanner with a patient lying supine for axial scans.

approximately 14,400 simultaneous equations needed to compute a single CT image could be made in 4 1/2 minutes.

These calculations created an image made up of 80 rows of 80 picture elements called *pixels*. The numerical values of the picture elements were converted to gray shades, displayed on a television monitor, and recorded on film for permanent storage.

Modern, state-of-the-art CT scanners function much the same as the original EMI scanner. The patient is not held in a water bath but still must be restrained in a comfortable head holder to prevent even the slightest motion. The pair of detectors has been replaced by a sophisticated array of detectors capable of making large numbers of simultaneous measurements of x-ray absorption. Spiral CT scanners can produce up to 30 slices, each 1.0 mm in thickness, per minute.

Modern CT images are much more detailed. A picture with 512 x 512 data points can now be computed in a matter of seconds. The resolution of such systems is within 1.0 mm for high-contrast objects such as bone (Fig 2-1). Each data point has a numerical value called a *CT number* (also called *Hounsfield units* in honor of Godfrey Houndsfield, the inventor). These numbers range from –1,000 to +1,000. Each number represents a different amount of attenuation of x-ray. Air is assigned the value –1,000; water is assigned the value 0; and dense material, such as bone, is assigned the value +1,000.

Choice of Scanners

Most commercially available CT scanners are capable of producing the high-resolution images needed for the evaluation of the jaw for dental implants. Not all scanners produce images of the same quality, however. It is therefore incumbent on the referring surgeon to compare the images produced by the different equipment available in the geographic

area of his or her patients. In our clinical practice, we have found that the General Electric (GE) 9800 and Siemens high-resolution scanners produce the best dental examinations. There are many scanners that we have never used and therefore cannot compare to the GE 9800. It is our experience that images made with Picker scanners (Picker Medical Systems) appear less sharp.

Probably the most important single variable in determining which scanner to use is the experience of the technologist operating the scanner. The dental CT examination is very operator-dependent. It requires far more attention to detail than do most CT procedures. Most CT operators have never examined dental patients and are unfamiliar with the requirements of the examination.

The experience of the radiologist supervising the procedure is also important, because the radiologist is ultimately responsible for quality control. The interpretation of the scan is less important than the quality of the images. It is very unusual to find some unexpected abnormality on the scan that would produce a diagnosis other than periodontal disease. Of the approximately 5,000 patients scanned in our practice over the last 8 years, in only one was a diagnosis of an unsuspected tumor made from the scan. The diligent attention of the radiologist supervisor will help to ensure routinely high-quality dental scans.

Direct Coronal CT Scans of the Jaw

Computerized tomography scanners were originally called *computerized axial tomography (CAT) scanners* because they were designed to produce images in the axial plane. That means that the cross sections are along the long axis of the body. It was obvious in the early days of CT scanning that frontal views would be very helpful in the evaluation of head and neck abnormalities. Direct coronal CT images were first produced in the late 1970s.[5–7]

It is possible to produce coronal scans with the patient either prone or supine. The prone position is considered advantageous in most patients. The head is hyperextended, and the scanner gantry is angulated to produce images approximating the coronal plane. Some elderly patients find it impossible to lie still in the prone position with the head in hyperextension as a result of cervical arthritis. In those instances, the patient can be placed supine with his or her shoulders elevated off the table. The head is draped backward in hyperextension, and the gantry is angulated appropriately. These views can be used to evaluate the jaw[8–10] for maxillofacial surgery.

The first scans made for the evaluation of dental patients were done in the coronal plane. There are several major drawbacks to this type of scanning. The first and most important is that it is very difficult to obtain scans truly perpendicular to the alveolar ridge. Scanners have a limited ability to tilt, and elderly patients cannot bend their necks very

much. The result of these two factors is images that are not truly coronal. Measurements made on these films overstate the height of the alveolar ridge[11] (Fig 2-2). Direct coronal scans are most precise along the lateral arches and least precise in the area of the canines because of the curvature of the bone. Coronal scans do not produce perpendicular cross sections of the anterior mandible or maxilla.

In the coronal plane, the x-ray beam traverses the crowns of the teeth. Restorations will produce prominent streak artifacts. Heavy metal restorations, wires, and pins absorb nearly all of the x-rays passing through them. Consequently, the detectors in line with the metal see no radiation. The data are contaminated, resulting in streaks. These streaks are most pronounced between two parallel restorations. Metal artifacts make it difficult or even impossible to see the alveolar bone and make measurements (Fig 2-3).

For all of the aforementioned reasons, direct coronal scanning for the evaluation of implant sites has never attained any degree of acceptance in the dental community.



Fig 2-2 Patient in position for direct coronal CT scans.

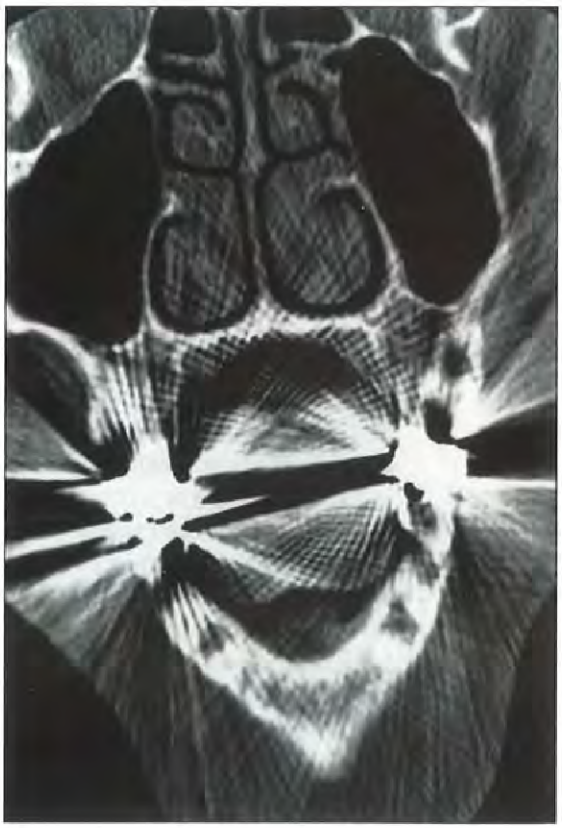


Fig 2-3 Direct coronal CT scan with dramatic artifact caused by dental restorations. (From Schwarz MS, Rothman SLG, Chavetz N, Rhodes M. Computed tomography in dental implantation surgery. Dent Clin North Am 1989;33:577. Reprinted with permission.)

The Reformatted Axial CT Examination

Patient preparation

Reformatted sagittal and coronal spinal CT became standard in the early 1980s.[12] With that technology well established, it was logical to adapt the same process to dental CT. The patient reclines supine on the scanner table with his or her head immobilized in the scanner's head holder. Soft sponges are placed around the head to prevent even the slightest motion. The head is angulated so that the plane of scanning is parallel to the occlusal surface of any residual teeth. In completely edentulous patients, the plane of scanning is parallel to the superior surface of the alveolar ridge.

A lateral digital radiograph is made on the scanner to allow the technologist to define the upper and lower limits of the scan volume (Fig 2-4). If the patient's head is not properly aligned, the angulation can be corrected at this time. The patient is instructed to breathe slowly and quietly and to refrain from swallowing. The minimal motion from a swallow can cause a minor artifact that will make measurement difficult. A gauze-covered tongue depressor or some other soft intraoral space filler is positioned between the patient's teeth to eliminate mandibular motion.



Fig 2-4 Digital lateral scout view indicating the proper position and angulation for mandibular scanning.

Scanning technique

The scanning sequence is begun and all of the data are acquired very rapidly from a series of very thin axial sections. For evaluation of the mandible, the patient is advanced into the gantry in 1.0-mm intervals. The total examination creates a series of 20 to 40 thin axial sections 1.0 mm apart. The CT slice thickness is determined by the technologist and varies depending on which scanner is in use. It has been found empirically that, for best evaluation of the mandible, the slice thickness should be no greater than 1.5 mm. For scanners whose minimum slice thickness is 1.5 mm (eg, GE 9800), it is necessary to overlap the axial scans to optimize the geometric resolution of the reformatted images. On spiral scanners and those scanners whose minimum slice thickness is 1.0 mm, contiguous scans with no overlap are used. It has been found that the average error of measurement generated by this technique will be in the range of 0.8 mm.[13] Scanners with a minimum slice thickness greater than 1.5 mm are best not used for dental examinations.

Evaluation of the mandible is more technically demanding than the evaluation of the maxilla. It requires the maximum resolution power of the scanner to visualize the inferior alveolar nerve canal in many patients. It is not as critical to perform 1.0-mm-thick slices every 1.0 mm to assess the maxilla; it is adequate to scan the maxilla with 1.5-mm slices every 1.5 mm.

The entire scan should take no more than 5 minutes to complete once the patient is properly positioned within the scanner. If both arches are to be studied on the same day, the patient should be allowed to rest and move his or her head and neck between the two halves of the examination. A second digital scout view is performed to align the occlusal plane of the other jaw and to set the limits of the second scan. The second set of images is then completed as quickly as possible. If it is obvious that the patient is moving during data acquisition, the sequence should be terminated. The technologist should attempt to determine what, if any, problem the patient is experiencing and remedy the situation. Generally, patients can hold still for the few minutes required. If the patient has a tremor or is agitated, it is unlikely that an adequate study can be performed.

Multiplanar reformation

Once the axial CT data are acquired, the patient is free to leave unless the technologist has reason to believe there is patient motion on the scan. It generally requires several minutes for the axial pictures to completely reconstruct. If the technologist suspects that there is patient motion on the scan, the patient can remain on the table until the reconstruction of the data is completed. A single-slice reformation should be performed using the scanner's own on-line program to reformat and to evaluate the extent of motion artifact. After consultation with the radiologists, the technologist can repeat the scan if the reformation is very

degraded. Minor motion may not cause an artifact severe enough to cause significant measurement errors. It is best to allow the referring dentist to decided whether a second scan is justified.

Most of the computer programs that were designed to produce images for the evaluation of dental implants are minor modifications of the original DentaScan software produced by Multiplanar Diagnostic Imaging Co and are now available from General Electric Medical Systems. The programs vary slightly in their display formats, and it is very simple for anyone familiar with one program to understand and to interpret images on other programs. The setup technique and formatting for the DentaScan program will be described. 3D/Dental software (Columbia Scientific) will also be discussed, because it has slightly changed how the printed formats are used.

Two basic types of reformatting program are available: those that run on the scanner's on-line computer or a second operator's console provided by the manufacturer (eg, DentaScan; 3D/Dental; Siemens MPR/MPD, Siemens Erlangen) and those designed to run on free-standing independent computer workstations (eg, ToothPix, Cemax Inc; Allegro workstation, ISG Technologies). The axial CT data must be transferred to the workstation on a diskette or tape. The processing can be performed at the convenience of the technologist. The images can be photographed on x-ray film or photographic paper or stored on disk for further processing on a personal computer.

Setup procedure (DentaScan)

Regardless of which type of reformatting software is being used, the setup procedures are similar. For the purpose of the following discussion, the DentaScan program will be used. At the conclusion of this section, representative images will be displayed from some of the other commonly used programs.

At the completion of the CT examination, the operator has a stack of axial scans stored on the disk drive. A representative scan from that stack (usually the center slice) is displayed on the viewing screen. Using a trackball, the technologist identifies a series of data points buccal to the midzone of the bone. The computer then creates a curve by connecting the dots through the alveolar ridge. This curve should parallel the inner and outer cortices (Fig 2-5a).

Once the technologist is satisfied that the curve is smooth and is likely to produce symmetric panoramic views, a command is given to draw a series of equally spaced lines that are perpendicular to the original curve. These lines are calculated to represent true cross-sectional oblique views. They are not parallel to each other because the inner cortex of the jaw makes a tighter curve than the outer cortex. The space between these cross-sectional oblique images is variable. An interval of 2.0 mm between slices appears to be adequate in nearly all patients. The lines are then numbered sequentially, and the television screen image is updated with the new information (Fig 2-5b). If all appears correct to the operator, the command is given to begin the reformation process.



Fig 2-5a Axial CT slice through the mandible showing the curve drawn by the technologist through the center of the bone.

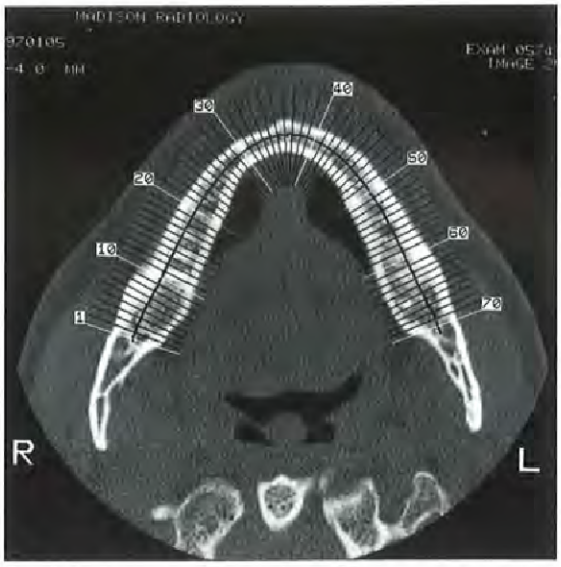


Fig 2-5b Same axial scan after the computer has calculated the position of the cross-sectional oblique pictures.

The first part of this process is for the computer to dig into the stack of axial slices and identify all the picture elements along each of the drawn cross-sectional oblique lines. These picture elements are then rearranged into images and displayed as a sequence of oblique cross sections, which are numbered from right to left. On the second cross-sectional image from the left in the upper row, the letters *BCL* and *LNG* are added to the film to identify the buccal and lingual sides to prevent confusion (Fig 2-6).

Tick marks are appended to each image to facilitate localization of visualized anatomic structures. The tick marks along the side of each small image represent the location of each individual axial scan. If there are 30 scans in the stack, there will be 30 tick marks. The distance between each tick mark is equal to the amount that the scanner table moved between each slice. In most instances, that will be 1.0 mm for mandibular scans and 1.5 mm for maxillary scans (on GE 9800 scanners). It is therefore very important for the referring dentist to know exactly how the scan was performed. It is critical to realize that the interval between the tick marks represents a specific distance, for example 1.0 mm, because the distance may not actually measure 1.0 mm on the film.

Typically, the computer images are photographed on x-ray film. Each camera is different. There may be distortion along either the horizontal or vertical axis. It is critical for the operator to calibrate the camera. If the photographed tick marks do not measure as they should, the camera must be serviced and corrected. The referring dentist should check the calibration occasionally.

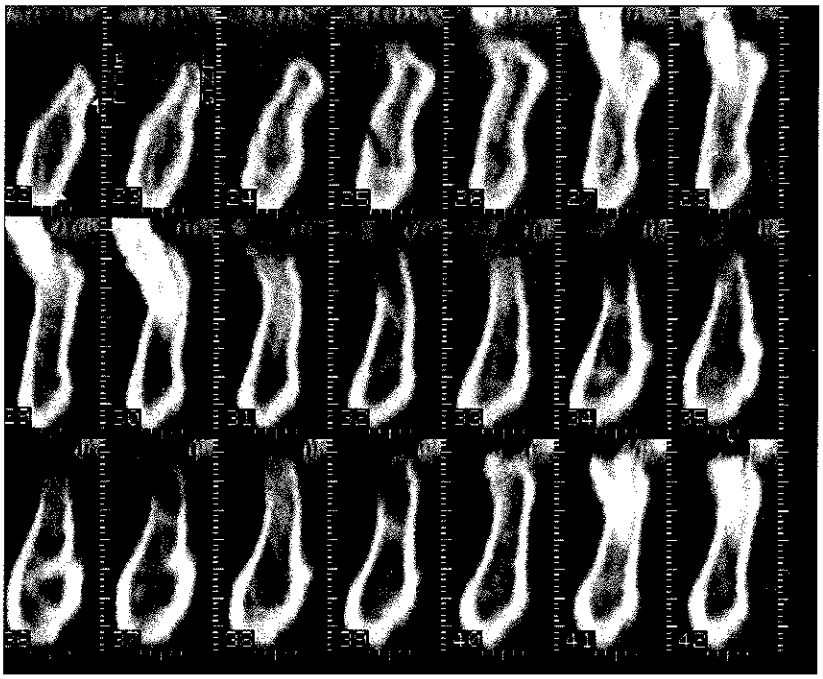


Fig 2-6 DentaScan display format for oblique cross-sectional reformations.

The measured distance on the film will depend on the amount of magnification or minification created by the camera that makes the images. If proper filming technique is used and the camera is carefully maintained, the photographed images can be made life-sized and all measurements can be made directly from the sheets of x-ray film. To prevent errors, a millimeter ruler, labeled *mm,* is displayed below the axial scans on each set of images. This ruler allows calculation of the magnification factor of the film.

To ensure the most precise determination of the magnification factor, the distance between 100 tick marks should periodically be measured. That distance should actually measure 10.0 cm. (It is best to measure a relatively large number of tick marks to decrease the total error caused by measuring short distances with relatively thick rulers.) If 100 tick marks on the film measure less than 100.0 mm, any measurement made directly from the film will underestimate the actual distance. If this difference is less than 4.0 mm, the scan should be considered as if it were life-sized, because this small error will provide a safety margin for the surgeon; that is, there will be very slightly more bone present than was expected.

If the measured distance is significantly greater than the expected 100.0 mm, the magnification factor is calculated by dividing 1.0 by the amount of the actual measurement. Measurements made directly from the film are corrected by multiplying the measured distance by the magnification factor. Any error made under these circumstances will suggest

to the surgeon that more bone is available than there actually is, thereby reducing the margin of safety.

The tick marks along the bottom of each cross-sectional oblique image represent the position of the panoramic reformations. After completing the series of oblique cross sections, the computer goes back into the data set and draws four curves that parallel the original curve created by the technologist. Two curves are buccal and two lingual to the original curve. The program then dissects the stack of axial scans and computes panoramic pictures from the same axial data. The five panoramic images are displayed sequentially and numbered from 1 through 5. A series of tick marks are appended to these images (Fig 2-7).

The tick marks at the bottom of each panoramic view correspond to the location of each of the cross-sectional images. Every fifth tick mark is elongated to facilitate counting. The tick marks along the side of each panoramic view indicate the position of each axial slice. Consequently, the number of tick marks alongside the images and the spacing between them will be identical on the panoramic and cross-sectional oblique images.

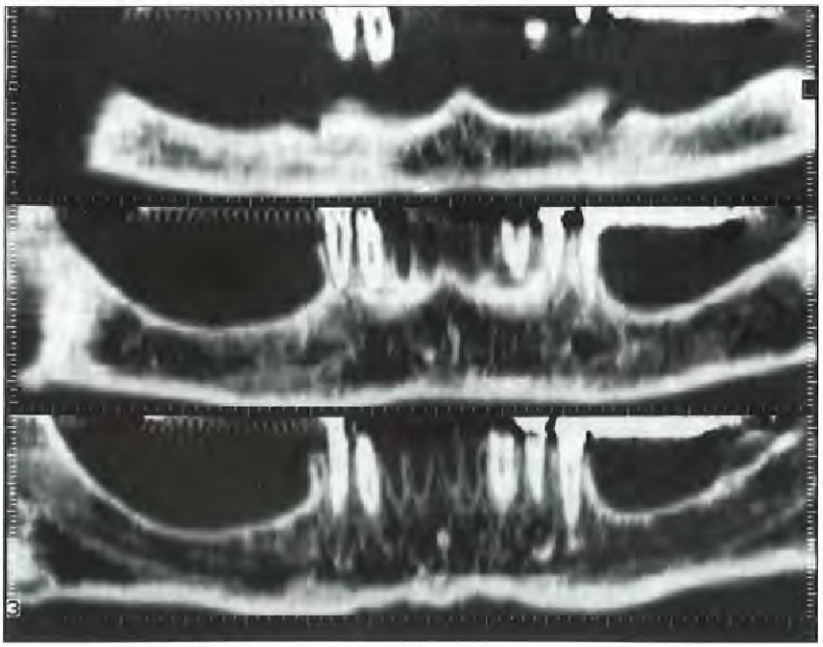


Fig 2-7 DentaScan display format for panoramic reformations.

It is useful to practice localizing an anatomic structure in all three planes, for example, the extraction sockets highlighted on the axial image in Figure 2-8, on the cross-sectional oblique views in Figure 2-6, and the panoramic views in Figure 2-7. In Figure 2-8, the most right-sided extraction is at the position of the 32nd tick mark. The larger tick mark, numbered 30, is just distal to the bony concavity. The 32nd tick mark is small. This localizes the area of interest to the 32nd cross-sectional oblique image. Thus, in Figure 2-6, oblique cross-sectional image 32 shows the extraction socket. The lower tick mark closest to the bone cavity indicates which panoramic view to evaluate. To locate that tooth on the panoramic view, the lower tick marks are counted to 32. The numbers begin on the left and continue to the right. With this technique, it is possible to locate any anatomic structure on all three views. For practice, the reader should try to locate the bony defects visible on oblique cross sections 34, 37, and 39.

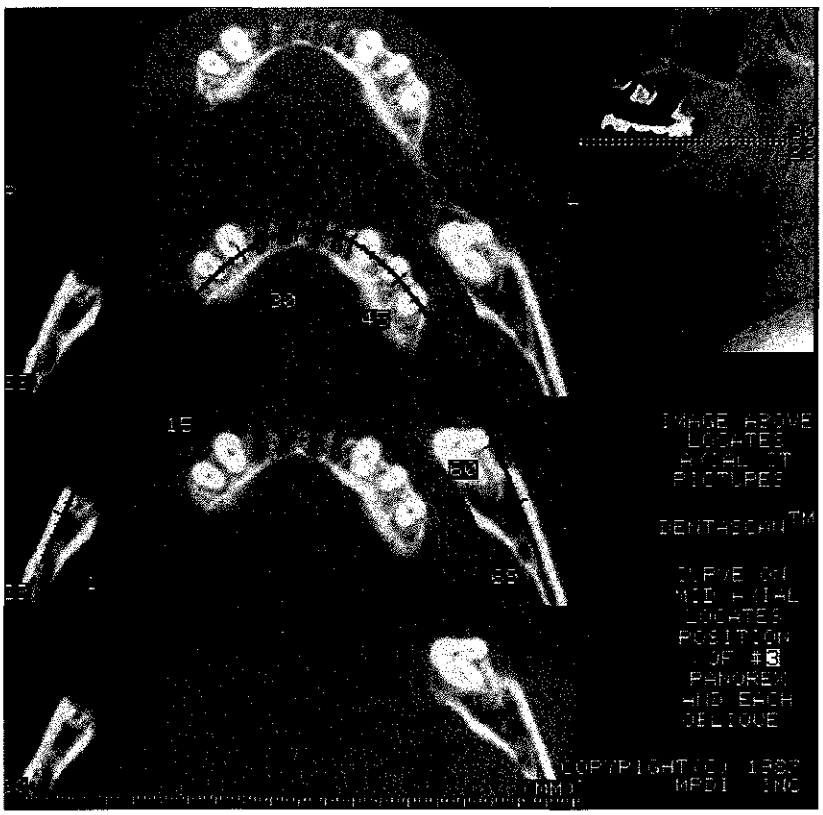


Fig 2-8 DentaScan display format for mandibular axial views.

The DentaScan program was designed to be frugal with film. Three contiguous axial views are displayed simultaneously, each one within the concavity of the adjacent sections (see Fig 2-8). The slices are numbered sequentially, and the left and right sides of the image are marked. For the DentaScan program, the patient's right side is displayed on the left side of the printed image. The central axial view of each triplet is annotated with a curve that marks the position of the middle panoramic section and all of the cross-sectional oblique views. The software displays four contiguous maxillary scans in each camera frame. The lower two axial images are annotated with the curve and tick marks for slice localization (Fig 2-9). There are several lines of text below the images. The distance between the axial slices is defined in that text.

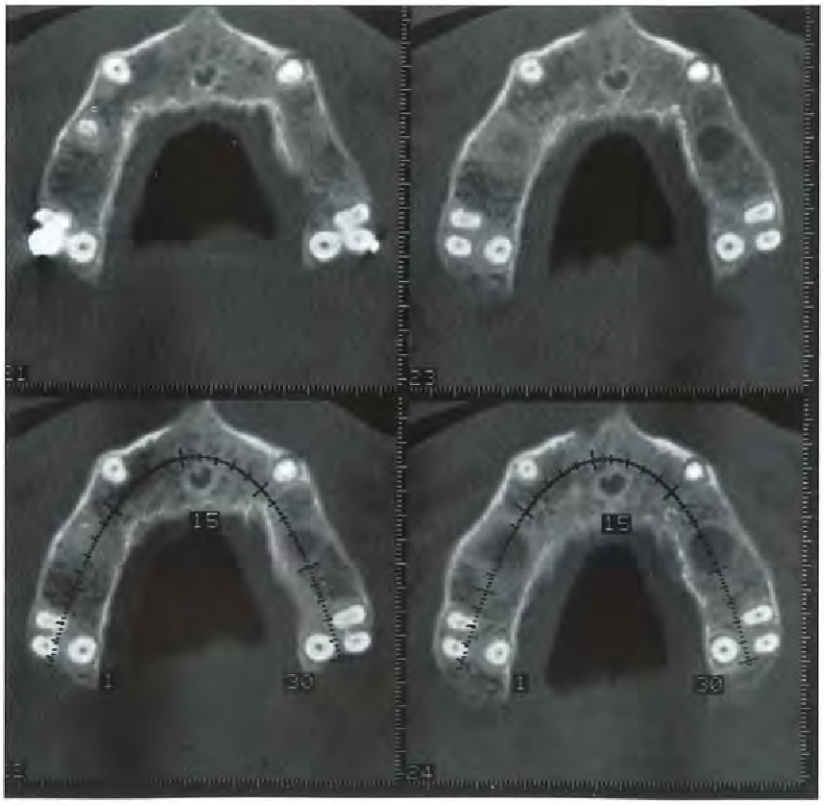


Fig 2-9 DentaScan display format for maxillary views.

The 3D/Dental program

The 3D/Dental program is very similar to DentaScan. Since initially introduced, it has undergone several revisions that make it more user friendly to the dentist. A patient identification image displays the digital scout view and the midline axial scan with the annotated curve and markers indicating the position of the cross-sectional oblique views (Fig 2-10). Two 5.0-cm rulers are displayed, one in the horizontal plane and one in the vertical plane, making it easy to check for geometric distortion of the image or camera error.

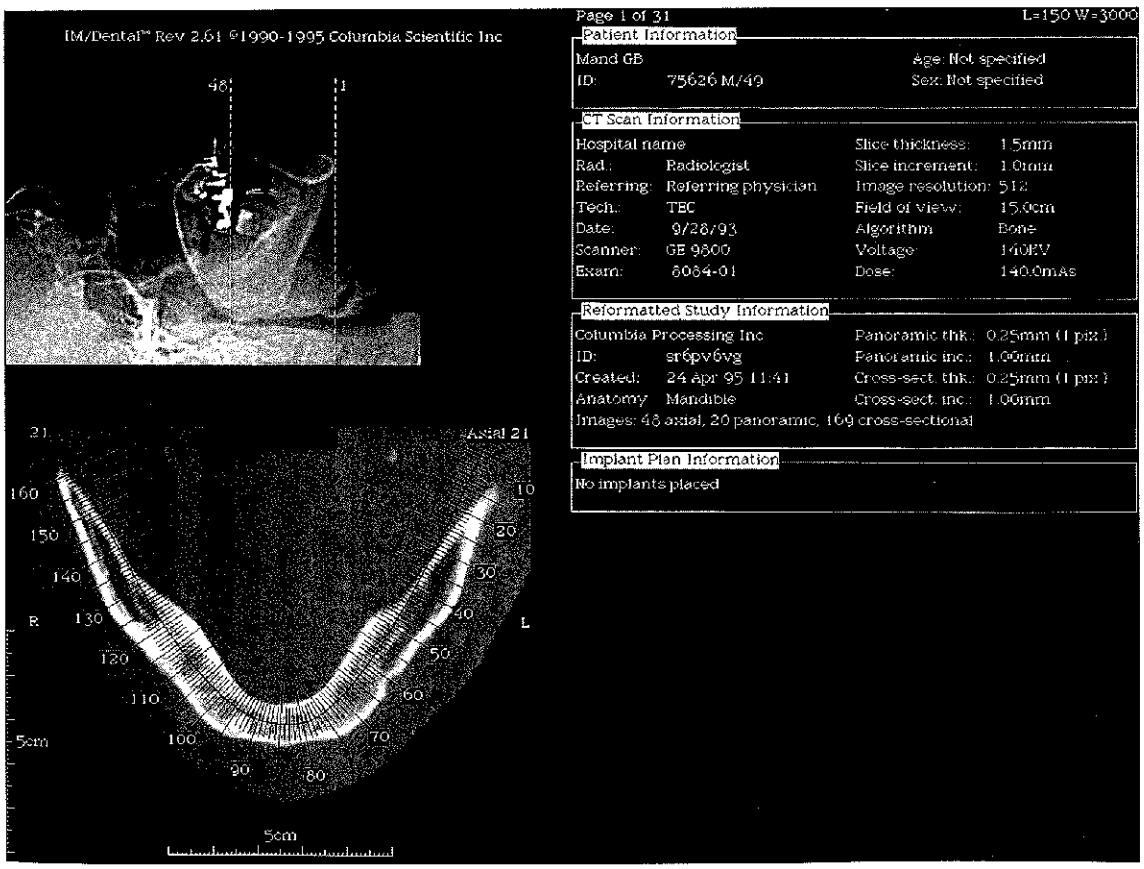


Fig 2-10 3D/Dental display format for patient identification and localization of the cross-sectional oblique reformations.

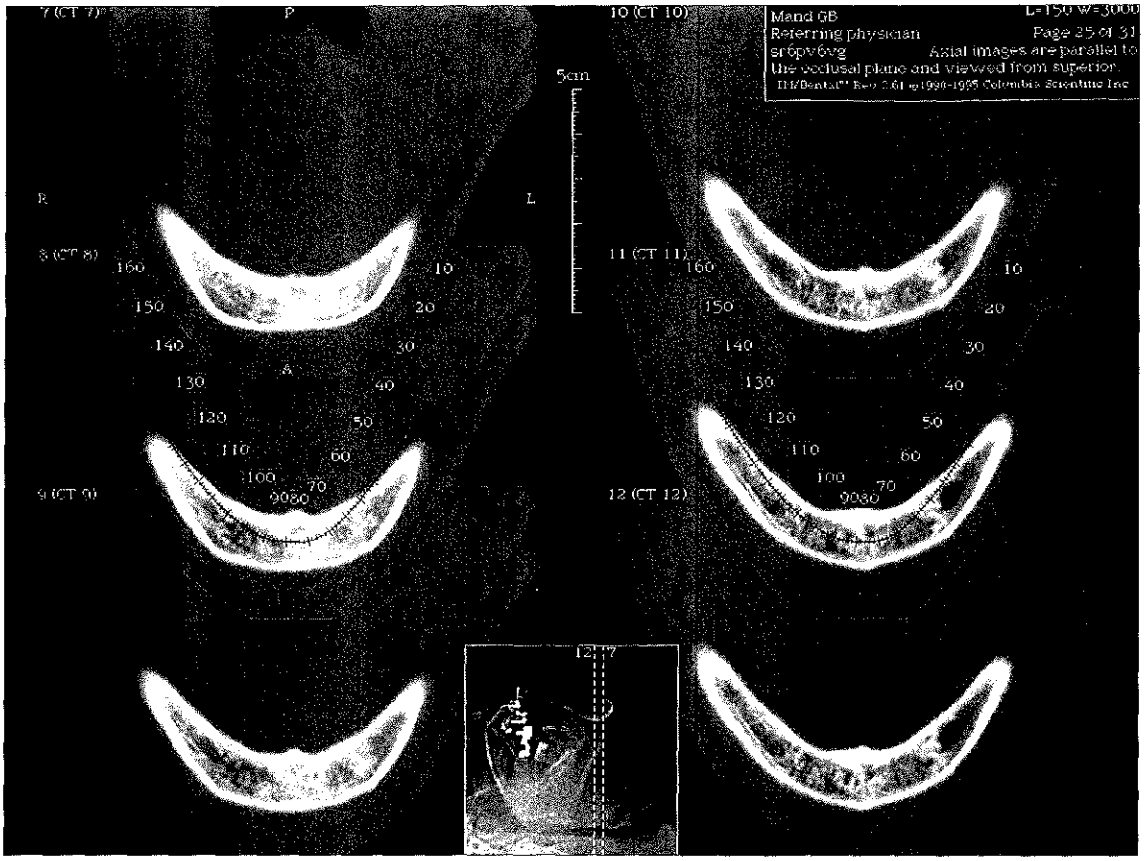


Fig 2-11 3D/Dental display format for mandibular axial views.

The axial images of the mandible have been inverted so that the observer is looking down on the mandible as the dentist would see it while looking down into the mouth (Fig 2-11). A minified digital radiograph indicates the position of the displayed axial slices. A single 5.0-cm ruler is included with each set of images. The patient's right is on the left side of the picture and is appropriately marked.

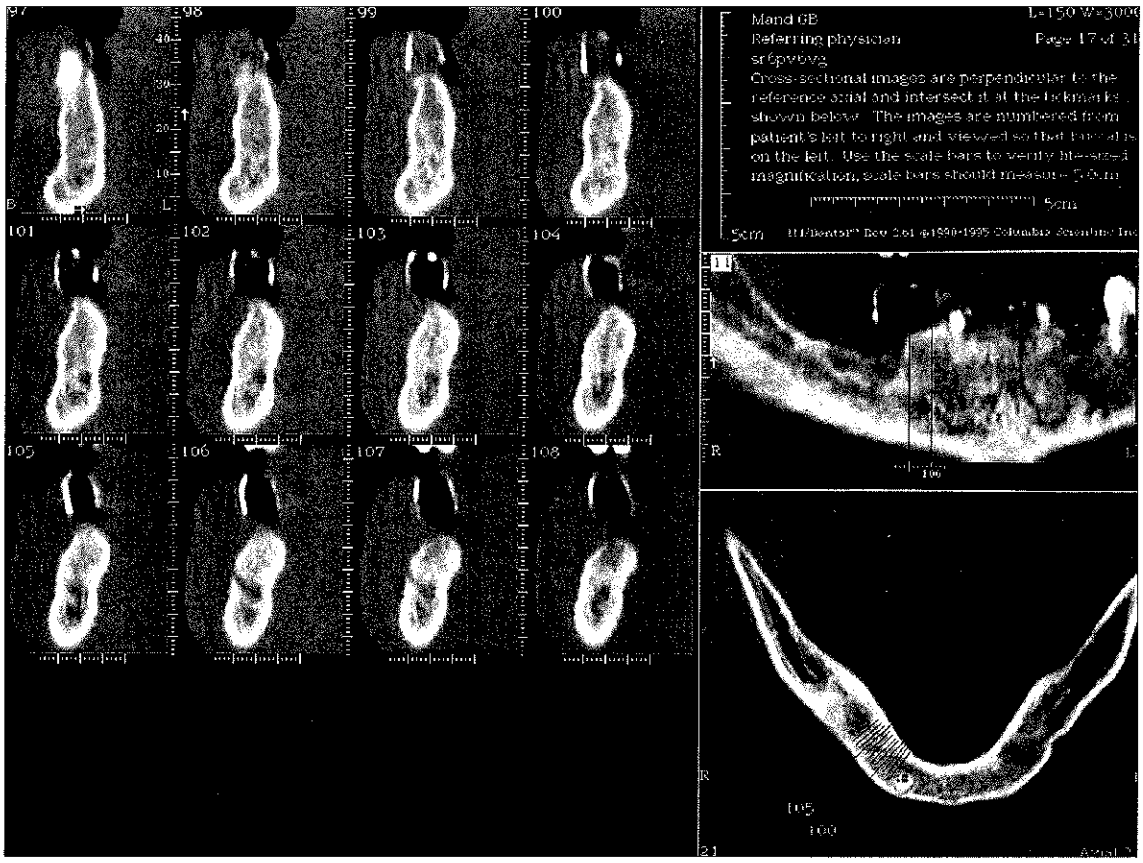


Fig 2-12 3D/Dental display format for cross-sectional oblique reformations.

The cross-sectional images are displayed sequentially (Fig 2-12). Panoramic and axial views have been affixed to the right side of each series of images with the position of the cross sections identified. Buccal and lingual markers are present as part of the upper left-hand image. The tick marks below each cross-sectional image correspond to the 20 panoramic reformations produced by this program.

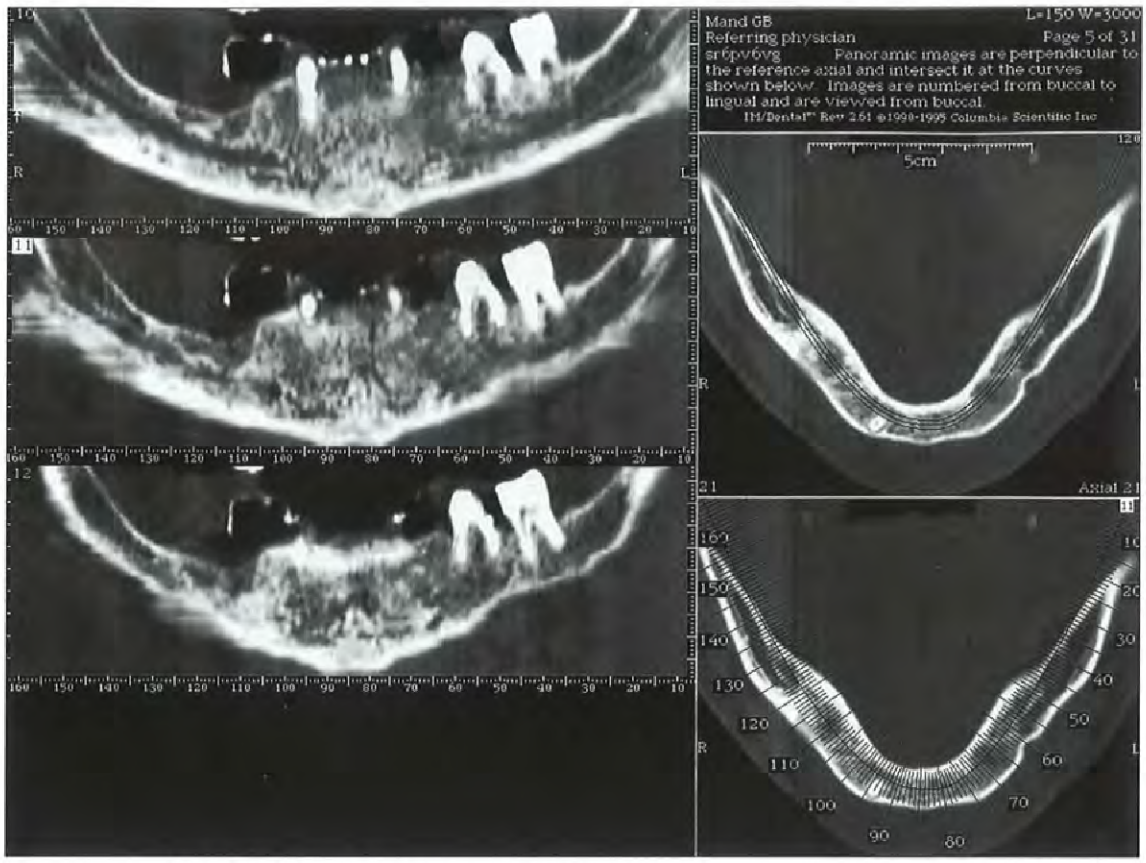


Fig 2-13 3D/Dental display format for panoramic reformations.

The panoramic views are displayed in sequence with an attached pair of axial views (Fig 2-13). The upper axial view indicates the position of the panoramic slices within the bone, and the lower indicates the position of the oblique cross sections.

The maxillary axial views are displayed as they are in the DentaScan examination. The observer is looking up into the maxilla as the dentist would look up into the mouth. Eight sequential views with an attached digital scout view are photographed as a unit (Fig 2-14).

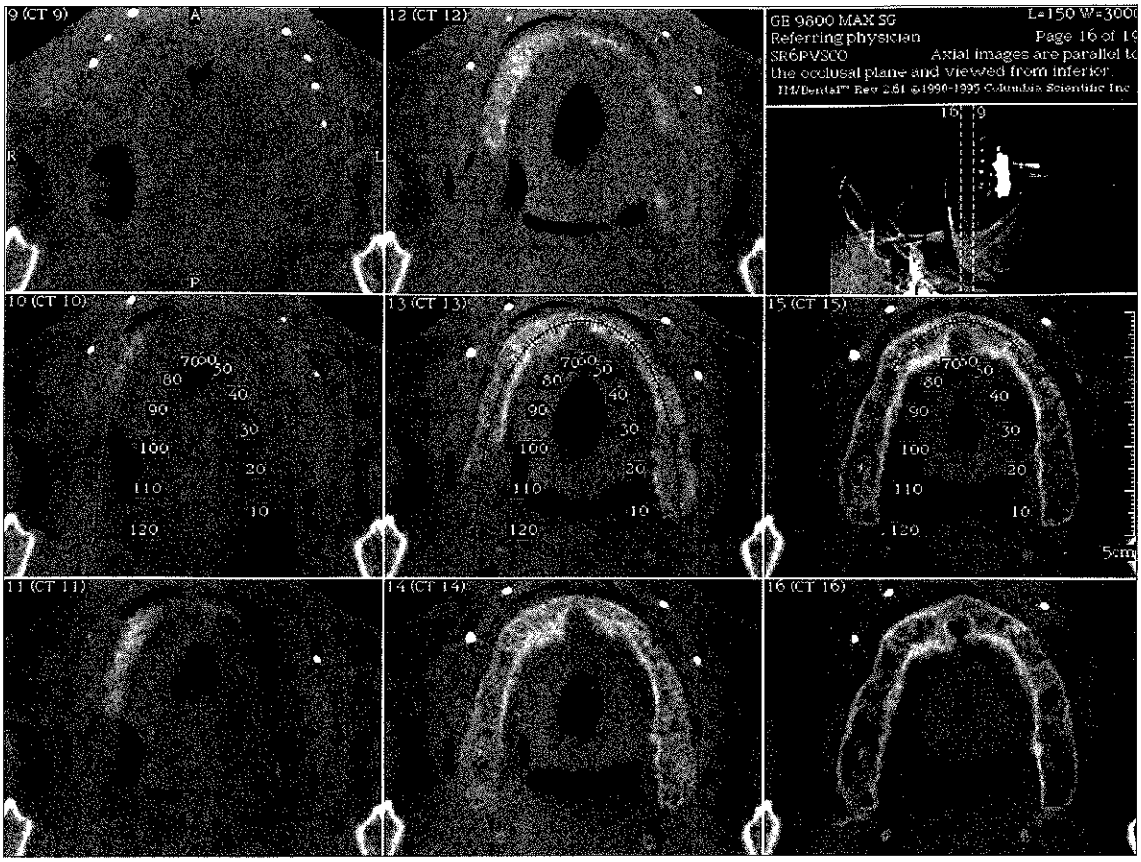


Fig 2-14 3D/Dental display format for maxillary axial views.

The 3D/Dental film format is designed to provide the maximum information in all three planes on the fewest number of films. For a partially edentulous patient, it is possible to include all of the critical information on a single film. This reduces the amount of time needed to make the preoperative measurements.

Allegro Workstation

The ISG technology Allegro Workstation is a high-end stand-alone image processing and display system. It is capable of producing a dental examination very similar to the two programs previously described. Axial views are oriented similar to those in the DentaScan program. A three-dimensional rendering of the jaw, rather than a digital radiograph, is used to localize the position of the axial scans. The axial views are minified, and rulers surround the image so that a magnification factor can be calculated (Figs 2-15a to 2-15c). There is little difference in the display of the cross-sectional oblique and panoramic views between this program and DentaScan.

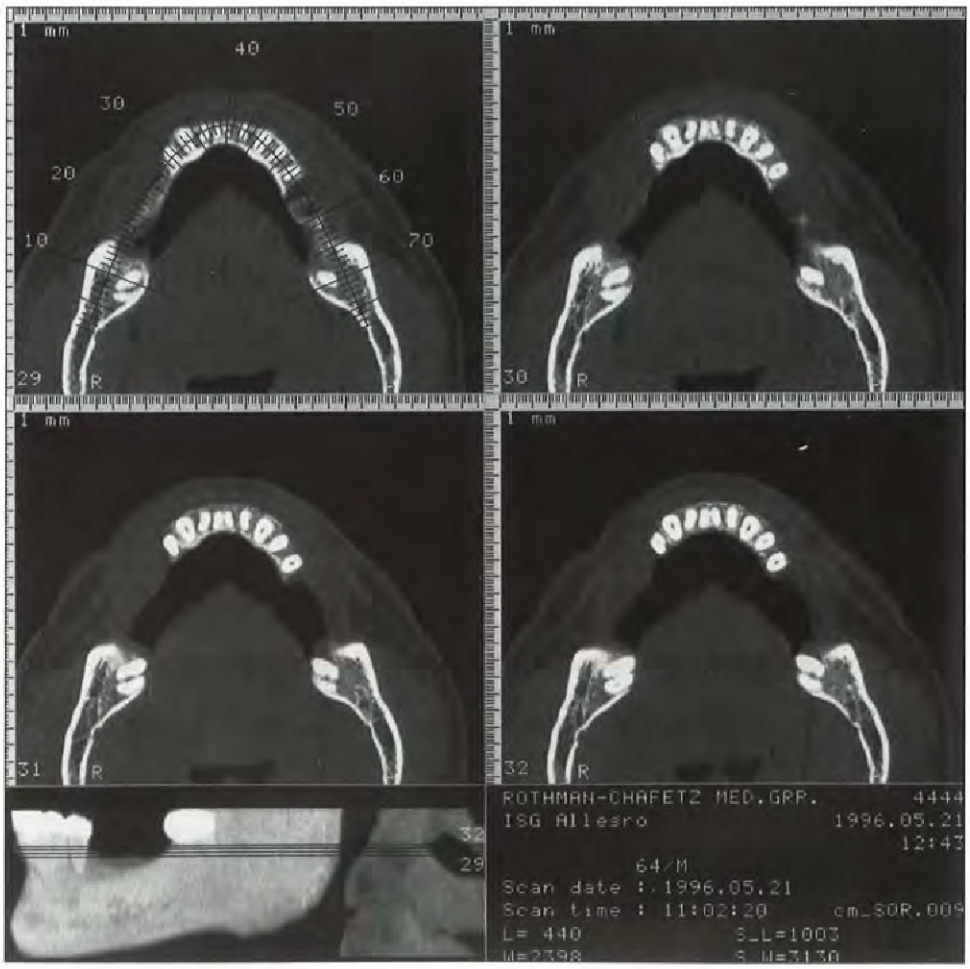


Fig 2-15a Allegro workstation display format for axial views.

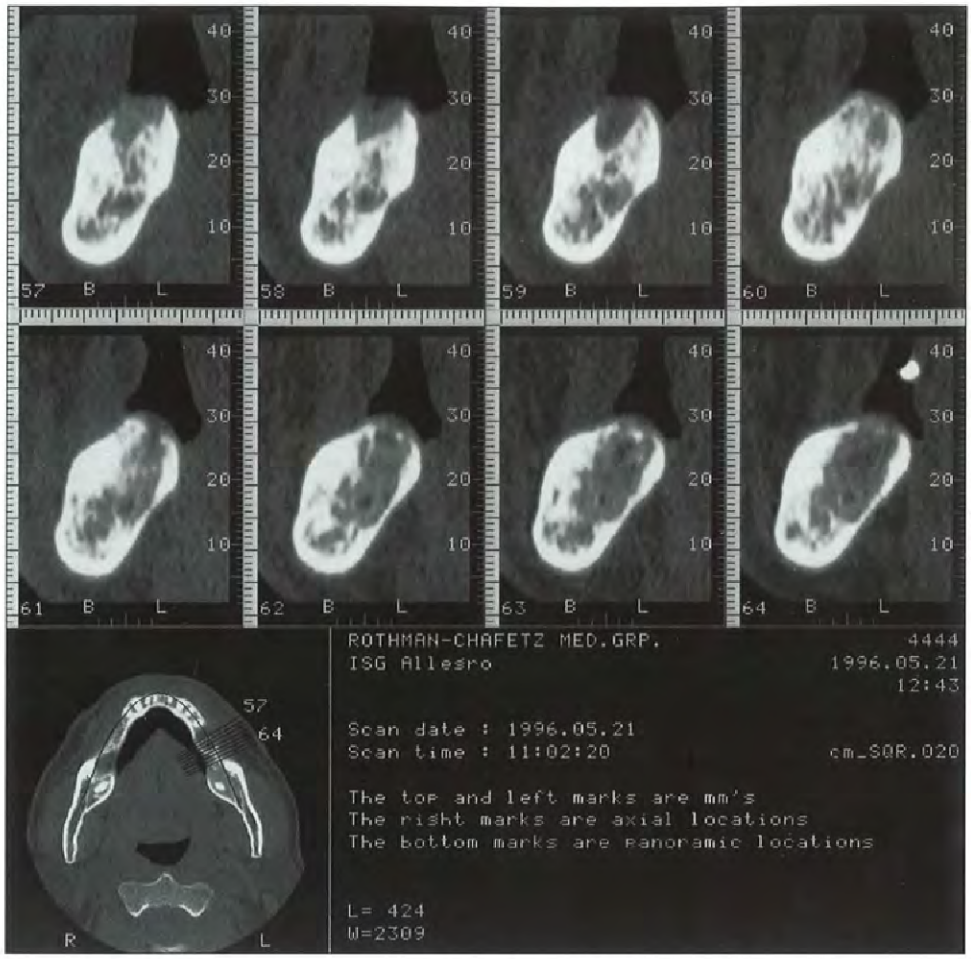


Fig 2-15b Allegro workstation display format for cross-sectional oblique reformations.

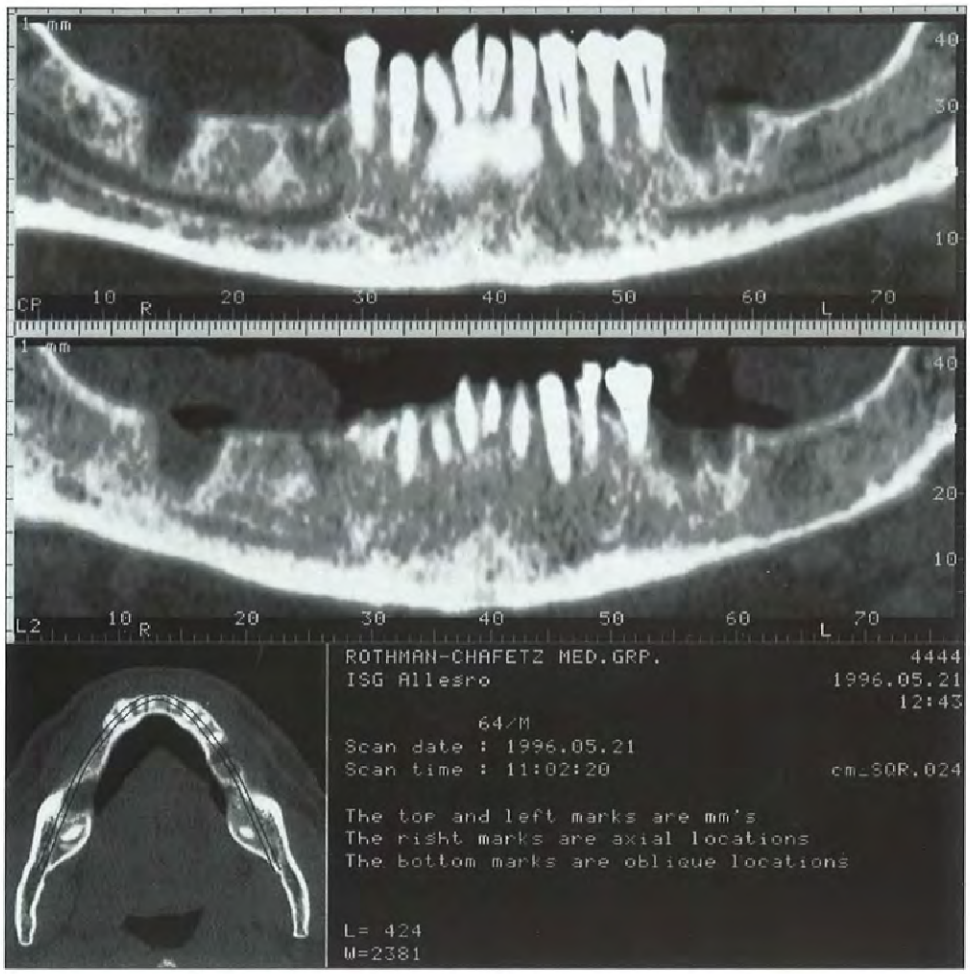


Fig 2-15c Allegro workstation display format for panoramic reformations.

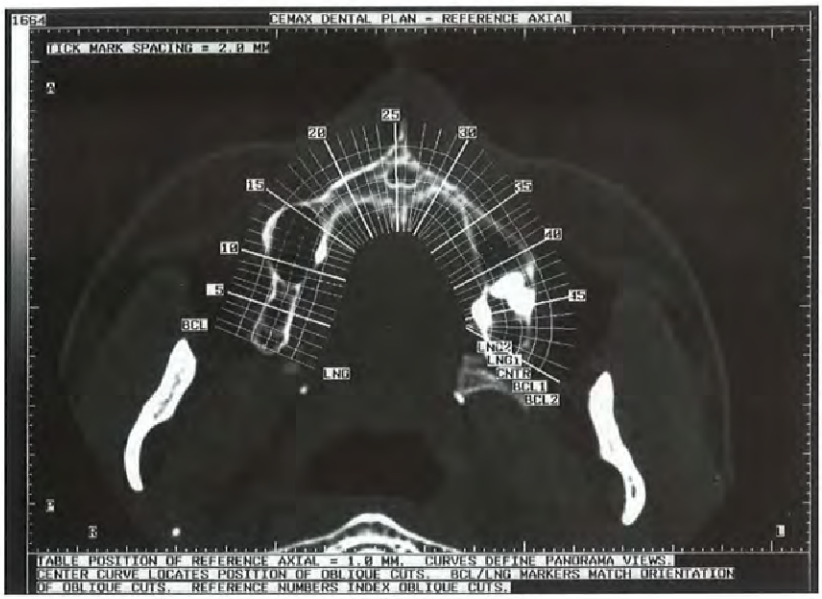


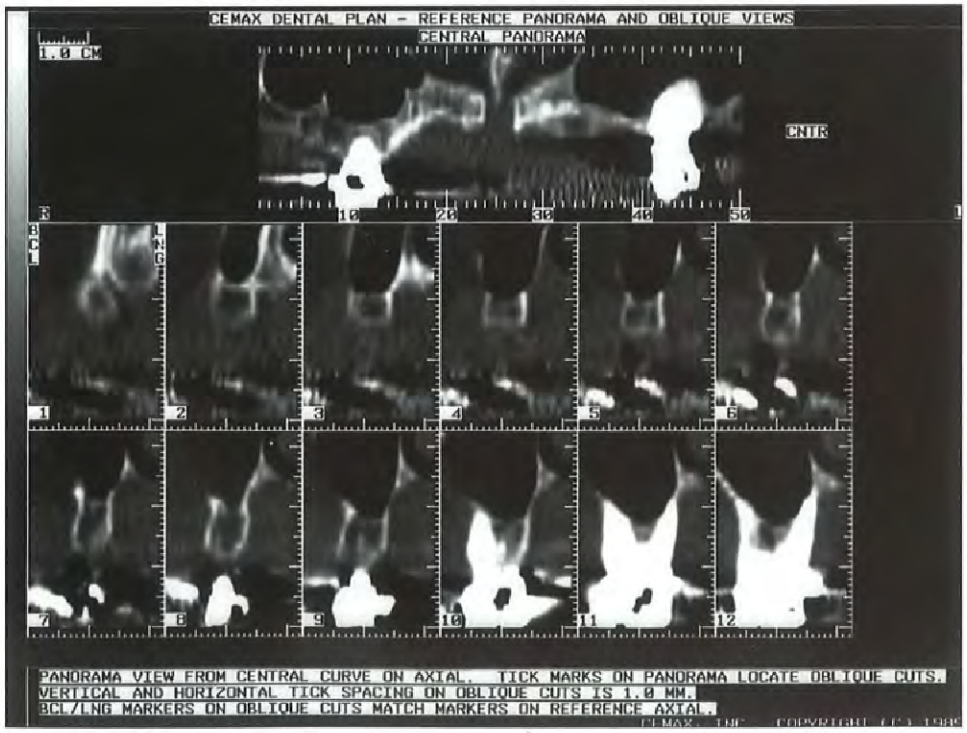
Fig 2-16 Allegro three-dimensional renderings of the mandible. The inferior alveolar nerve has been colored red. In one view *(upper right)*, the external surface of the bone has been rendered transparent, so that the nerve is visible within the bone. In another projection *(lower left)* the mandible is displayed from another angle, and the alveolar nerve canal is exposed.

The Allegro workstation is most outstanding for the three-dimensional renderings it performs. This and most workstations are capable of displaying an entire volume of data from a large number of angles. It therefore allows the operator to define the picture elements that make up the osseous structures. The jaw can be turned in space and viewed from any angle. The inferior alveolar nerve can be colored and displayed through the bone as if the bone were transparent. The program also allows the operator to dissect away layers of bone to visualize any deep structure (Fig 2-16).

The display formats of several other manufacturers are depicted in Figures 2-17a to 2-17c.

Figs 2-17a to 2-17c *Other reformation formats.*





Figs 2-17a and 2-17b Cemax dental plan formats.

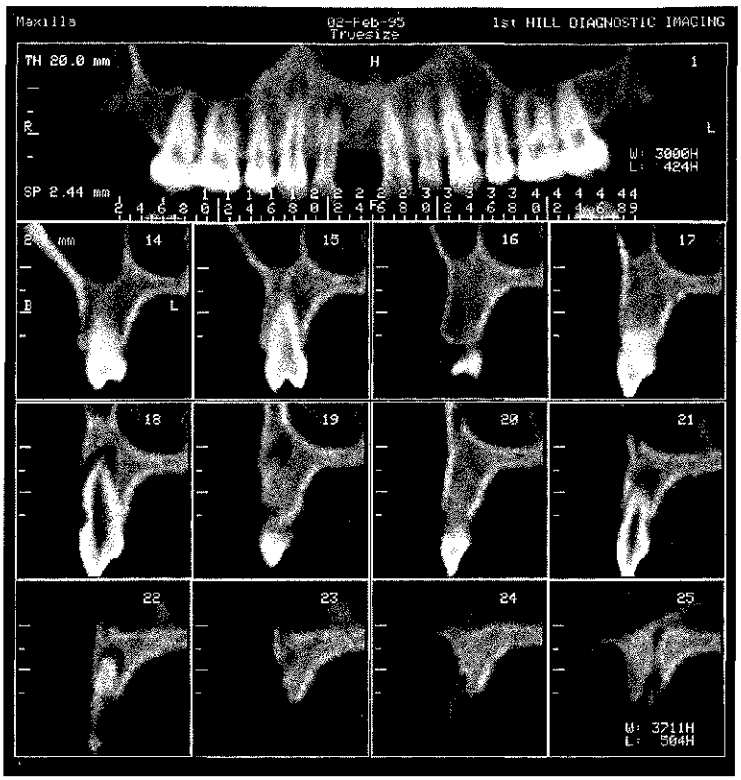


Fig 2-17c Dimensional Medicine formats (DMI).

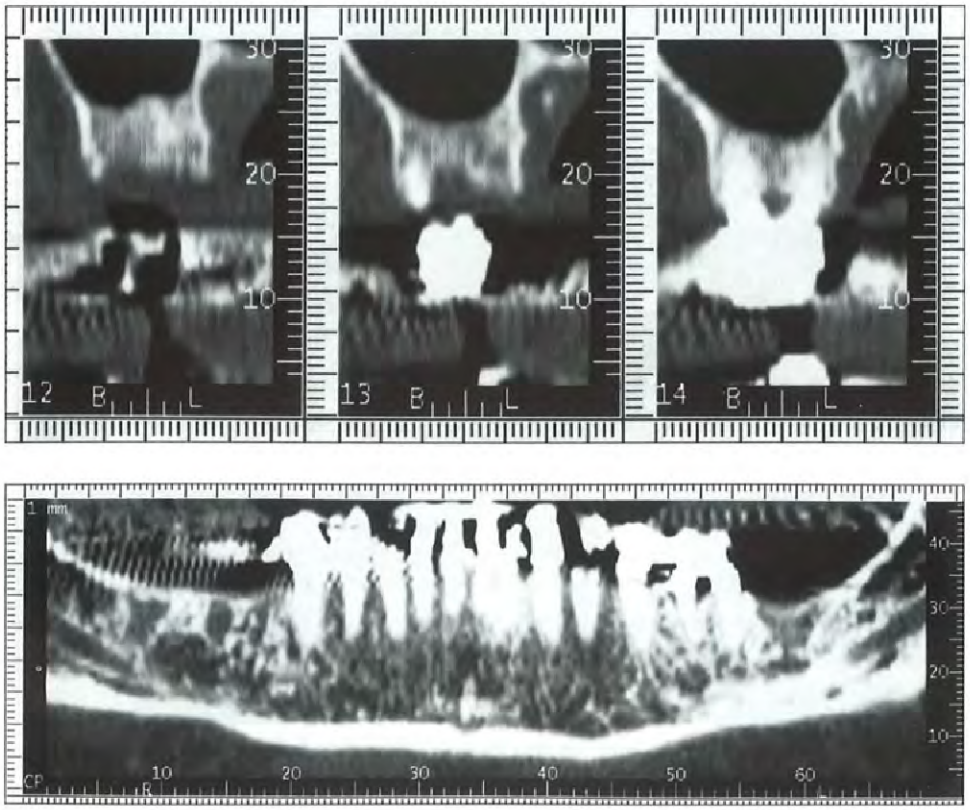
Artifacts

The most common artifacts of the dental examination are those caused by the presence of metal within the jaw or teeth and those resulting from patient motion. Direct coronal CT has already been shown to be degraded by restorations because the x-ray beam traverses the entire depth of the metal crown or restoration. This type of artifact also degrades the reformatted CT examination, but not nearly as much.

Proper positioning of the patient in the scanner projects crowns and restorations above the plane of the alveolar bone of the mandible and below the plane of the alveolar bone of the maxilla. This is because the edentulous areas typically atrophy and resorb. The axial scans superficial to the alveolar bone are degraded, while those through the bone are not. The reformatted images, therefore, project the artifact off the cortical bone of the alveolar ridge (Fig 2-18a to 2-18c). If the technologist positions the patient incorrectly, so that the head is tilted too much, the artifact from a restoration may project through the alveolar bone (Fig 2-18d). Only patients with metal pins implanted in the bone or other interosseous metal will show an artifact on properly positioned scans. The larger the number of pins, the more interosseous artifacts will be found.



Fig 2-18a Axial CT scan at a level where there are numerous restorations. Note the remarkable streak artifact. The anatomy is very distorted.



Figs 2-18b and 2-18c Reformatted cross-sectional oblique and panoramic views showing that the artifact projects well away from the alveolar bone.



Fig 2-18d Improperly angled CT scan with artifact projecting into the alveolar bone. (From Schwarz MS, Rothman SLG, Chavetz N, Rhodes M. Computed tomography in dental implantation surgery. Dent Clin North Am 1989;33:578. Reprinted with permission.)

The reformatted CT examination may not be oversensitive to metal artifacts, but it is extremely sensitive to the most minute patient motion. It is impossible to perform an adequate scan on patients with a tremor or another neurologic motor disorder. Speaking, swallowing, coughing, or sneezing will produce motion artifact. There are two types of motion artifact. Patients may move during the data acquisition of any axial scan. In that case, it is obvious that the data set is distorted because the axial scan looks blurry, as if it were double exposed (Fig 2-19). All other axial scans that do not contain motion are sharp.

Motion in the interval between axial scans does not distort the axial views. The cross-sectional oblique and panoramic reformations, however, will be distorted. The cortical edges become irregular at each point where there is motion between the slices (Fig 2-20). If the motion is very minor it may not interfere with measurement of the height of the alveolar bone. If, however, there is a large amount of motion, measurements should not be made from the films. Occasionally the motion artifacts will be on slices inferior to the inferior alveolar nerve canal. In those cases, measurements can be made because the bone in the surgical field is well depicted free of artifact.

On rare occasions, a black line will be seen on the reformations extending all the way through the image (Figs 2-21a and 2-21b). This represents drastically degraded data resulting from the total failure of one of the axial scans to process correctly. The axial scan will demonstrate bold streaks across the entire field of view, and no normal anatomic structures will be visible on the picture.



Fig 2-19 Axial CT scan of the mandible with obvious motion artifact. There appears to be a "double exposure."

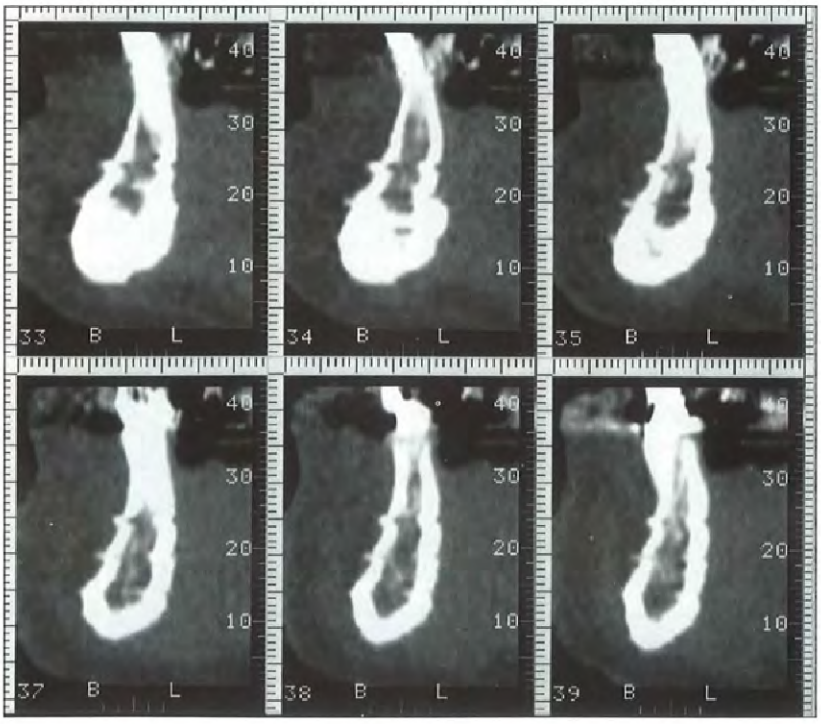
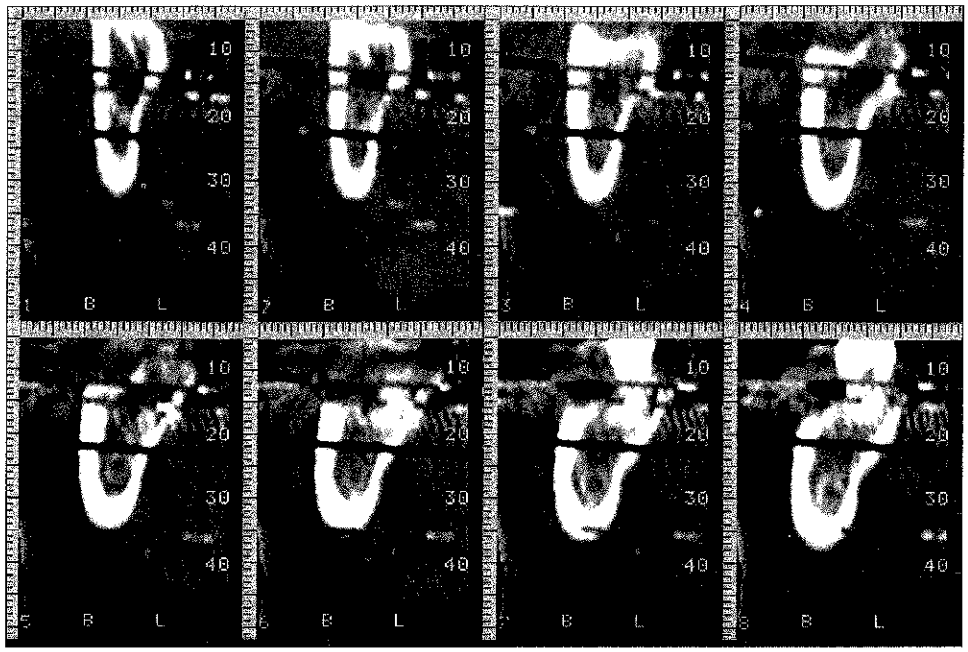
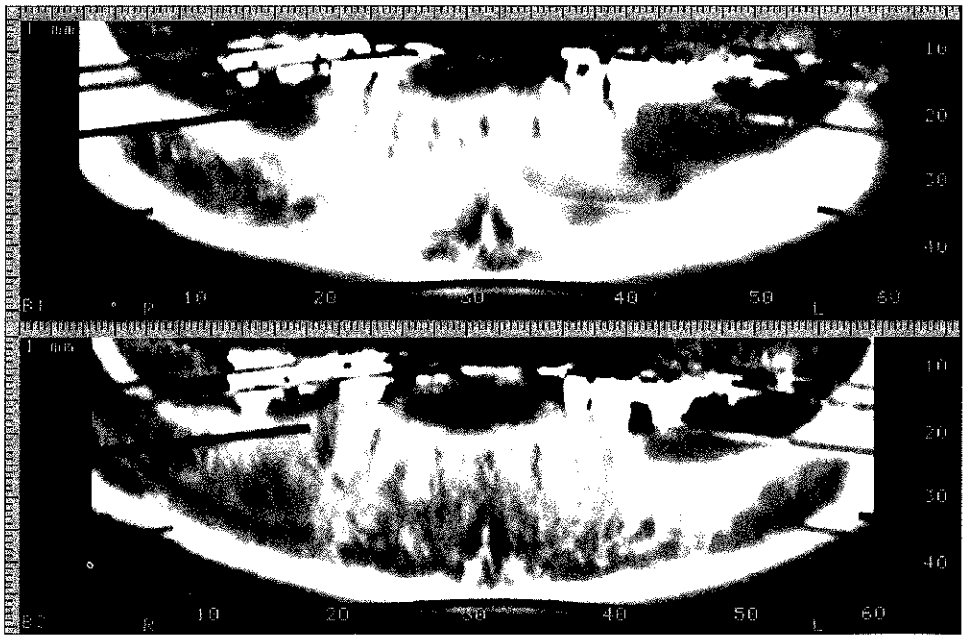


Fig 2-20 Cross-sectional oblique reformation revealing several motion artifacts. The apparent small linear projections of bone are artifacts caused by very slight patient motion.





Figs 2-21a and 2-21b Cross-sectional oblique and panoramic reformations showing an artifact resulting from the loss of data from three axial scans. There are areas of complete data dropout because of the failed axial slices. The study is still useful because the geometry of the scan is not distorted.

Intraoral stents

Many implant dentists find it difficult to locate the prospective implant site on the CT scan, particularly in completely edentulous bone. It is also helpful to know the location of the teeth to determine if the implants must be tilted so that the prosthesis parallels residual teeth. To solve these problems, it is possible to fabricate an acrylic resin intraoral stent to mark the location for optimal implant placement. A stent is prepared from an impression of the alveolar ridge and adjacent teeth area. Radiopaque markers, which will be visible on the CT scan, are placed in the stent.

Various types of markers have been used, including metallic balls and wires, barium-coated dentures, and gutta-percha.[14–17] Gutta-percha is moderately radiopaque, easy to handle, and found in most dental offices, where it is used for provisional restorations. It is, therefore, the optimal marker.

In a recent review, Borrow and Smith[14] described the appearance of the most commonly used opaque markers for dental CT. Metal balls, which are typically used for site localization in conventional radiographs and panoramic views, tend to produce the most artifact and therefore are least desirable for use with CT scans. Radiopaque tooth indicators are useful to allow a simulation of the final dentition to be displayed on the CT image.

Holes 1.0 to 2.0 mm in diameter are drilled in the stent along its gingival surface at the positions that would produce optimal fixture placement. These holes are packed with gutta-percha. This material is visible on the CT image but does not cause streak artifact. It is important that the gutta-percha be placed as closely as possible to the gingiva, to ensure that the CT examination will include the markers. If the holes are not totally filled with the gutta-percha they can still be identified, because the residual air within the holes acts as a negative contrast within the acrylic resin.

Figures 2-22a to 2-22c provide a good example of how markers in a stent aid in surgical planning. The three markers were placed in the stent in the positions determined to be optimal for supporting the necessary prosthesis. It is obvious from the scan that this will be a difficult case. The surgeon can evaluate these images and make measurements in the desired locations.

The stent can also be used as an interoperative guide for the localization of the implant site at surgery. The sterilized stent can be modified and the desired holes can be used as drill guides for the implants. Stents are accurate as markers only if they are properly positioned at the time of surgery. The patient needs to know how to insert the stent properly, and the technologist must verify that it is in position prior to beginning the scan.

Figs 2-22a to 2-22c *Mandibular scan taken with a stent in place.*

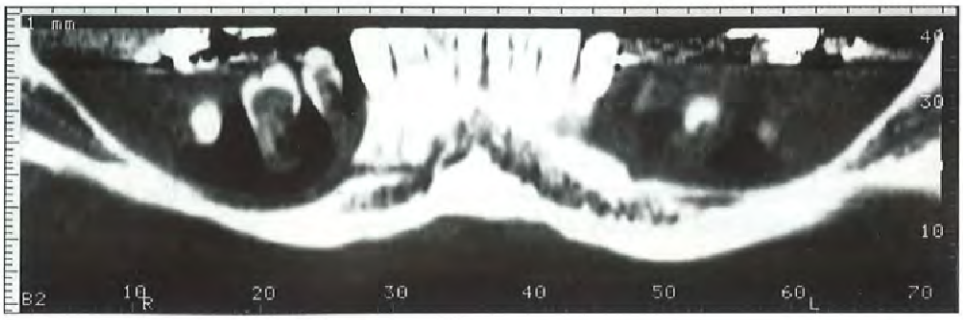


Fig 2-22a Panoramic reformation.

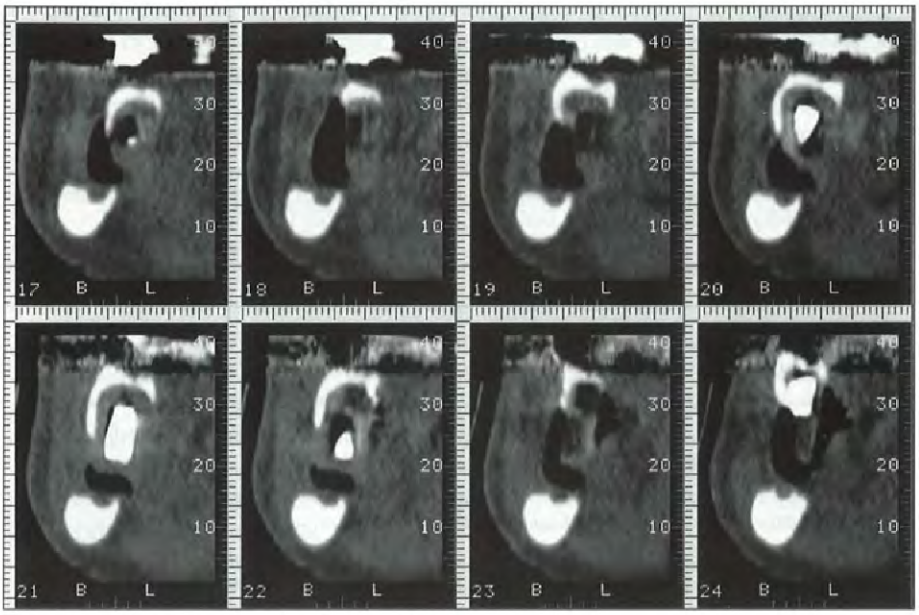


Fig 2-22b Cross-sectional oblique reformation.



Fig 2-22c 3D/Dental reformation of a partially edentulous mandible of a patient who was scanned with a mockup of the final prosthesis in place. Note the position of the opaque material *(blue)* above the markedly atrophic mandible.

Conclusion

As a matter of practicality, it should be assumed that the CT measurements are accurate to 1.0 mm. It is probable that in most patients the measurements are more accurate than that, but it is best to underestimate the available bone by 1.0 mm. Problems rarely are caused by underestimation of the thickness of bone. Overestimation of the bone height could lead to injury of the alveolar nerve.

References

1. Eisenberg RL. Radiology and Illustrated History. St Louis: Mosby-Year Book, 1992:467–471.
2. Hounsfield GN. Computerized transverse axial scanning (tomography). Part 1. Description of system. Br J Radiol 1973;46:1016–1022.
3. Cormack AM. Representation of a function by its line integrals with some radiological applications. J Appl Phys 1964;35:2908–2913.
4. Radon JH. Uber die Bestimmung von Funktionen durch ihre integralwerte langes gewisser Mannigfaltigkeiten. Berl Vehr Sachs Adad Wiss 1917;69:262–277.
5. Mass S, Norman D, Newton TH. Coronal computed tomography: indications and accuracy. AJR 1978;131:875–879.
6. Tadmor R, New PF. Computed tomography of the orbit with special emphasis on coronal sections. Normal anatomy. J Comput Assist Tomogr 1978;2:24–34.
7. Tadmor R, New PF. Computed tomography of the orbit with special emphasis on coronal sections. Pathological anatomy. J Comput Assist Tomogr 1978;2:35–44.
8. North AS, Rice J. Computed tomography in oral and maxillofacial surgery. J Oral Surg 1981;39:199–207.
9. Wishan M, Bahat O, Krane M. Computed tomography as an adjunct in dental implant surgery. Int J Periodont Rest Dent 1988;8(1):31–47.
10. McGivney GP, Haughton V, Strandt DT, et al. A comparison of computer assisted tomography and data-gathering modalities in periodontics. Int J Oral Maxillofac Implants 1986;1:55–68.
11. Quirynen M, Lamoral Y, Dekeyser C, et al. The CT scan standard reconstruction technique for reliable jaw bone volume determination. Int J Oral Maxillofac Implants 1990;5:384–389.
12. Rothman SLG, Glenn WV Jr. Multiplanar CT of the Spine. Baltimore, MD: Baltimore University Park Press, 1985.
13. Solnick M, Abrahams J, Faiella RA. A comparison of the accuracy of periapical, panoramic, and computerized tomographic radiographs in locating the mandibular canal. Int J Oral Maxillofac Implants 1994;9:455–446.
14. Borrow JW, Smith JP. Stent marker materials for computerized tomography–assisted implant planning. Int J Periodont Rest Dent 1996;16:61–67.
15. Abrahams JJ. Dental implants and multiplanar imaging of the jaw. In: Som PM, Curtin HD (eds). Head and Neck Imaging. St Louis: Mosby, 1996:362–363.
16. Israelson H, Plemons JM, Watkins P, Crysup S. Barium coated surgical stents and computer-assisted tomography in the preoperative assesment of dental implant patients. Int J Periodont Rest Dent 1992;12:53–61.
17. Schwarz MS, Stauts B. Fixture placement. Achieving acceptable aesthetics with implant anchored prostheses is becoming a more predictable procedure. CDA J 1987;45:45–50.

3 Computerized Tomography of the Mandible

Definition of Terms

Radiologists and dentists use different terms to describe anatomic structures. It is important for the radiologist to learn the dental lexicon. The fully dentate mandible contains 16 teeth. The teeth are numbered sequentially from the left posterior molar, tooth 17, across to the right posterior molar, tooth 32. The portion of the tooth extending above the bone is the crown, the portion within the bone is the root.

The tooth has five different surfaces. The biting surface of the tooth is called the *occlusal surface*. The outer surface of the incisors and canines, facing the cheek and lip, is termed the *labial surface*. The outer surface of the molars and premolars is the *buccal surface*. The inner surface, facing toward the tongue, is the *lingual surface*. The remaining surfaces face adjacent teeth; the surface projecting toward the midline is called the *mesial surface*, and that facing posteriorly is called the *distal surface*.

These same terms are used to describe direction. *Mesial* means anterior toward the midline; *distal* means posterior toward the ramus. The occlusal direction faces the opposing tooth; the *apical direction* faces the depth of the root socket.

The Edentulous Mandible

The edentulous mandible is not a static structure. Periodontal disease, which is the most common cause of tooth loss, produces local erosion about the diseased teeth. The pattern and extent of erosion and bone loss may change rapidly. When a tooth is removed, there is often very dramatic remodeling of the residual bone, with loss of alveolar height.[1] Definition of the contour and shape of the alveolar process is one of the most important aspects of dental computerized tomography (CT).

Definition of the internal structure of the bone is also very important to the implant dentist. The pattern of medullar trabeculation, the amount and position of marrow fat, and the position of the inferior alveolar neurovascular bundle are critical anatomic variables that must be considered in the preoperative evaluation of every patient who will undergo root-form dental implantation.

The pattern of ossification of the mandible is variable among patients. The relative amount of osseous tissue and fat is different from one patient to the next. It is even very variable within the same patient from side to side and from centimeter to centimeter. Because of this, it is very difficult to determine what "normal" ossification is. This is especially true in an analysis of the mineral content of the medullary bone. Rather than describe "normal" and "abnormal," this chapter will display the spectrum of variations within the mandible.

Currently it is possible to describe the medullary bone according to its ability to attenuate an x-ray beam. The more mineral present, the more x-rays are absorbed by a volume of bone. The CT attenuation number, as calculated by the scanner, is a representation of the amount of mineral within the bone. If a phantom of known calcium content is scanned concurrently with the patient, it is possible to compute the calcium content of the bone. An estimate of the calcium content of the bone can be made easily from the CT images just by looking at the film with an experienced eye. It is possible to grossly distinguish very osteoporotic bone from normally ossified bone.



Normal Anatomy of the Mandible

The mandible is made up of a curved body and two rami extending posteriorly to articulate with the base of the skull. Only the anatomy of the body is important to the implant surgeon, and therefore it alone will be described here. The base of the mandible can be thought of as the platform on which sits the alveolar process. The alveolar process is small at birth and expands with development of the dental alveoli. In the fully developed adult mandible, the height of the alveolar process is approximately the same as the height of the base. The grooves, ridges, and tubercles that make up the inner and outer surfaces of the bone form in response to the attached muscles, the neurovascular structures, the salivary glands, and the teeth.[2]

Internal surface of the mandible

The dominant feature of the internal surface of the mandible is the mylohyoid line, which is the origin of the mylohyoid muscle. The mylohyoid muscle separates the submandibular space from the sublingual space. Anteriorly, just above the mylohyoid muscle, there is a smooth area where the submandibular gland lies. Posteriorly, just below the line, is an indentation for the submandibular gland. The mandibular foramen, which lies near the center of the ramus, is the internal opening for the inferior alveolar nerve. This lies just inferior to the mylohyoid groove. There is an indentation in the internal surface made by the neurovascular bundle. The concavity is obvious on CT scans as an area of lucency. Rarely, though, this may appear unusually prominent.



Fig 3-1a Axial reformation.

Figs 3-1a and 3-1b *Mandibular tori. Symmetric densities project lingually from both sides of the mandibular archs.*

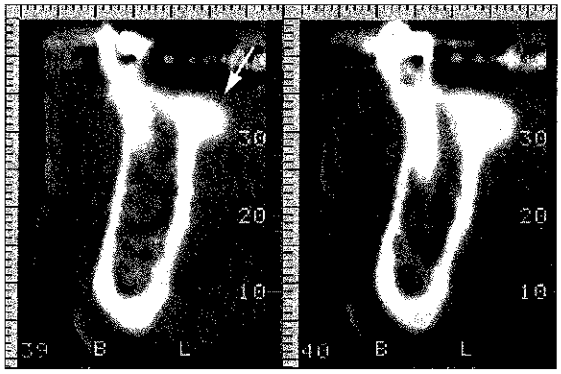


Fig 3-1b Cross-sectional oblique reformation.

Anteriorly, there are two pairs of spinelike projections of bone to which attach the genioglossus and the geniohyoid muscles. On occasion there is very prominent bony buildup along the inner surface of the bone; this is called *torus mandibulare*. It is generally of no consequence, although it is rather striking on CT scans (Figs 3-1a and 3-1b).

External surface of the mandible

The external surface of the mandible is marked anteriorly by the symphysis mentalis, which is a small ridge at the point of fusion of the two halves of the fetal mandible. The mental protuberance is the round forward projection of the mandibular base.

The mental foramen, through which exits the mental nerve, lies inferior to the second premolar tooth at a level near the center of the bone. It is the most important external landmark for the implant surgeon. The mental foramen should be visible on all mandibular CT scans. It appears as a crescentic lucency in the external cortex on the axial views, a forward-projecting opening on the coronal reformation, and a downward-projecting channel on the cross-sectional oblique images (Figs 3-2a to 3-2c). As the alveolar ridge atrophies, the mental foramen comes to lie more superiorly. In patients with severe atrophy, the mental foramen may actually lie on the superior surface of the bone (Figs 3-3a and 3-3b).

Figs 3-2a to 3-2c *Most common appearance of the mental foramen. The foramen opens posteriorly; consequently, the anterior wall of the foramen is more distinct than the posterior wall.*

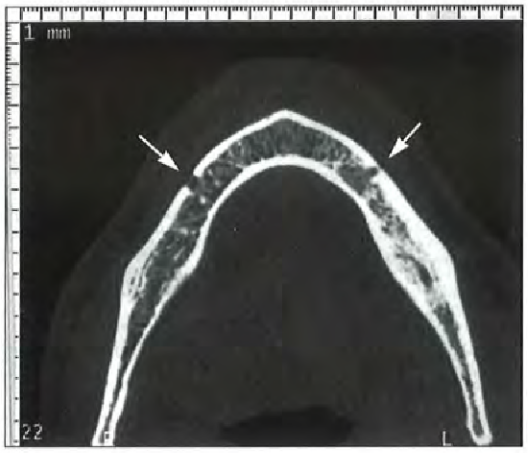


Fig 3-2a Axial reformation.

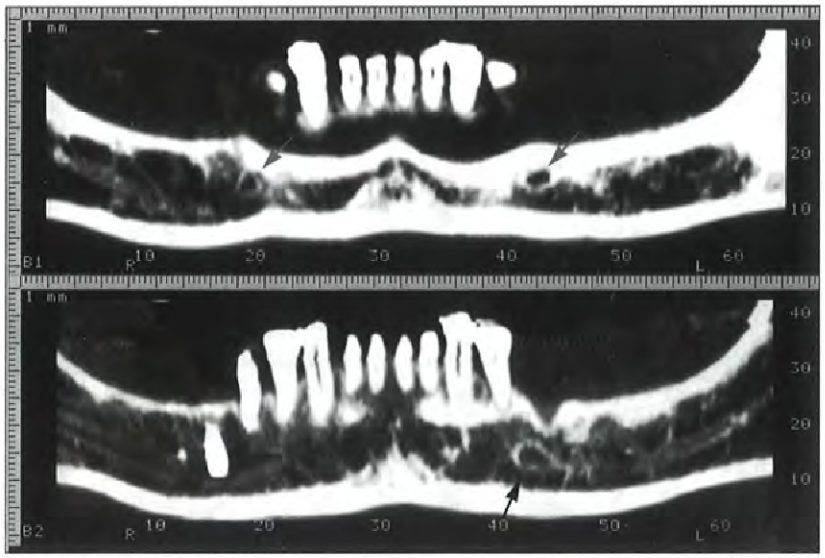


Fig 3-2b Panoramic reformation.

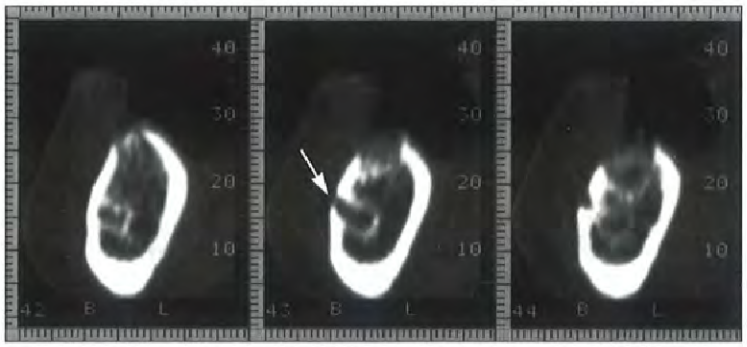


Fig 3-2c Cross-sectional oblique reformation.





Figs 3-3a and 3-3b Three-dimensional reformations demonstrating the position of the inferior alveolar nerve *(red)* along the superior surface of the mandible.

Inferior alveolar nerve and mandibular canal

The internal architecture of the mandible is quite variable. The lacy osseous framework is interspersed with fatty bone marrow.[3] The relative amount of fat increases with increasing age. The amount of bone and fat varies considerably within any mandible. It is important to define the relative amount of bone at a proposed implant site to determine the optimal time to leave the fixture at rest prior to attachment of the prosthesis.

Besides the teeth, there is little internal structure of importance other than the inferior alveolar neurovascular bundle and the surrounding canal. The inferior alveolar nerve is the main sensory nerve for the lower third of the face. It descends through the mandibular foramen into the mandibular canal, where it gives off branches to the roots of the teeth. It terminates near the mental foramen, where it divides into the mental nerve, which is the sensory nerve to the chin and lower face, and the incisive branch, which innervates the anterior teeth (Fig 3-4). There may be several small branches to the teeth, lying in separate small bony channels. Small accessory dental nerves arise within the adjacent muscles and penetrate the mandible to join the internal neural plexus. From the perspective of the implant surgeon, the dental branches are of little importance. Only the main trunk of the nerve is important, because if it is invaded by an implant the lower face will become numb.

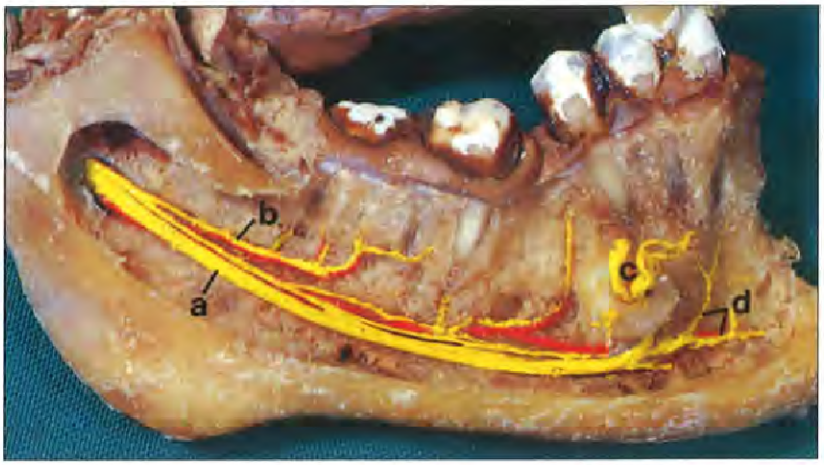


Fig 3-4 Mandible of a 57-year-old man, viewed from the right side, with the mandibular canal opened and the periosteal sheath removed. a = Inferior alveolar nerve; b = dentogingival nerve; c = mental nerve; d = incisor (anterior inferior alveolar) nerve. (From van der Zypen.[1] Reprinted with permission.)

The neurovascular bundle forms early in fetal development. It is present prior to chondrification or ossification of the mandible.[2] The mandible forms around the neurovascular bundle, completely encapsulating it. The nerve is covered by a periosteal sheath that, in well-mineralized bones, is associated with a rim of bone. The inferior alveolar canal is visible on most CT scans. Its identification is critical for the evaluation of the implant patient.

The course of the inferior alveolar nerve is constant, although its position within the mandible is somewhat variable. In the completely dentulous mandible, the nerve lies just inferior to the roots of the teeth. A branch emanates from the neural plexus to innervate the root of each tooth. The buccolingual position of the canal is variable. It enters the bone along the buccal surface at the mandibular foramen and exits on the labial surface at the mental foramen. The nerve is therefore more lingual in the distal portion of the bone and more labial in the anterior portion. Through much of its course it can lie near the center of the bone and cause difficulty for the implant surgeon (Figs 3-5a to 3-5c).

The downward-sloping curve of the inferior alveolar nerve is very constant. The angle of the hyperbolic sweep will vary only slightly, depending on the shape of the mandible, but the overall sweep of the mandibular canal is constant. It would be extremely unlikely for the canal to undulate in the superior-to-inferior plane. As the nerve extends anteriorly, it will always descend slightly relative to the roots of the teeth for the first several centimeters. It then remains nearly flat for some distance and begins to ascend again toward its final bifurcation, which lies just mesial to the mental foramen.

The inferior alveolar nerve *always* extends more mesially than does the mental foramen (Figs 3-6a and 3-6b). At its most anterior point, the

Figs 3-5a to 3-5c *Variations in position of the inferior alveolar nerve.*

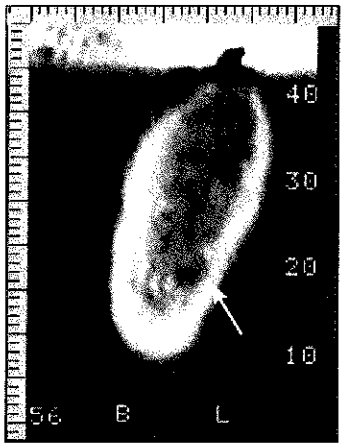


Fig 3-5a The proximal cross section shows the nerve to lie adjacent to the lingual cortex.

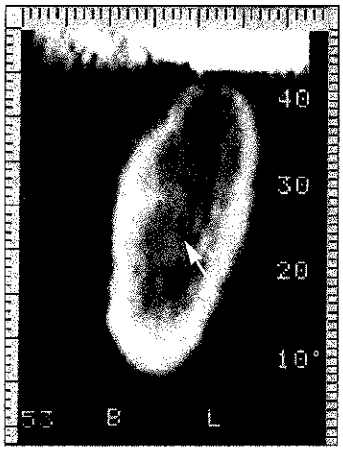


Fig 3-5b On the cross section near the midportion of the canal, the nerve lies near the middle of the bone.



Fig 3-5c At the mesial end of the canal, near the mental foramen, the nerve is on the labial side.

nerve divides into the mental nerve, which curves back on itself and sweeps upward and toward its labial exit at the mental foramen. The terminal branch continues in one or more very small bony canals to provide sensory branches to the roots of the anterior teeth. These bony canals can be identified on the CT scans.

The anterior portion of the nerve forms a genu from inferior to superior. The length of the genu varies considerably. It is generally thought to extend approximately 3 mm forward of the mental foramen, but in some patients the main trunk of the nerve has been found to project a full 1 cm beyond the foramen. Recognition of this anatomic variation is very important in the anteriorly edentulous patient. The diagnosis is most easily made on the panoramic reformations, where it is possible to see most of the curve on a single image (Figs 3-7a and 3-7b).

The presence of a long genu is also confirmed of the cross-sectional oblique reformations. Because, in effect, there are two mandibular canal cross sections present in the bone in this location, the lower coursing forward and the upper backward, there will be a "figure 8" appearance within the bone (Fig 3-8a). If the oblique cross section fortuitously falls at the tip of the curve, the canal will have an elongated appearance (Fig 3-8b). Cross sections mesial to the genu will generally demonstrate a bony channel for the dental branches to the anterior teeth that is considerably narrower in diameter than the mandibular canal (Figs 3-8c and 8-d).

The implant surgeon will, under normal circumstances, expect to use the mental foramen as a surgical landmark. The closest implant will usually be placed several millimeters mesial to the foramen. If there is a forward-projecting genu, there is greater likelihood that the nerve will be injured by the implant.

Figs 3-6a and 3-6b *Course of the inferior alveolar nerve.*

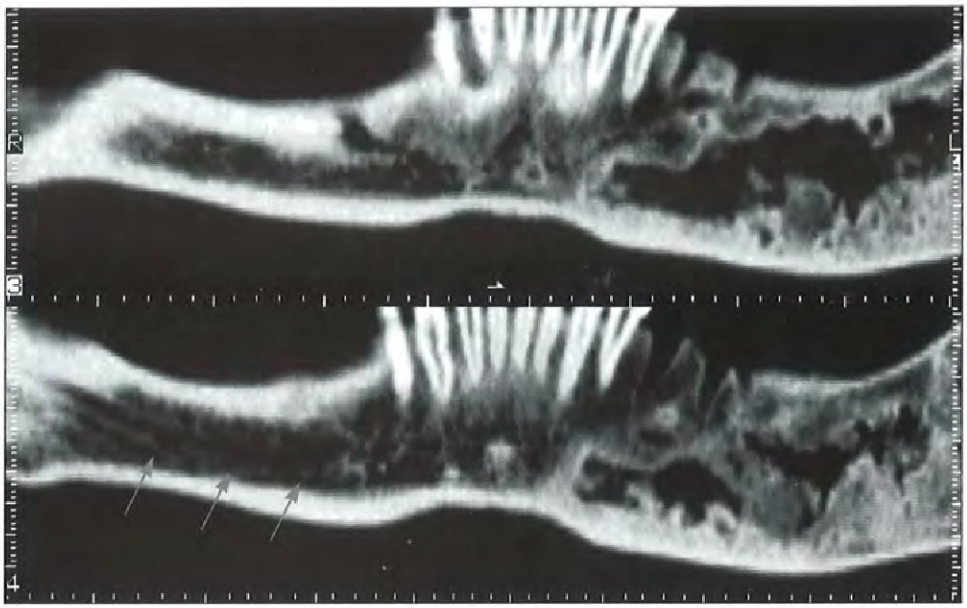


Fig 3-6a Panoramic reformation along a plane demonstrating the mandibular canal. On the right, the anterior genu extends anterior to the mental foramen. Fibrous dysplasia can be seen on the left.

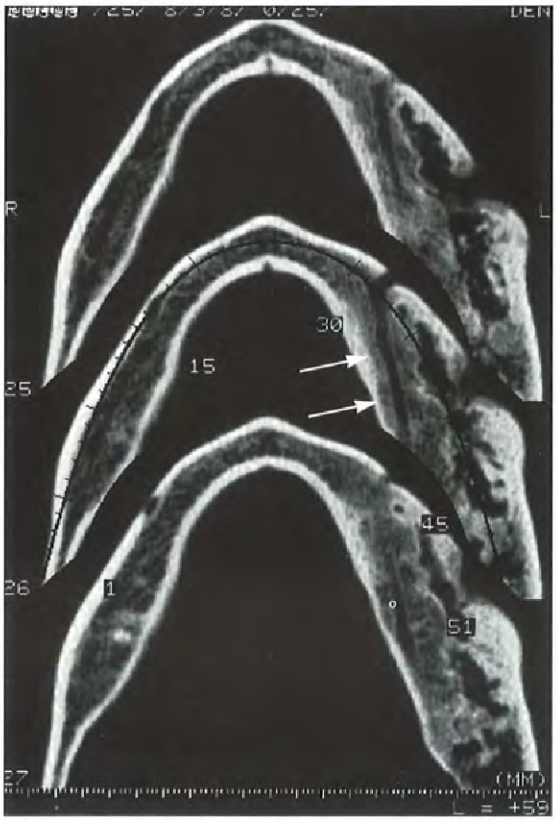


Fig 3-6b Because of the increased density within the bone, the nerve canal is unusually clear on the axial image.

Figs 3-7a and 3-7b *Variations of the genu of the inferior alveolar nerve. (From Schwarz MS, Rothman SLG, Chavetz N, Rhodes M. Computed tomography in dental implantation surgery. Dent Clin North Am 1989;33:566. Reprinted with permission.)*

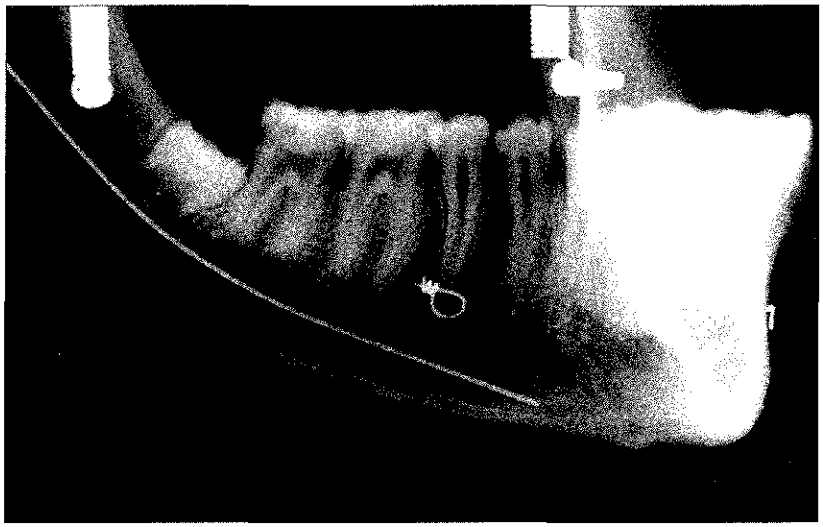


Fig 3-7a Radiograph of a mandibular specimen with a wire within the mandibular canal and a circular marker indicating the position of the mental foramen. The wire projects well forward of the mental foramen.

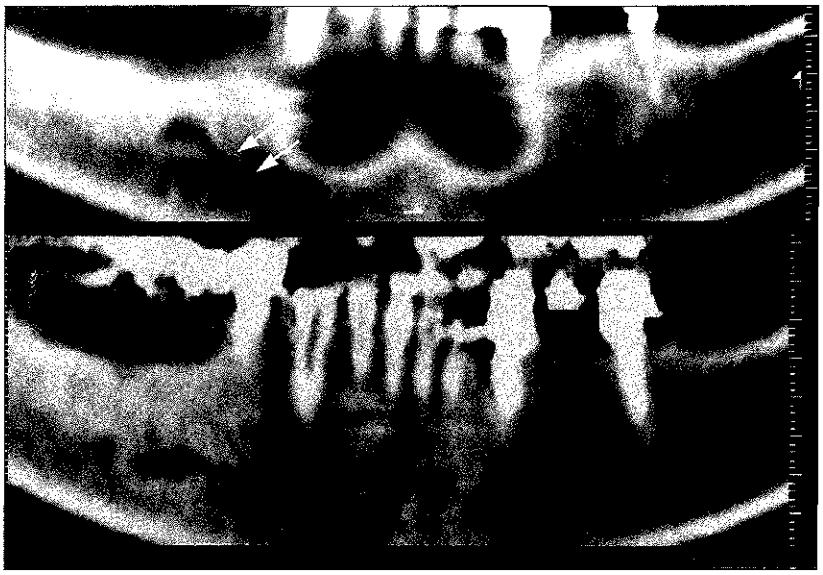


Fig 3-7b Reformatted panoramic image of a patient whose genu extends more than 1 cm forward of the mental foramen.

Figs 3-8a to 3-8d *Genu of the inferior alveolar nerve.*

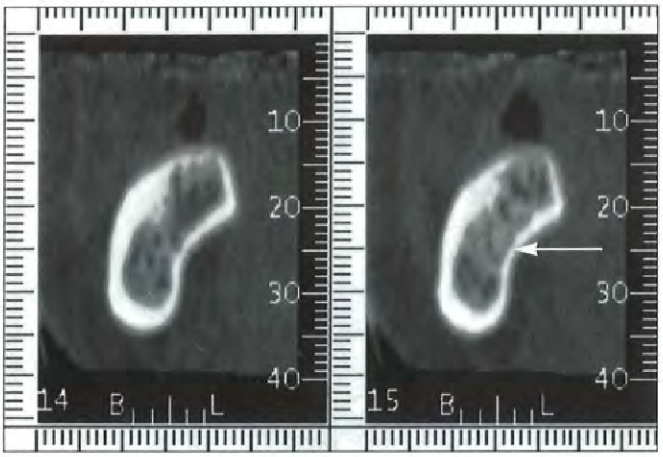


Fig 3-8a Cross-sectional oblique view of a "figure 8" caused by a long genu. The inferior bony circle contains the proximal portion of the nerve and the superior circle contains the distal portion of the nerve.

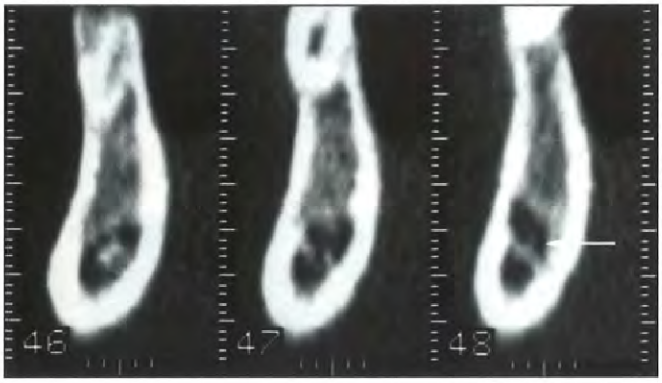


Fig 3-8b Crescentic appearance of the canal at the tip of the genu.

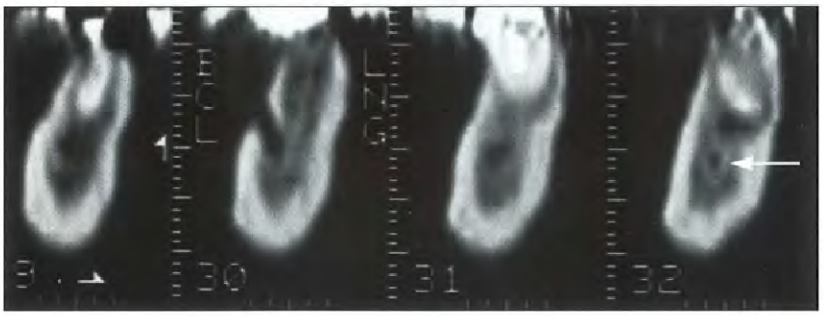


Fig 3-8c Cross section mesial to the genu demonstrating the terminal dental branch in its narrow bony canal.



Fig 3-8d Panoramic view demonstrating medial projection of the dental branch from the alveolar nerve.

Computerized Tomography Evaluation of the Mandible

Assessment of anatomic parameters

Five anatomic parameters must be assessed when the mandible is evaluated for dental implants:

1. The height of the alveolar bone
2. The buccolingual dimension of the ridge at the implant site
3. The contour of the ridge
4. The relative amount of bone and fat at the implant site
5. The position of the inferior alveolar nerve

Height of alveolar bone

The edentulous mandible will demonstrate generalized loss of height of the alveolar ridge because of diffuse atrophy of the bone. It may also show localized bone loss at any extraction sites. Periodontal disease can cause asymmetric destruction and remarkable localized destruction. All these components combine to produce a shrunken and deformed alveolar ridge (Figs 3-9a to 3-9c).

Once the optimal implant sites have been chosen by the implant dentist, the height of the alveolar bone is measured on the cross-sectional oblique CT image from occlusal surface to the internal edge of the inferior cortex. Measurements can be confirmed on the appropriate panoramic view. In completely edentulous patients, an attempt is made to place from four to six implants in the zone between the mental foramina. The implants can be long and can be sunk into the cortical bone inferiorly (Figs 3-10a and 3-10b). There is no worry about injuring the inferior alveolar nerve except near the mental foramen, where it typically courses forward of the mental foramen.

In partially edentulous patients who require implants near, or posterior to, the mental foramen, the measurement must be made from the occlusal surface to the superior edge of the alveolar canal (Fig 3-10c). If the occlusal surface is deformed or unusually thin and tapered, the measurement is made from a point below the occlusal surface where the width of the ridge is capable of supporting an implant (Fig 3-10d).

Figs 3-9a to 3-9c *Atrophy of the alveolar ridge.*

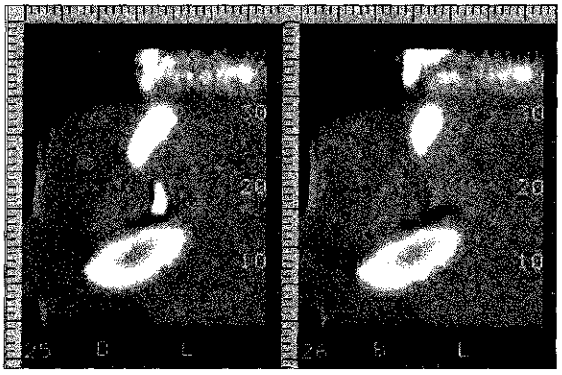


Fig 3-9a Diffuse atrophy with loss of height of the alveolar process. Cross-sectional oblique reformations reveal profound symmetric bone loss.

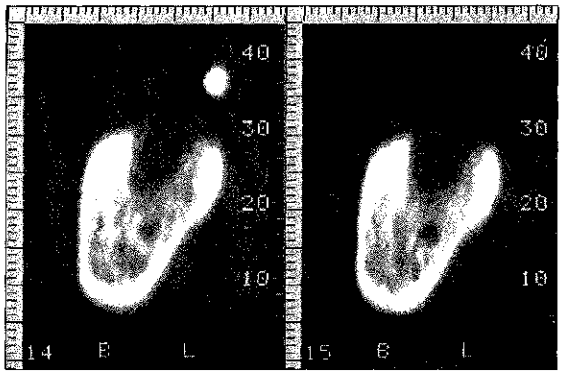


Fig 3-9b Cross-sectional oblique reformations demonstrating prominent residual extraction sockets. A tapering, craterlike deformity is found where teeth have been removed.

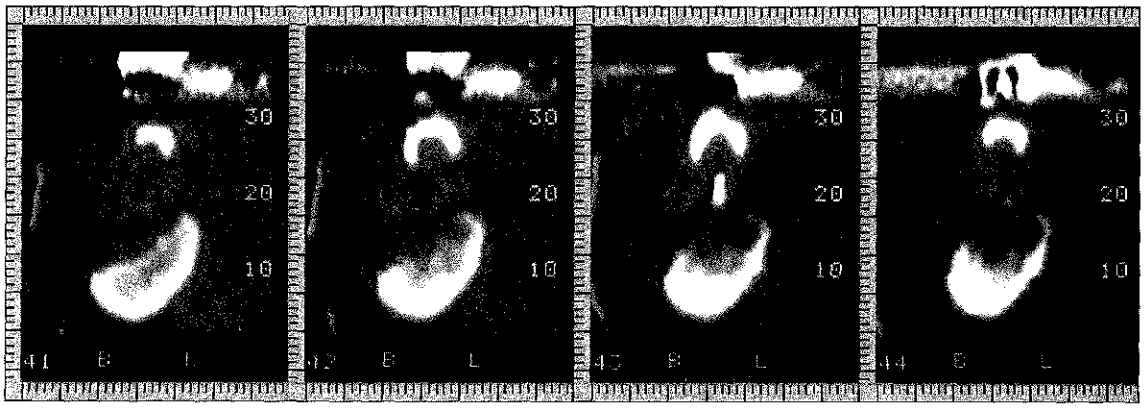
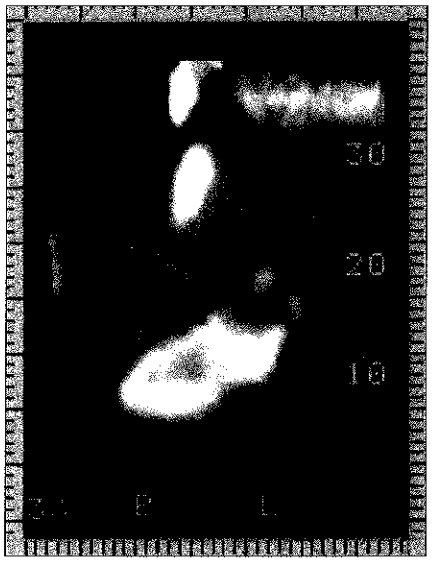
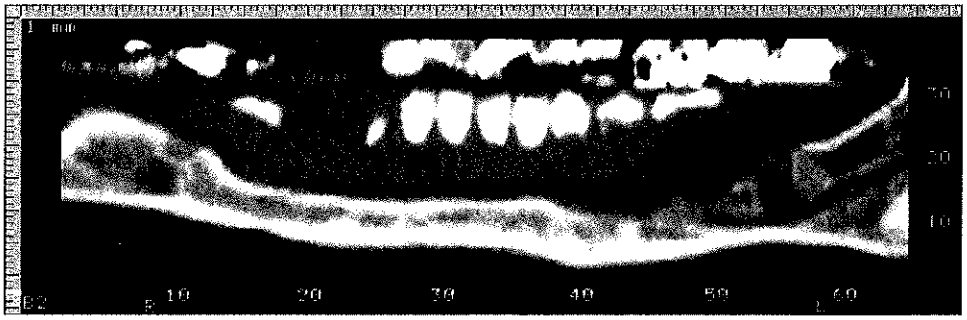


Fig 3-9c Localized bone destruction caused by extensive localized bone loss.

Figs 3-10a to 3-10d *Measurement of alveolar height.*



Figs 3-10a and 3-10b In the anterior edentulous area, measurements are made from cortex to cortex (8 mm).



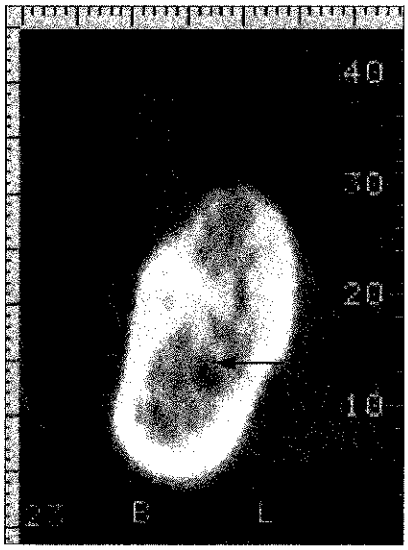


Fig 3-10c In the posterior edentulous area, the measurements are made from the occlusal surface to the inferior alveolar canal (16 mm) and, if appropriate, also to the cortical bone below.

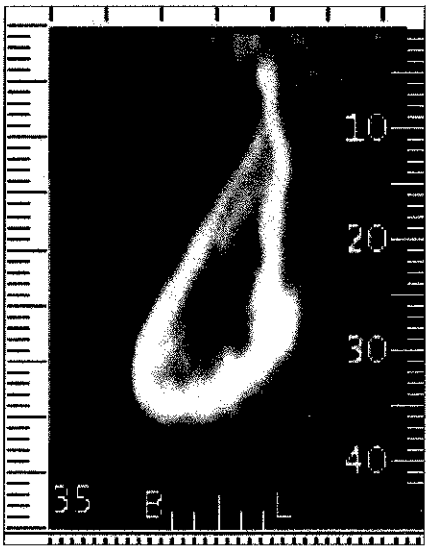


Fig 3-10d In the tapered alveolar ridge, the width is first measured. The height is calculated from a point inferior to the occlusal surface where the ridge is wide enough to accommodate a fixture (20 mm).

Buccolingual dimension of the ridge

The buccolingual dimension is measured on the cross-sectional oblique images. There is no way of confirming this measurement on the panoramic views, but it can be confirmed by measuring the internal dimension on the appropriate axial view. This is accomplished by identifying the height of the axial slice by counting tick marks from the bottom of the image to the level where the buccolingual width was measured. That axial scan is identified, and the location of the cross-sectional oblique image that was used as a reference is identified from the locator curve. The width of the ridge can be measured at this location (Figs 3-11a and 3-11b).

Even patients who appear to have adequate height to their alveolar processes may have profound buccolingual atrophy. The bone may be symmetrically atrophied and the ridge thin and knifelike. This is especially true in the anterior mandible and maxilla (Fig 3-12). Asymmetric loss of the labial bone is also very common in the anterior mandible. Usually the labial cortex is lost to periodontal disease and the medullary bone atrophies. Only the lingual cortex may remain. Implantation may not be possible in such patients.

Figs 3-11a and 3-11b *Measurement of alveolar width.*

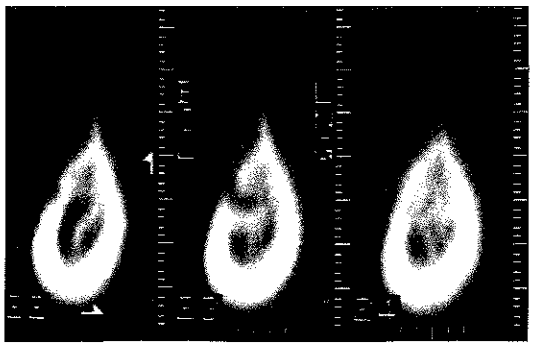


Fig 3-11a Cross-sectional reformation 23 extends through the mental foramen. The width of the ridge at the level of tick mark 16 is 6 mm.

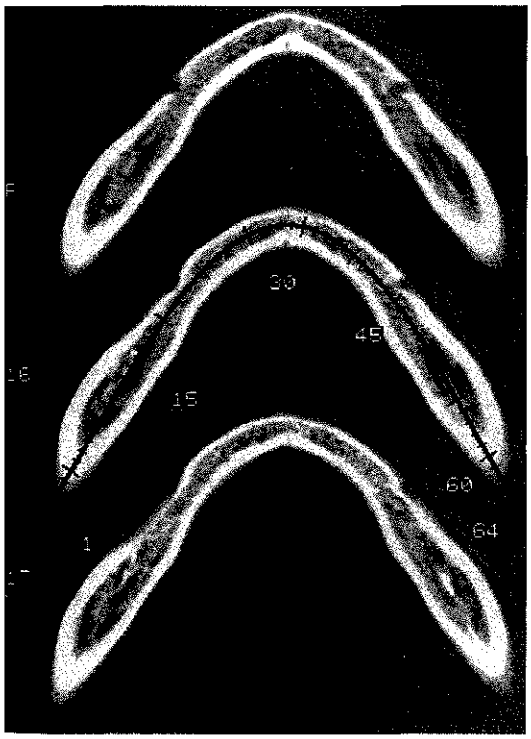


Fig 3-11b In axial view 16, the width of the alveolar ridge is confirmed by measuring the intercortical distance at the site of cross section 23.

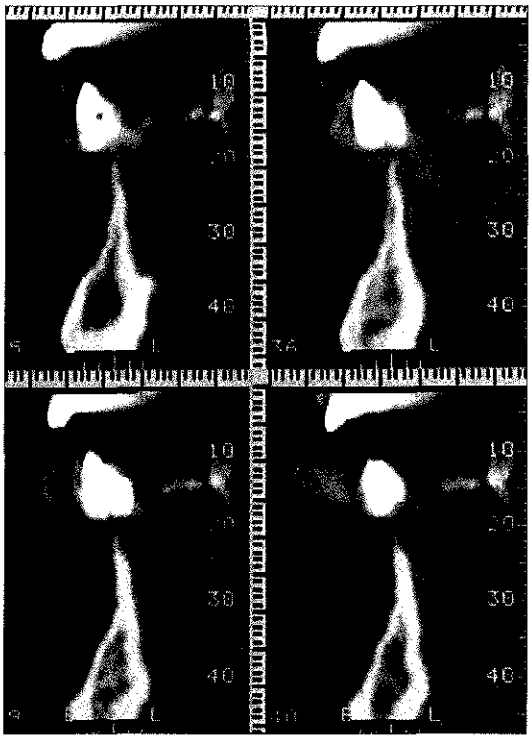


Fig 3-12 Buccolingual atrophy. Cross-sectional oblique reformations demonstrate remarkable symmetric atrophy of the alveolar ridge with a tapered, knifelike edge.

Contour of the ridge

In addition to losing thickness as a result of atrophy, the ridge may be deformed by underlying periodontal pathosis. Apical periodontal abscesses cause local bone destruction (Figs 3-13a and 3-13b). If an abscess is left untreated and the tooth is removed, the extraction socket may enlarge. The cavity it produces may be so large and irregular that it may preclude implantation (Fig 3-14). The full extent of the cavity is difficult to assess on conventional radiographs. It is impossible to determine whether there is adequate bone adjacent to the cavity to support an implant.

Figs 3-13a and 3-13b *Periapical pathosis and dental abscess. There is localized erosion around the root of the tooth on sections 60 and 61.*

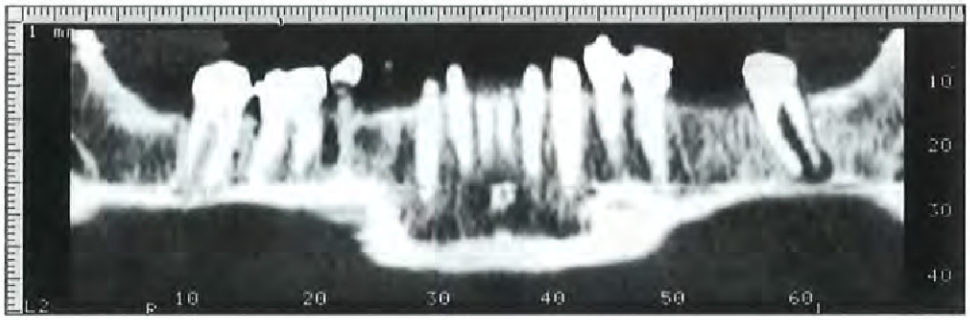


Fig 3-13a Panoramic reformation.

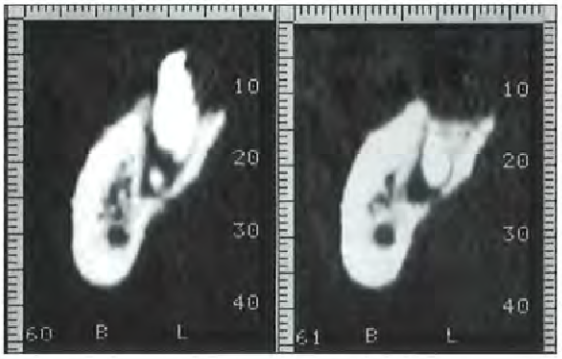


Fig 3-13b Cross-sectional oblique reformations.

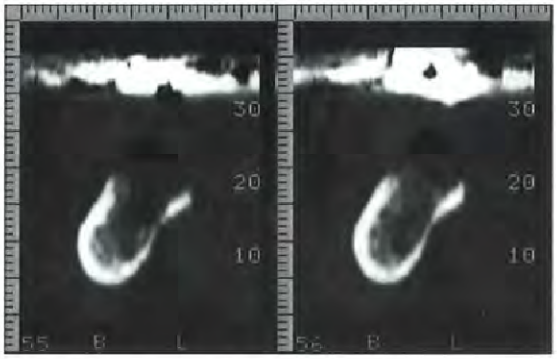


Fig 3-14 Extraction socket. An expanded extraction socket has deformed the entire alveolar ridge, leaving no room for implantation.

Mineralization of the mandible

It is possible to define three different types of mandibles based on the relative amount of intramedullary bone observed on CT scans.

In young people, the medullary space can be well ossified. Medullary bone appears dense and homogeneous on the images. The inferior alveolar canal is very visible on the CT scans because of the relatively homogenous medullary bone (Figs 3-15a and 3-15b). Most mandibles are not uniformly ossified; for example, in Figures 3-15a and 3-15b, the left side of the mandible is much more densely ossified than the right.

Figs 3-15a and 3-15b *Densely ossified mandible. Dense medullary bone is present on the left side of the mandible. There is a fairly dramatic difference in bone density on the two sides. The bone is much whiter on the left than on the right. The mandibular canal is very clearly visible because of the contrast between the dense medullary bone and the neurovascular structures in the canal.*

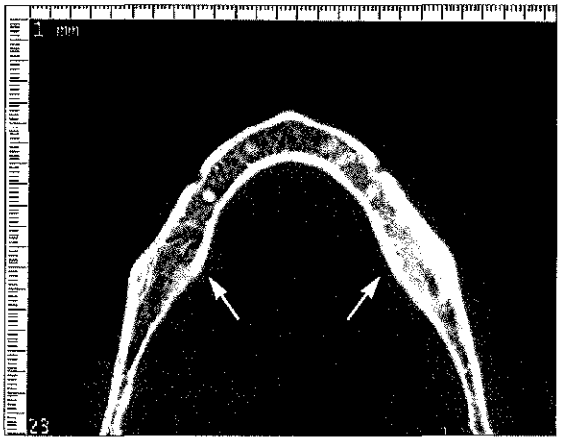


Fig 3-15a Axial reformation.

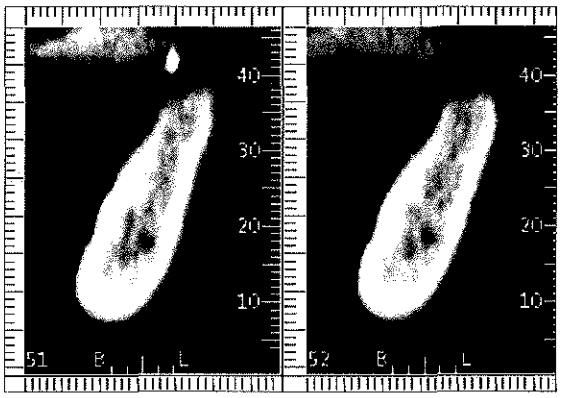


Fig 3-15b Cross-sectional oblique reformation.

The majority of patients have very heterogenous mandibles. There may be some areas where the mandible contains a relatively large amount of dense bone; other areas may be relatively demineralized. The mandibular canal is often visible because of a thin shell of bone that can be seen surrounding the nerve. The rim of bone is sometimes complete, but often the rim only partially encircles the nerve (Fig 3-16). It is not always easy to distinguish the mandibular canal from an area of fatty marrow surrounded by thickened trabeculae. If there is doubt about the position of the nerve on the key cross section, it is necessary to locate the nerve on adjacent images and trace back from there to the image in question.

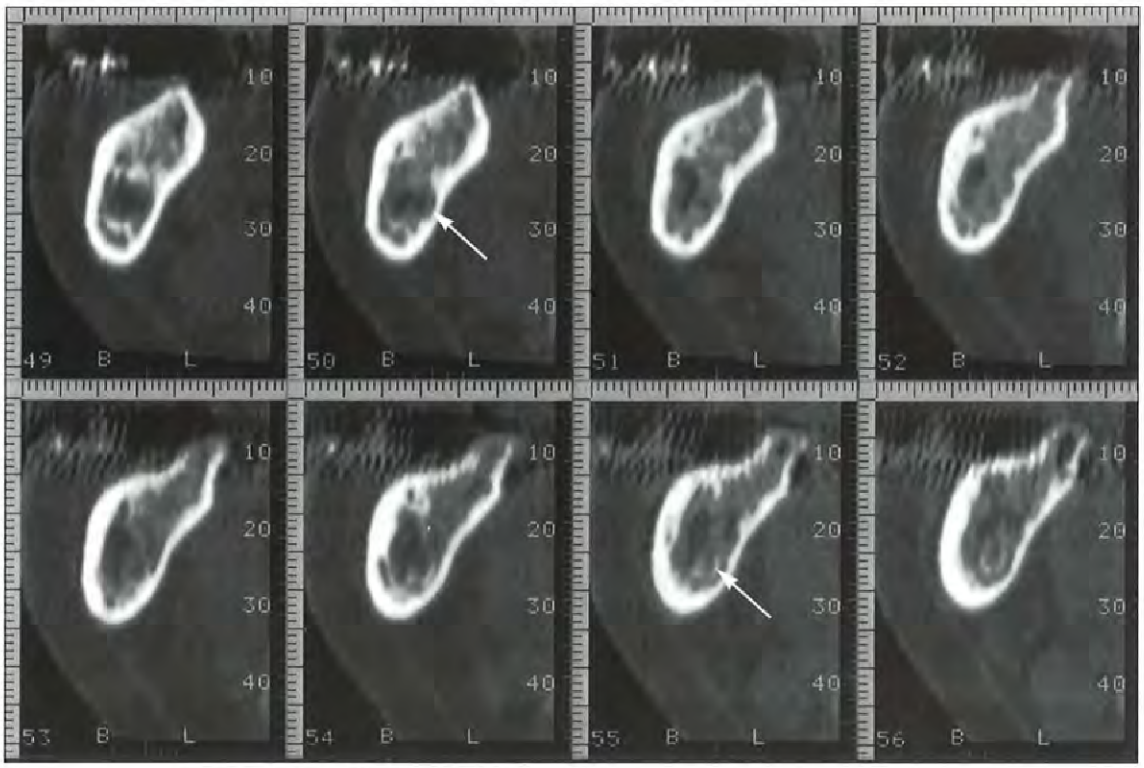


Fig 3-16 Moderately heterogenous mandible. The mandibular canal is very obvious on cross-sectional oblique reformation Nos. 53 to 56 because of a thin circumferential rim of bone around the inferior alveolar nerve. In contrast, in cross sections 49 to 52, the bone is indistinct centrally; on these views, it is very difficult to identify the canal.

The oldest patients and those with osteoporosis have the most demineralized mandibles. Fatty marrow has replaced most of the hematopoetic marrow by this stage in life. Osteoporosis reduces the number and size of the medullary bony trabeculae and thins the cortical bone. Periodontal disease destroys the alveolar process as previously described. The jaw requires constant mastication to maintain the integrity of the bone matrix. The loss of teeth leads to a dramatic decrease in the compressive forces applied to the bone, leading to further bone loss. It is a process equivalent to disuse atrophy in a nonmobile or paralyzed extremity. The internal structure of the bone appears very low in density on the CT images.

Quantitative assessment of mineral content

The mineral content of the mandible can be estimated from the CT scan. The "region of interest" feature common to most CT scanners is used to identify a volume of bone by depositing a box over the area to be measured. The computer averages the CT number of all the pixels in the box. This number represents the mean attenuation value for that volume of bone. The more fat within the volume, the lower the mean CT number will be. By definition, the CT number of water is 0 Hounsfield units. The CT number of fat is in the range of -80. The CT number of cortical bone is greater than 100 units. The lower the measured mean CT number, the more fatty marrow and the less osseous tissue are present in the measured volume.

It is likely that the amount of medullary bone at the implant site is important to the overall success rate of the surgical procedure. In an attempt to determine what effect bone mineral content has on the success or failure of implants, a series of patients in whom one or more implant failed to integrate were studied. The preoperative CT scan data, which had been stored on computer tape, were reloaded on the scanner's computer. The area of the bone that was implanted was identified by the surgeon and marked on the scan. Two measurements each of the CT number were made through an area of successful implantation and through the area where one of the implants failed. The mean CT numbers of the two sites were compared (Figs 3-17a and 3-17b).

Figs 3-17a and 3-17b *Bone mineral measurement.*



Fig 3-17a Axial CT scan of a patient who has had two implants. The average CT number has been calculated from the two marked locations.

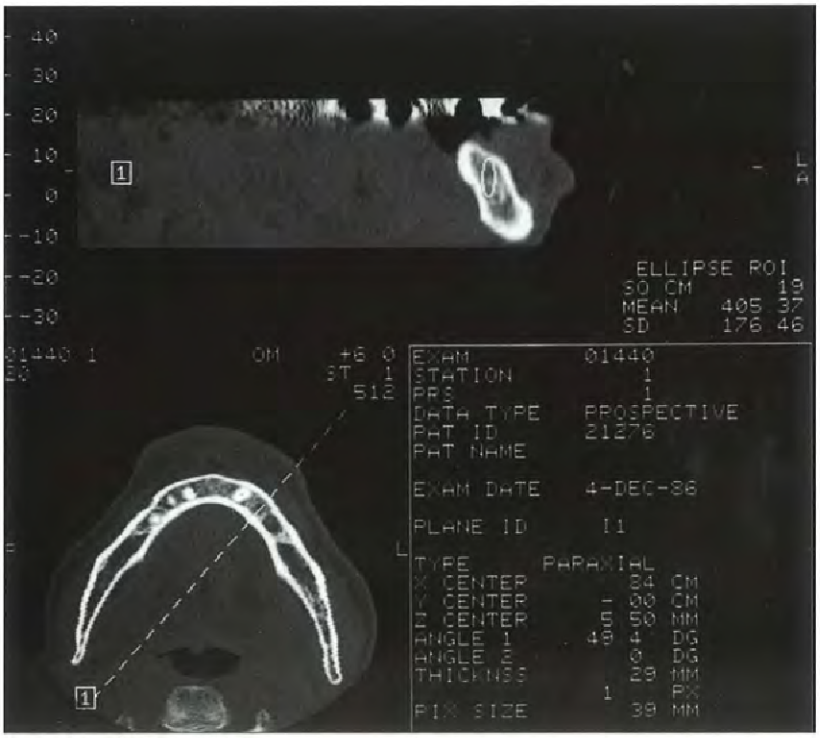


Fig 3-17b Oblique reformation showing the technique of measurement of a cylindrical volume of bone.

Some interesting data were obtained from these observations. It was found that the average CT number of the bone in the majority of the failed mandibular implants was higher than that of the bone in which the implants integrated. This means that there was more than the usual amount of bone matrix at the implant site. It was postulated that the failure was likely due to the dense bone. The two most likely explanations are that the denser bone is less well vascularized than the more fatty bone or that the drill heats the dense bone more than the fatty bone. In either instance, the integration may be affected.

In the maxillas, the failed implants were found to have been placed in inadequate bone most of the time. The increased density did not appear to be a problem. If the implant site has a very low CT number, the implants may benefit from being left in place longer than usual before the prosthesis is attached. If the implant site is denser than average, extra care should be taken not to heat the bone with the drill.

Position of alveolar nerve

The mandibular canal is often extremely difficult or impossible to identify in patients, because no medullary bone is present surrounding the inferior alveolar nerve (Figs 3-18a to 3-18c). In this type of mandible, it is sometimes possible to estimate the position of the nerve at the desired implant locations even if it is impossible to see at that location. This is because the anatomy of the mandibular canal is so constant. The downward-sloping inferior alveolar nerve makes a constant curve within the bone. Therefore, if the mandibular canal can be identified proximal and distal to the desired implant site, it is possible to draw a line from the superior margin of the canal on the most distal visible cross section to the superior margin on the mesial cross section. The inferior alveolar nerve must lie below this line.

As an exercise, the reader should attempt to locate the inferior alveolar nerve on the patient displayed in Figure 3-19. The canal can be identified on cross-sectional oblique view 55, which is distal to the implant site, and on oblique section 51, which is mesial to the site. The reader should draw a line with a clear plastic ruler from the top of the canal on both of these images. The nerve will lie below this line on all of the intervening cross sections. This is true in the majority of the bone, except near the mental foramen. The inferior alveolar nerve begins to curve superiorly within 1 cm of the mental foramen, and therefore the previous method cannot be used (Fig 3-20).

Figs 3-18a to 3-18c *Variations in the anatomy of the mandibular canal.*

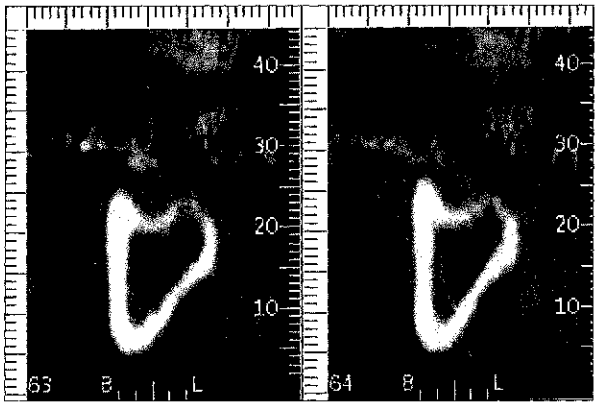


Fig 3-18a Markedly demineralized mandible showing no visible mandibular canal. The medullary bone consists primarily of fatty marrow. No surrounding bony rim is identifiable.

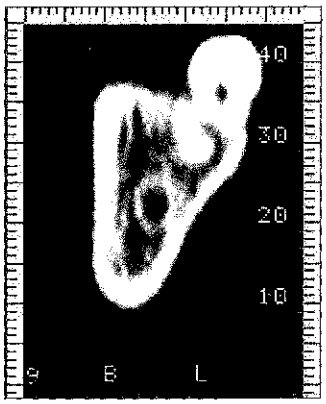


Fig 3-18b Complete cortical rim surrounding the nerve.

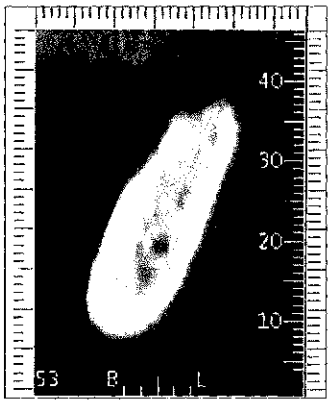


Fig 3-18c Nerve surrounded by homogenous dense bone.

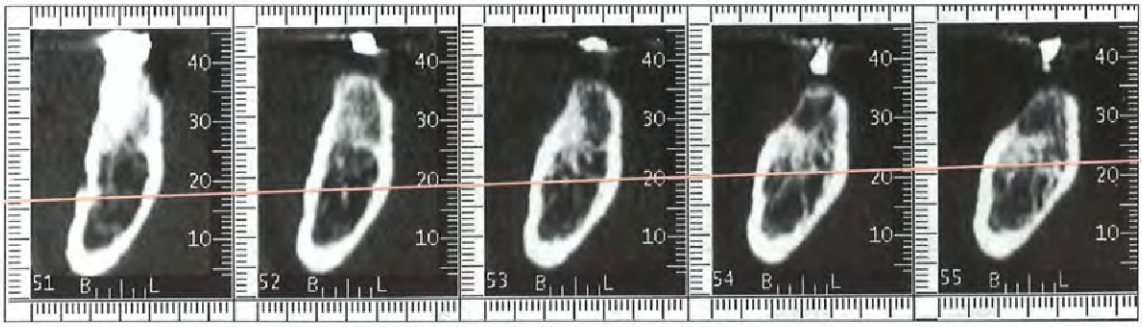


Fig 3-19 Demineralized mandible. In this series of cross-sectional oblique reformations, the mandibular canal is not visible throughout most of the potential implant sites. It is possible to see the canal on image 55 distally and 51 mesially. By connecting the superior border of the canal on the two images, it is possible to determine the most superior possible position that the nerve can reach.

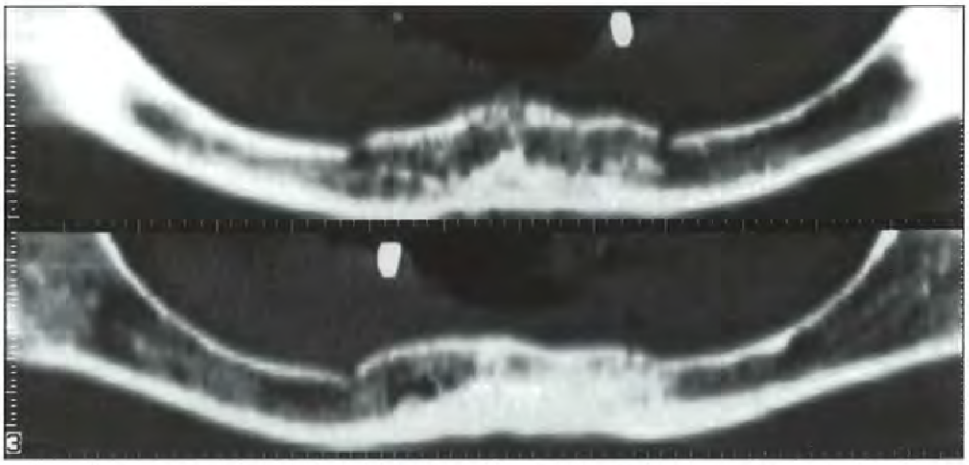


Fig 3-20 Distal end of the mandibular canal. The distal end of the inferior alveolar nerve curves superiorly in 1 cm distal to the mental foramen.

Completely edentulous mandible

In completely edentulous mandibles, there is a wide spectrum of bone loss, depending on the age of the patient and the amount of time elapsed since the teeth have been lost. In younger patients without total alveolar loss, there is nearly always enough bone present to implant a series of fixtures anteriorly between the mental foramina. Originally, Brånemark's group attempted to implant six fixtures anteriorly. It has been found subsequently that four or five implants can adequately rehabilitate the jaw (Fig 3-21).

In older patients whose teeth have been gone for many years, there may be profound bone loss. The alveolar process has usually resorbed. Asymmetric erosion may leave either the labial or the lingual cortex relatively intact but cause profound central loss. The height of the remaining mandible may be so reduced that it cannot support even the shortest implants. In these patients, ridge enhancement procedures are occasionally attempted.

The lateral and posterior portions of the mandible distal to the mental foramen pose the most problems for the implant surgeon. With loss of the alveolar process, the inferior alveolar nerve may come to lie immediately below the eroded occlusal surface of the bone (Fig 3-22).

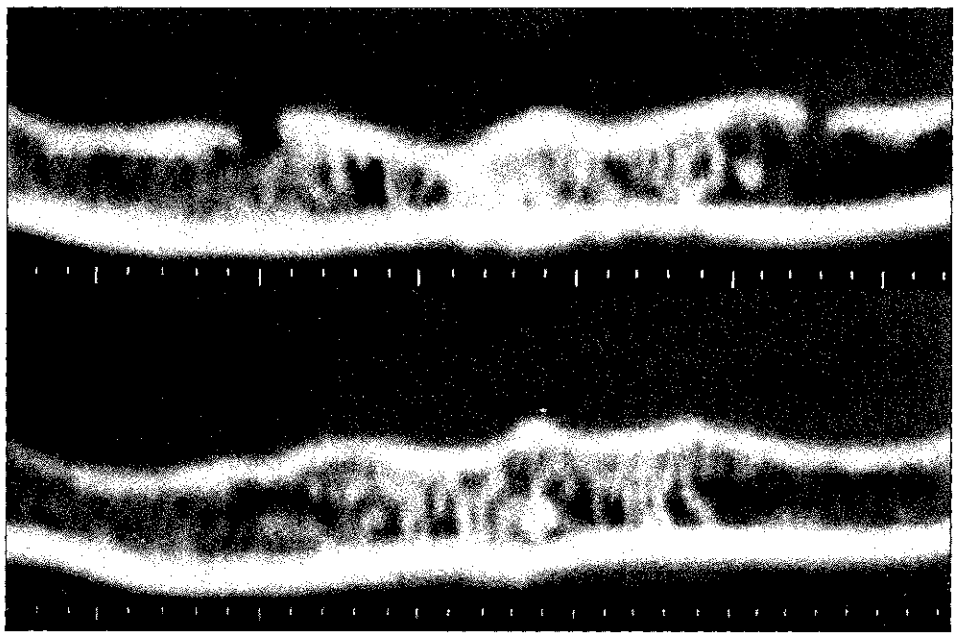


Fig 3-21 Completely edentulous mandible: There is moderate atrophy of the alveolar process, but not enough to preclude implantation. Five implants can be placed between the mental foramina.

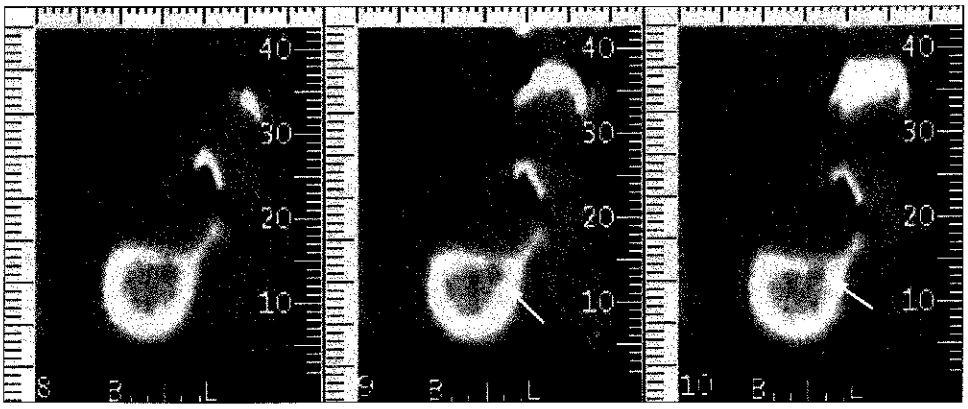


Fig 3-22 Long-standing completely edentulous mandible. The inferior alveolar nerve lies within the bone just beneath the superior surface of the bone.

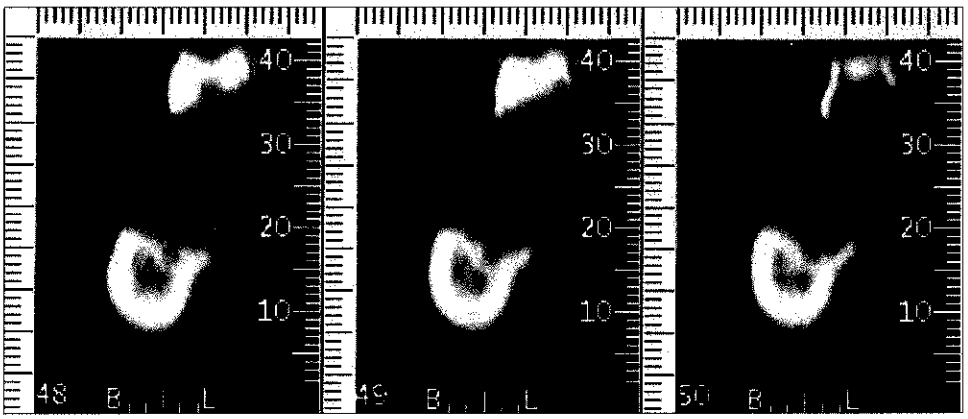


Fig 3-23 Severe erosion of the alveolar ridge. The inferior alveolar nerve lies outside the eroded bone

The nerve may lie centrally within the bone; this will preclude implantation. If the nerve lies along the buccal or lingual side, it may be possible to pass a fixture beyond the plane of the nerve into cortical bone.

In the worst cases, the height of the mandible will be reduced to a level inferior to the plane of the inferior alveolar nerve. In those cases, the nerve may actually lie along the surface of the bone, free of any osseous covering. This is obvious on the cross-sectional oblique reformations (Fig 3-23).

References

1. Cawood JI, Howell RA. A classification of the edentulous jaw. Int J Oral Maxillofac Surg 1988;17:232–236
2. Williams PL, Warwick R, Dyson M, Bannister LH (eds). Gray's Anatomy, ed 37. Edinburgh: Churchill Livingstone, 1989:367–369.
3. van der Zypen E. Anatomic basis of implantology. In: Schroeder A, Sutter F, Krekeler G (eds). Oral Implantology. Stuttgart: George Thieme, 1991:11–35.



Computerized Tomography in Patients with Implants and Other Metal in the Jaw

It has been obvious since the advent of computerized tomography (CT) that metallic material within the cross section degrades the image. This is caused by the absorption of x-rays within the metal. Gold, silver amalgam, and stainless steel will absorb nearly all the traversing radiation, allowing none to reach the CT scanner's detectors. Consequently, the scan data are degraded and linear streaks occur within the image. It was shown in Chapter 2 that this is the main drawback of direct coronal scanning of the jaw. It is impossible to eliminate the artifacts produced by dental restorations from the CT image.

Titanium is different from other metals. It has been used for decades within the human body and has never been found to be incompatible with tissue. It is the ideal material for dental implants for the following reasons[1]:

1. Titanium is very reactive. A coat of titanium oxide forms spontaneously around the implant. This oxide is one of the most resistant materials known, protecting the implant from tissue fluids.
2. Titanium is inert in tissue. Because of the oxide coating, there is virtually no release of titanium ions into the tissue.
3. Titanium is very strong. It is considerably stronger than the cortical or cancellous bone into which it will be implanted.
4. Titanium will form an intimate bond to bone.

Titanium implants produce virtually no artifact on the CT images. Titanium behaves like calcium. Its density on CT images is very similar to that of rods of hydroxyapatite or very dense bone. Because of this physical property of titanium, it is possible to produce diagnostic CT scans of patients postimplant.

Often it is not necessary to perform a CT scan on a patient with implants. The most common reason for scanning patients postoperatively is to plan for further implantation into other areas within the same jaw. The second most common indication is for the evaluation of postoperative pain syndromes. It is therefore imperative that the clinician be familiar with the appearance of osseointegrated and failed implants as well as the appearance of the most common complications of the implant surgical procedures.

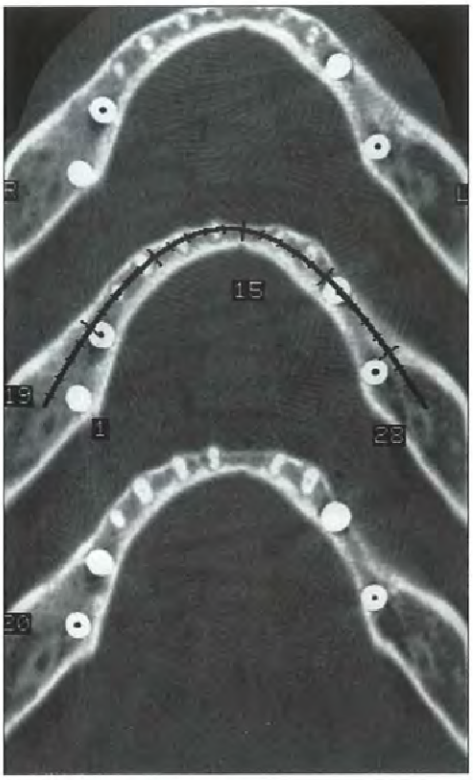
Evaluation of the Osseointegrated Implant

In the earliest days following implantation, before osseointegration has occurred, a very faint line is visible surrounding the implant. This line may not be continuous, depending on the intimacy of the contact between the bone and the implant. The osseointegrated fixture forms a solid chemical bond to the host bone (Figs 6-1a and 6-1b). Histologically bone can be identified in direct contact with the titanium surface. Scanning electron micrographic images have demonstrated penetration of the rough plasma-coated surface of implants by lamellar bone.[1]

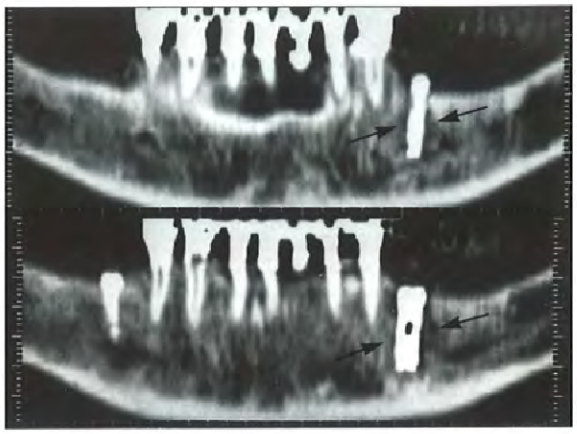
The osseointegrated implant demonstrates intimate contact with the host bone (Fig 6-1c). The space between the implant fills in, except for the most superficial portion of the implant. Depending on implant design, several millimeters of the implant may not be osseointegrated at the mucosal border. A faint halo can be seen on those axial CT slices near the mucosal border. Determination of the presence of osseointegration should be made on the axial views, because they are the images with the highest resolution.

In patients with two or more adjacent implants, there will often be a very subtle black space between the implants on the axial views (Figs 6-2a and 6-2b). This is a "beam-hardening" artifact caused by the passage of the x-ray beam through two relatively dense objects in a single plane. Some data dropout occurs in the bone between the two implants. In simple terms, the detectors that lie on a plane with the two implants see a smaller amount of x-ray than they should. A disproportionate amount of the x-ray beam is absorbed by the two implants, and an error occurs in those picture elements between the two implants.

The position and orientation of the implants are easily determined from the cross-sectional oblique reformations. It is ideal that the implants parallel the plane of adjacent teeth. The screw access hole will then lie in the center of the prosthesis. This is especially important in the anterior jaw. Figures 6-3a to 6-3c present a series of CT images of a patient with a single maxillary anterior implant. The axial view reveals that the implant is in the widest portion of the ridge. There is a zone of buccal bone loss immediately distal to the implant. The cross-sectional oblique view indicates that the implant is exactly parallel to the adjacent tooth.



Figs 6-1a to 6-1c *Computerized tomography in the early postoperative period.*



Figs 6-1a and 6-1b Axial and coronal reformations demonstrate lucency around the implants. Osseointegration has not had time to occur.

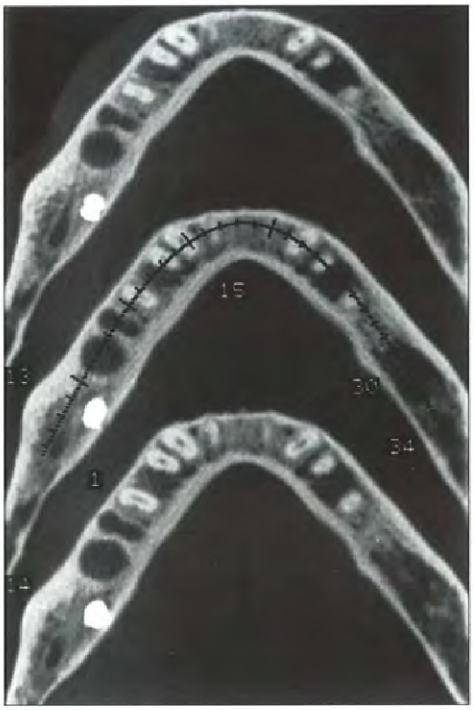


Fig 6-1c Axial scans of another patient with an osseointegrated implant lying just lingual to the inferior alveolar nerve. Note the intimate contact between the fixture and the bone.

Figs 6-2a and 6-2b *Two adjacent osseointegrated implants.*

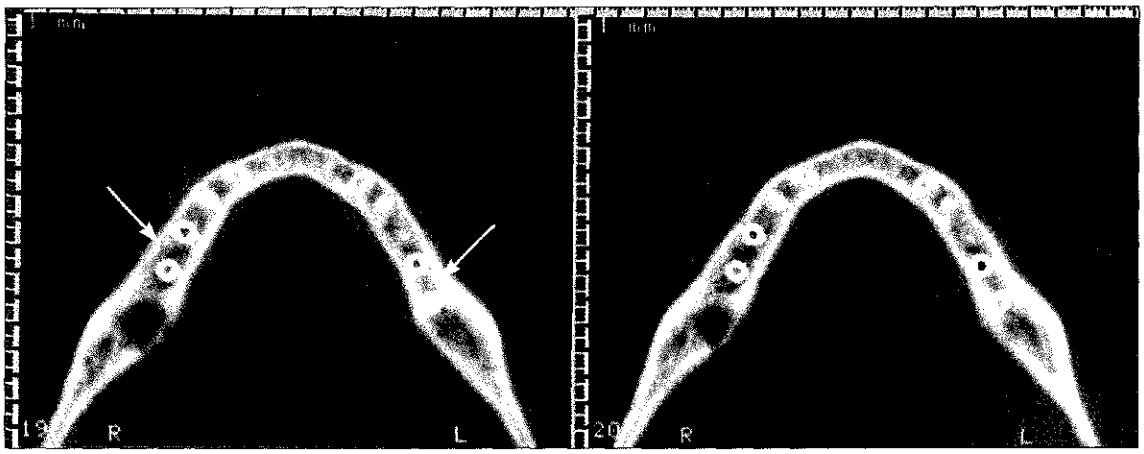


Fig 6-2a Axial reformation. There is a subtle band of low density between the implants. A prominent extraction socket is seen distal to the posterior implant.

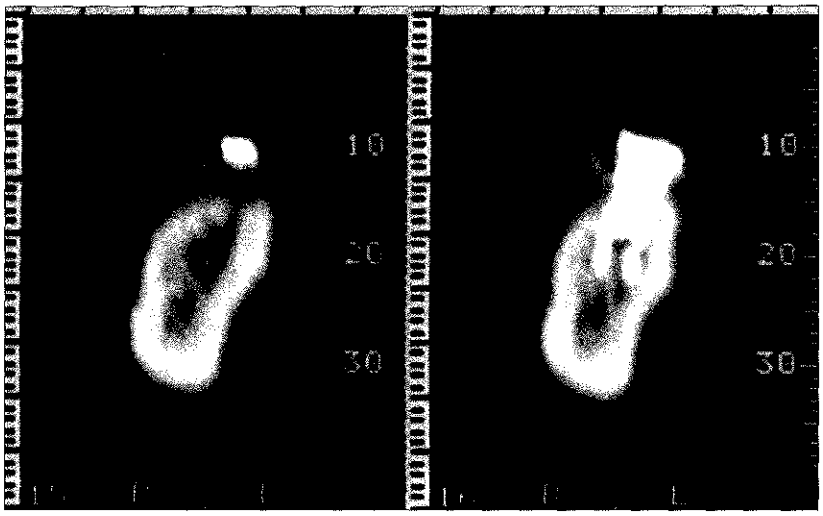
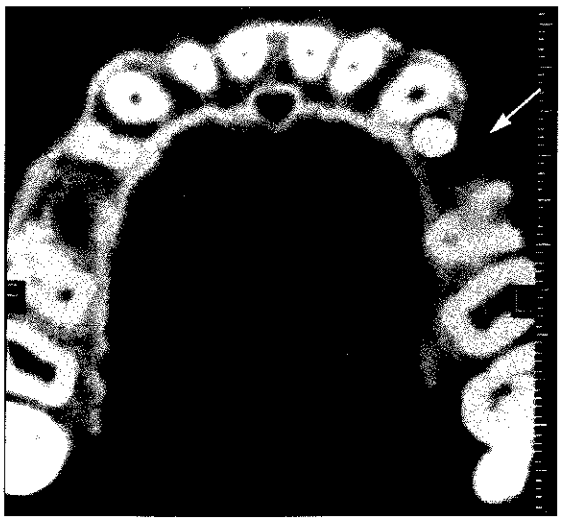


Fig 6-2b Cross-sectional oblique images showing intimate contact of the implant with the bone.



Figs 6-3a to 6-3c *Well-positioned and well-integrated maxillary anterior implant.*

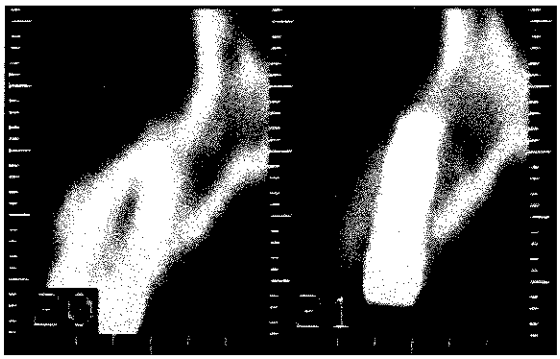


Fig 6-3a Axial reformation. There is intimate contact with the bone. There is a zone of localized bone loss distal to the implant.

Fig 6-3b Cross-sectional oblique reformation defining the angle of the implant. The implant perfectly parallels the adjacent tooth.

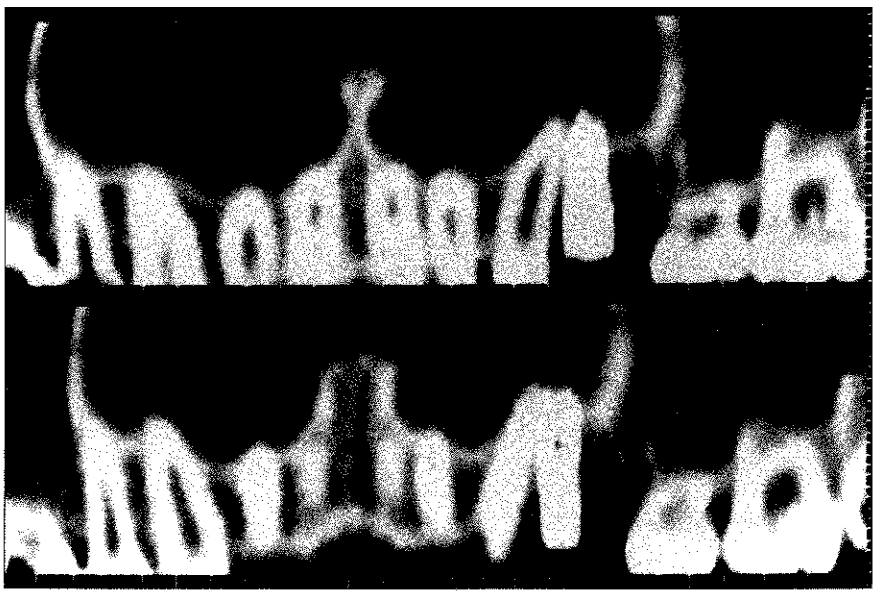


Fig 6-3c Panoramic reformation.

Figures 6-3a to 6-3c can be compared with the series of cross sections in Figure 6-4. The implant displayed in cross section 29 is oriented along the longest axis of the arch, rather than in the plane where the prosthesis should be. A long implant was used, but the implant points superior to the opaque marker placed in the patient's stent. The access hole of that implant will therefore project forward of the center of the prosthesis and compromise the esthetics of the final restoration.

The implant in Figure 6-5 is not oriented along the long axis of the maxilla. It is angled more toward the lingual side than would be ideal, but the esthetics of the final prosthesis will not be compromised because the access hole can be placed posteriorly without being visible or otherwise interfering with the prosthesis. Figures 6-6a and 6-6b depict a patient with an improperly placed maxillary anterior implant. The entrance of the drill into the alveolar ridge was made in the proper location, but the drill was inadvertently angled toward the labial side of the bone. The implant perforated the labial side of the bone and is, in part, lying in the anterior soft tissues.

Figures 6-7a and 6-7b present a series of CT images of another patient whose implants were placed distal to the mental foramen. The implants are well-positioned and perfectly angulated. The implant has been placed so that it engages the lingual cortical plate. The implant extends inferior to the plane of the alveolar nerve and lies lingual to it. This is an example of the ideal situation. The implant is longer than the space between the top of the alveolar ridge and the roof of the alveolar nerve canal. By carefully measuring the space between the canal and the cortex, the surgeon was able to determine that there was adequate room to drive the implant lingual to the canal without entering the canal and injuring the nerve.

Figures 6-8a and 6-8b present images of a patient in whom the mandibular implant was poorly positioned. The drill began in the proper location, but, as it descended into the bone, it perforated the buccal cortex, and the majority of the length of the implant lies outside the bone.

Figures 6-9a to 6-9c present a series of three-dimensional reformations of a patient with nine well-positioned implants. The relationship of the implants to the nerve is easily demonstrated on these images. Because of the position of the nerve near the center of the bone, it was not possible to sink any implants below the plane of the nerve. The posterior implants are therefore shorter than those placed anteriorly between the mental foramina.

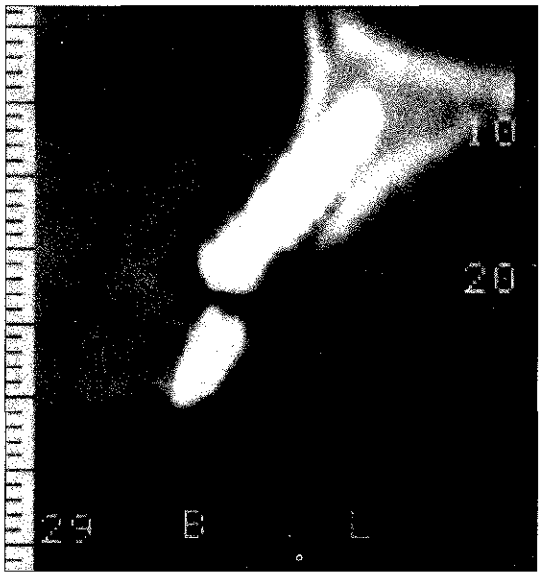


Fig 6-4 Less-than-ideal implant angulation. The cross-sectional oblique view reveals the implant to extend the length of the alveolar process. It points anterior to the opaque marker placed within the stent.

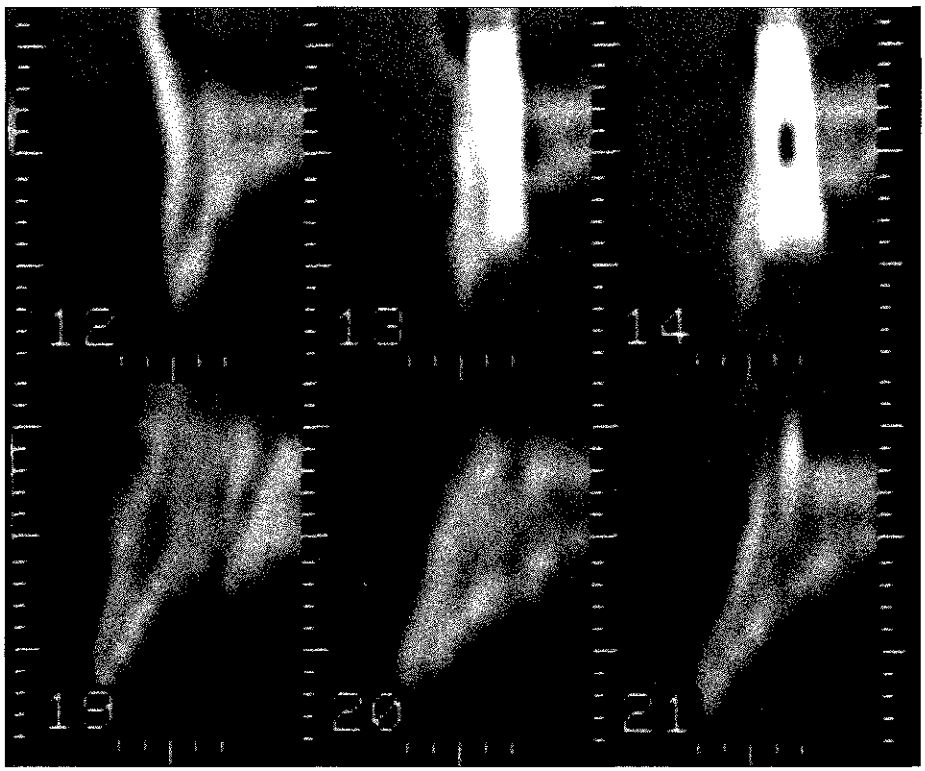


Fig 6-5 Less-than-ideal implant angulation. The cross-sectional views reveal that the implant is angled too far toward the lingual side of the ridge. It is unlikely that this will effect the final esthetic outcome significantly.

Figs 6-6a and 6-6b *Perforation of an implant through the buccal cortex of the maxilla.*

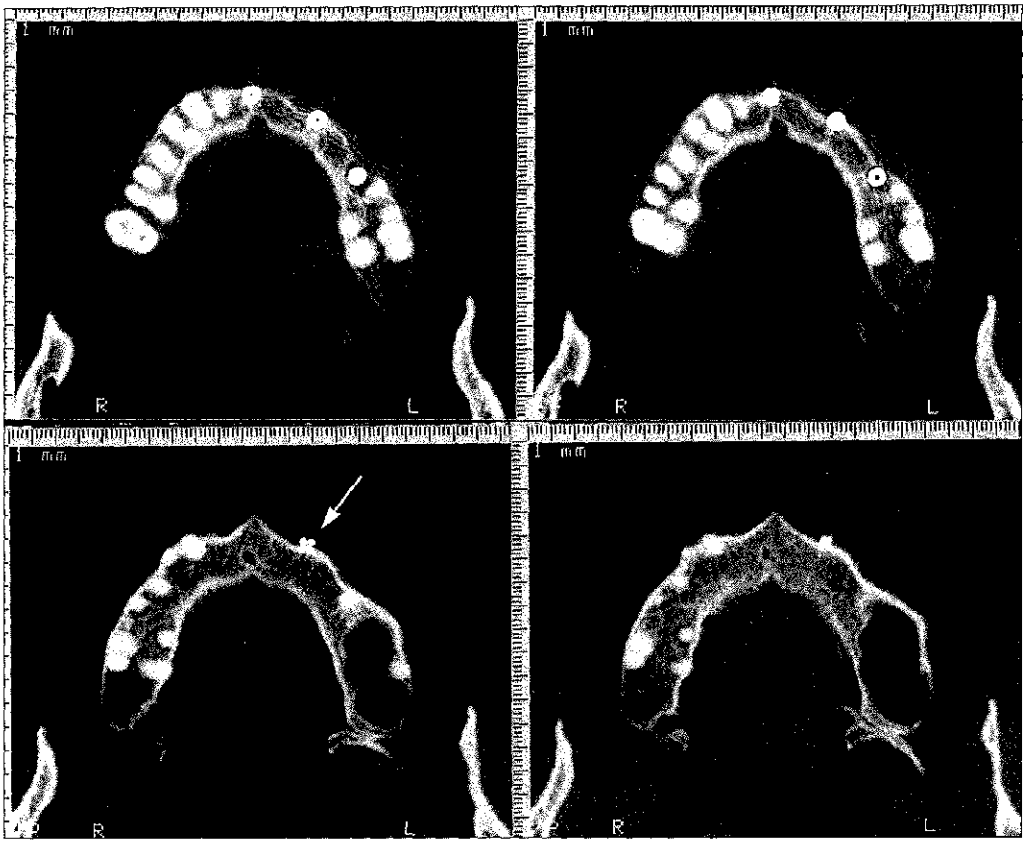


Fig 6-6a Axial reformation.

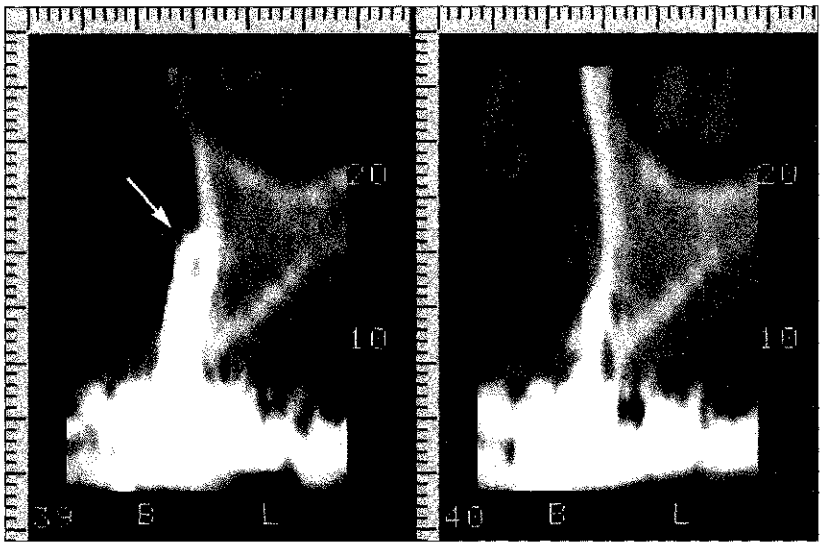


Fig 6-6b Cross-sectional oblique reformations.

Figs 6-7a and 6-7b *Well-positioned mandibular posterior implant.*

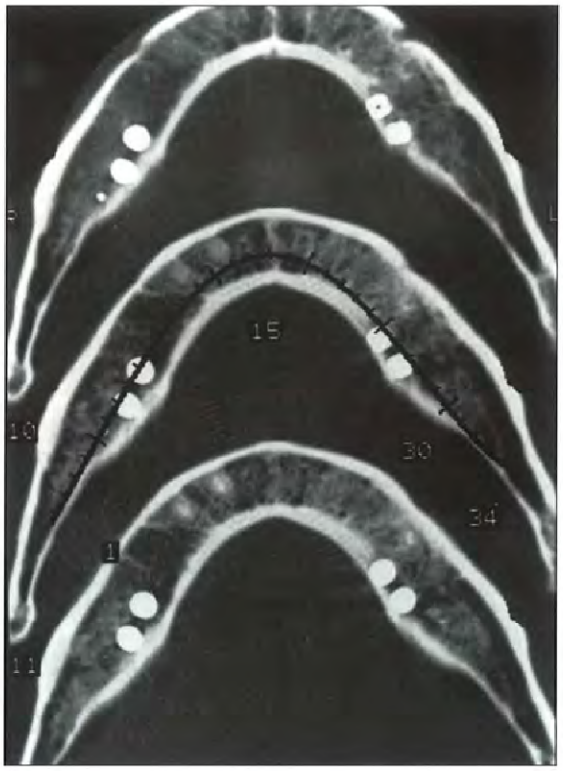


Fig 6-7a Axial views indicating the presence of four osseointegrated implants. The right-sided distal implant is found at cross-sectional oblique view 6.

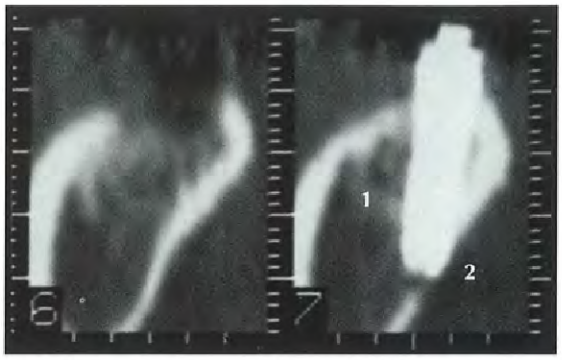
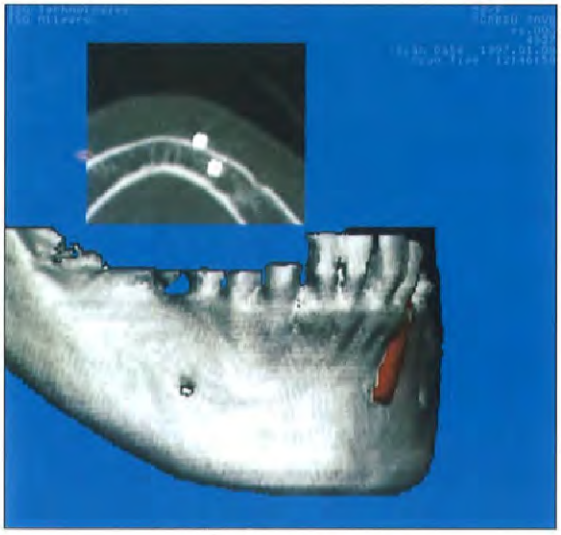


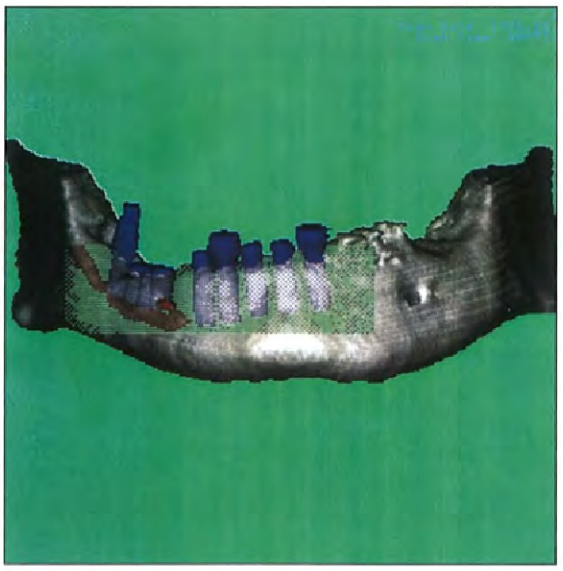
Fig 6-7b Cross-sectional oblique reformation demonstrating that the surgeon has placed the implant lingual to the inferior alveolar nerve (1). The distal end of the implant engages the lingual cortex below the plane of the nerve (2). (From Schwarz MS, Rothman SLG, Chavetz N, Rhodes M. Computed tomography in dental implantation surgery. Dent Clin North Am 1989;33:579. Reprinted with permission.)

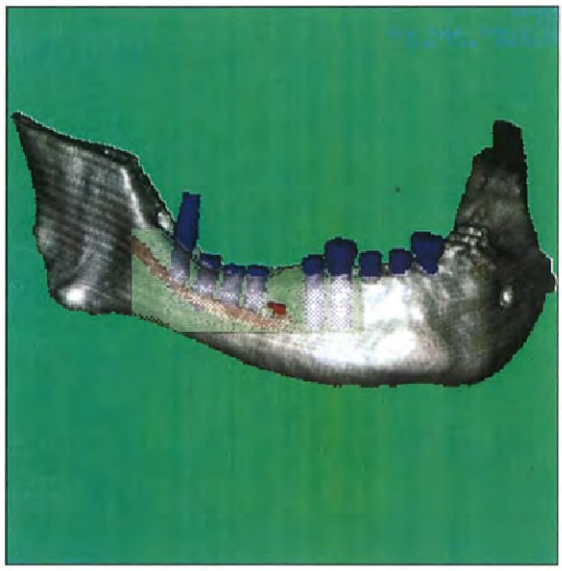




Figs 6-8a and 6-8b Perforation of an implant through the buccal cortex of the mandible. Three-dimensional reformations and axial and cross-sectional images of a patient in whom the anterior implant *(red)* enters the mandible in the proper location but perforates the buccal cortex and lies outside the bone throughout most of it's length.







Figs 6-9a to 6-9c Well-positioned mandibular implants. Three-dimensional images presented with the right side of the mandible made transparent. The implants *(blue)* lie above the plane of the inferior alveolar nerve *(red)*.

Evaluation of the Failed Implant

A review of the preoperative CT scans of a group of patients who had one or more failed implants was undertaken at our facility. The implant surgeon marked the location of the failed and osseointegrated implants on one of the CT images for each patient. The actual CT data were reviewed, and the bone mineral content of the tissue volume that was replaced by the implant was estimated. This was accomplished by evaluating the mean CT number of the volume directly from the scanner's computer using a region of interest measurement on both the axial CT data and on a volume of bone reformatted from the entire CT data set.

An attempt was made to determine the "normal" bone content of the mandible and maxilla by studying the CT numbers measured within the mandibles and maxillas of a series of patients. A special mandibular phantom was manufactured for the purpose. The idea was to perform a series of CT number measurements of patients' jaws and compare the data to measurements made of the phantom to calculate mineral content. This technique is routinely used to calculate the bone mineral content of the spine in osteoporotic patients. It became obvious immediately that the internal structure of the bone was so variable, and the measured CT numbers varied so greatly within each mandible and among patients, that an absolute standard could not adequately be defined. This is due to the wide variation in the relative amount of cancellous bone and fatty marrow in each volume of tissue. Bone raises, while fat lowers, the CT number of a tissue volume.

It was therefore decided that a comparison should be made between the implant sites that failed and those that osseointegrated within the same alveolar arch. Preliminary analysis of these data indicated that, in most cases, the CT numbers were higher at sites where mandibular implants failed than at the comparable successful sites. This means that there was more bone per unit volume at failed sites than at the well-integrated sites. The sites of maxillary implant failure, however, tended to show less than the usual amount of bone per unit volume. This suggests that maxillary implant failure was commonly caused by inadequate host bone.

A failed implant will not be bound tightly to bone. The axial CT will therefore demonstrate a halo of lucency surrounding the implant. This halo will extend the entire length of the implant, indicating total failure of osseointegration. In the maxilla, it appears that the most common cause for implant failure is inadequate host bone. There may be inadequate bone height or buccolingual width to support the implants. Figures 6-10a and 6-10b depict such a patient. There is very profound bone atrophy. The implant is seated in bone that is inadequate to support the length of the implant. In the mandible, less than 5% of implants fail to osseointegrate. Many of these implant failures occur even when there is adequate bone height or width.

Our data suggest that in areas where the bone content is high, there may be overheating of the tissue by the drill, resulting in devascularization or other tissue injury that accounts for implant failure. Special care must be taken during drilling of dense bone. In several patients, implant failure occurred in areas with dramatic osteopenia. When implanting into very fatty areas in elderly osteoporotic bone, the implants should remain uncovered for a longer period of time than usual to allow osseointegration.

Figs 6-10a and 6-10b *Failure of a maxillary implant because of inadequate bone. The alveolar ridge is remarkably atrophic. There is inadequate bone height. Short implants have been placed anteriorly. There is lucency surrounding the implants.*

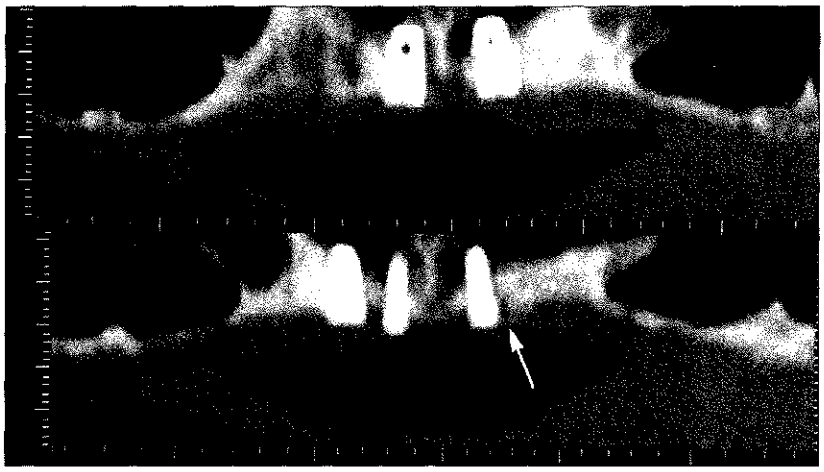


Fig 6-10a Panoramic reformations.

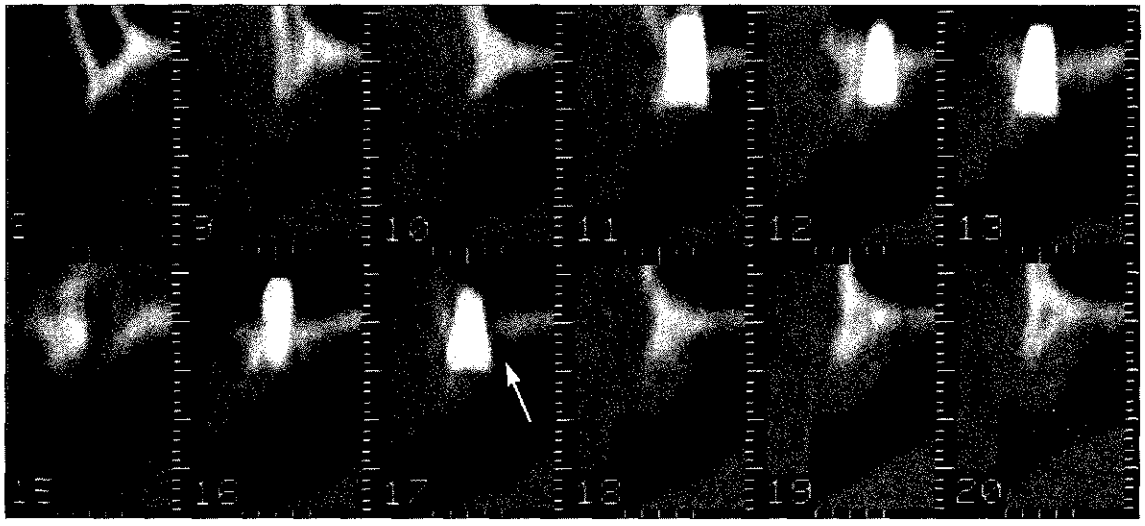


Fig 6-10b Cross-sectional oblique reformations.

Evaluation of the Symptomatic Implant

There are several clearly definable causes of postoperative symptoms following implantation. There are also rare patients who develop symptoms following implantation that do not correlate with any definable abnormality. One individual was convinced that he was receiving radio broadcasts over his implant. There is not much that postoperative CT can do for such patients.

Infection at the implant site is one of the common causes of pain in the immediately postoperative period. The diagnosis may be obvious clinically or on regular dental radiographs. A CT scan be useful in a minority of individuals where findings from the physical examination and radiographs are equivocal. The patient in Figures 6-11a and 6-11b developed pain in the jaw within 2 weeks of implantation. The routine dental radiograph was interpreted as being normal. A postoperative CT scan defines an area of localized bone loss at the base of the implant. Localized demineralization of the bone and a small abscess are present. This process involves the inferior alveolar nerve, which passes through the lucent zone. This is typical of acute infection of bone at the implant site. It is generally accepted that in the earliest stages of infection, bone dissolution remains invisible on routine radiographs. Bone loss must be significant to allow diagnosis. Computerized tomography, while more sensitive than regular radiographs, may also reveal no abnormalities in the very early stages of infection.

Neurologic dysfunction of the inferior alveolar nerve following implantation is generally caused by encroachment on the nerve by one of the implants. Computerized tomography is very useful in determining which of a series of implants is within the canal. Figure 6-12 depicts a scan of a patient with paresthesia of the face on the side of the implant. The cross-sectional oblique reformation reveals that the implant partially encroaches on the alveolar nerve canal. If the diagnosis is made in the early postoperative period, the implant can be slightly withdrawn. In the illustrated case, withdrawal of the implant by less than 2 mm will, perhaps, relieve the neural compression. If the diagnosis is not made in a timely fashion, and the implant is allowed to osseointegrate, removal of the implant becomes problematic.

In some instances, the implant is much too long or is so poorly positioned that it will require removal. Figure 6-13 depicts such an implant. It is obvious that the implant is much too long; it completely fills the cross section, almost down to the inferior cortex. This patient complained of anesthesia of the affected side of the face immediately following surgery.

Figs 6-11a and 6-11b *Implant failure caused by infection at the base of an implant. The bone is lucent at the tip of the implant. The space around the implant represents the abscess. The inferior alveolar canal is lost in this space.*

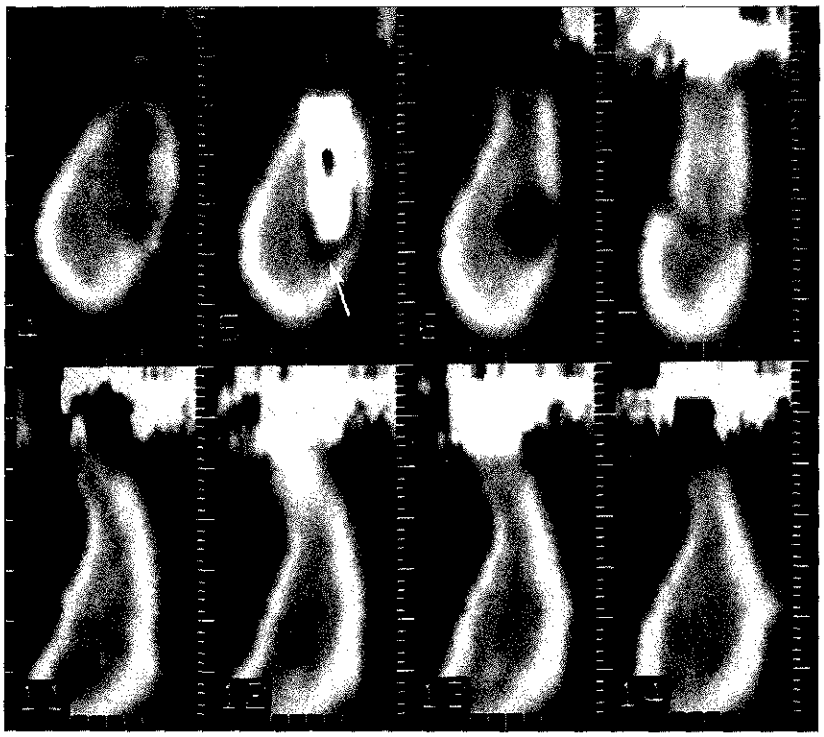


Fig 6-11a Cross-sectional oblique reformations.

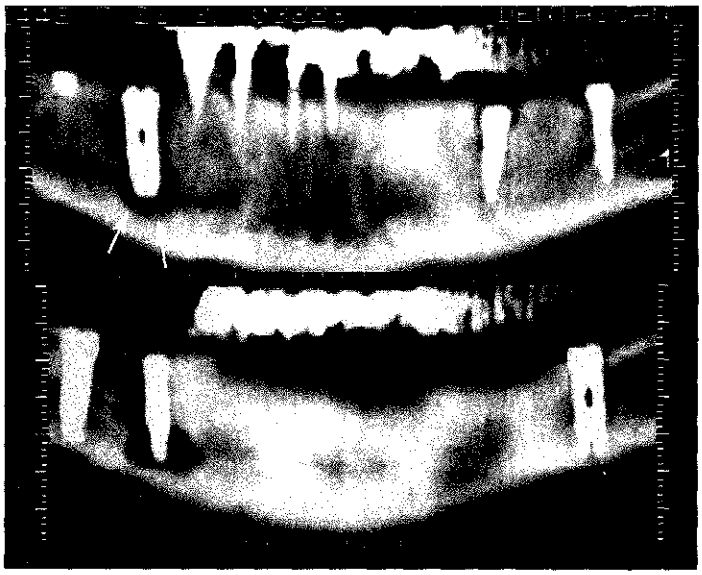


Fig 6-11b Panoramic reformations. (From Schwarz MS, Rothman SLG, Chavetz N, Rhodes M. Computed tomography in dental implantation surgery. Dent Clin North Am 1989;33:592. Reprinted with permission.)

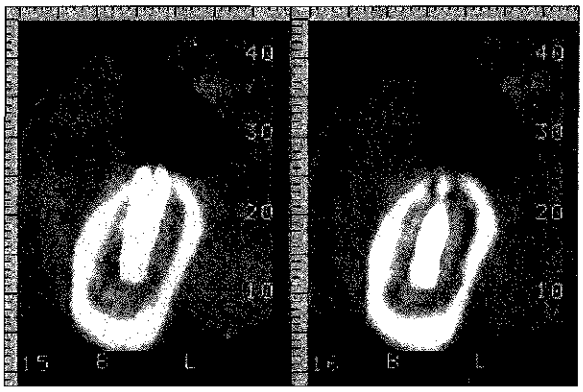


Fig 6-12 Implant partially encroaching on the alveolar nerve canal. Cross-sectional oblique views reveal that the implant has entered the canal and fills the superior half.

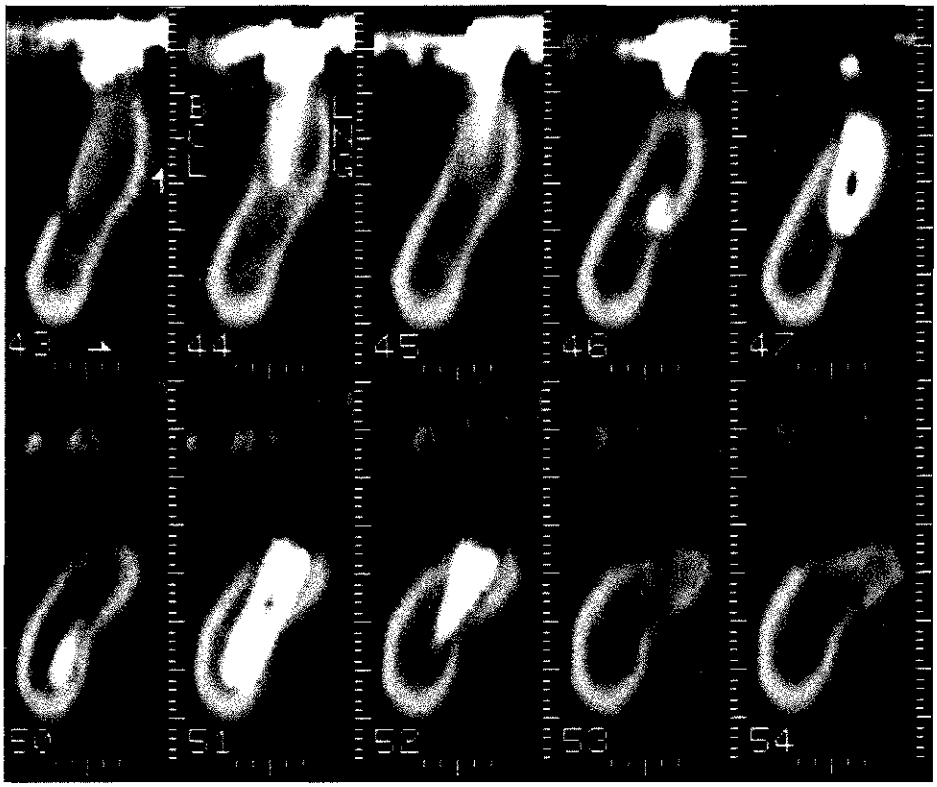


Fig 6-13 Implant completely transecting the alveolar nerve canal. Cross-sectional oblique view 51 reveals that the implant extends down through the canal and nearly engages the inferior cortex of the bone. The implant visible in images 46 and 47 is properly positioned.

It is unusual for a patient to develop pain in the jaw years after successful implantation. When this occurs, a stress fracture may have occurred in the bone. This complication is quite rare.[2] Tolman and Keller[3] described seven patients who developed fractures through implanted mandibles. Three of their patients developed spontaneous fractures at the site of implantation. In two of these patients, the fracture occurred in the zone of previously removed implants, and, in one patient, fracture occurred through an existing implant. Rothman and Schwartz[4] reported the CT appearance of two patients without severe atrophy who spontaneously developed stress fracture of the mandible through the bone surrounding well-positioned implants.

The patient depicted in Figure 6-14a was a 68-year-old woman who underwent implantation with three 13-mm implants. Her mandible was believed to be severely atrophic. Four weeks following surgery, she developed pain in the jaw. A CT scan demonstrated a fracture line extending lingually from all three implants. The patient in Figure 6-14b had uneventful implantation of five anterior implants. Four and a half months following implantation, the implants were uncovered and noted to have osseointegrated. The patient functioned normally for 3.5 years, at which time she developed acute pain in the area of the most distal implant on the right. Routine radiographs appeared normal, but a CT scan demonstrated a fracture through the distal implants. Results of the nuclear bone scan were positive in both patients.

The development of a stress fracture is rare. The use of CT should be considered if the cause of persistent pain is not found on routine dental radiographs.

Figs 6-14a and 6-14b *Stress fracture of the implanted mandible in two patient scans.*

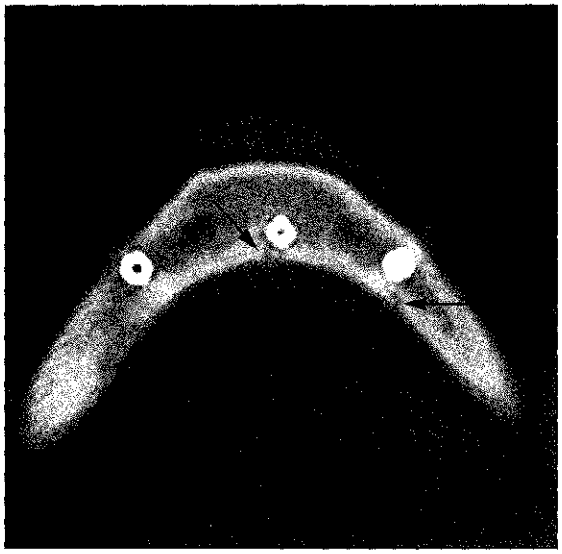


Fig 6-14a Patient 1 scan shows lucent lines extending lingually from all three implants.

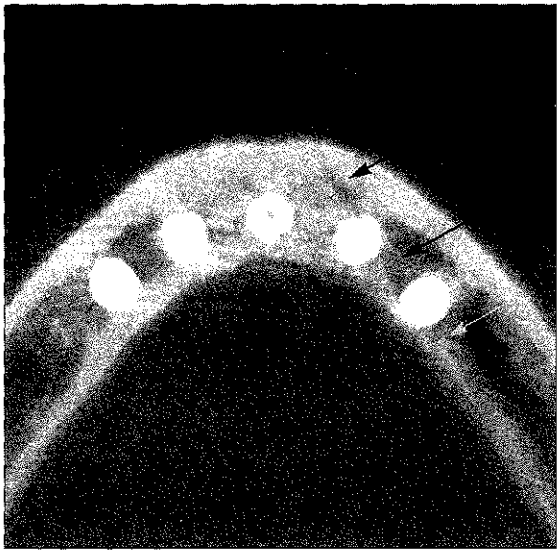


Fig 6-14b Patient 2 scan shows a single fracture through the two implants on the right.

Evaluation of Blade Implants

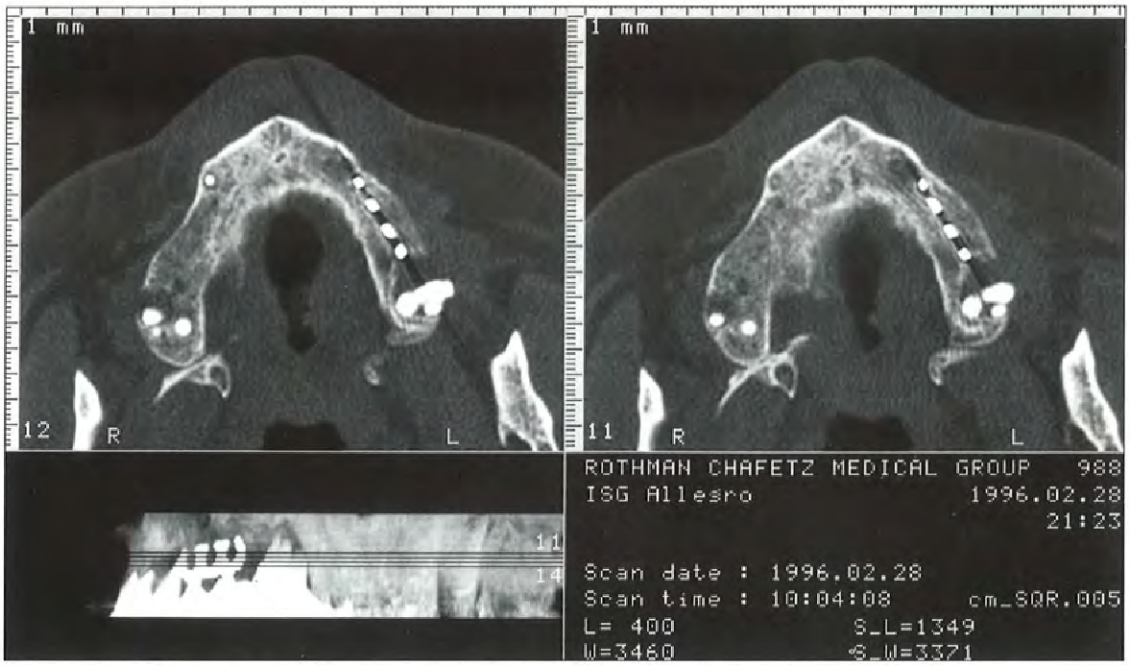
Narrow, blade-shaped implants have been used for years in patients with alveolar ridges that are inadequate in buccolingual dimension to support a cylindrical root-form implant. Blade implants are specifically designed to be placed into the mandible distal to the mental foramen, where there may not be adequate space between the nerve and either the buccal or lingual cortex to place a cylindrical implant. Blade implants were originally made of stainless steel and therefore would not undergo osseointegration. Titanium blade-type implants that will osseointegrate are now available.

Figures 6-15a to 6-15d present well-positioned and well-integrated blade implants in two patients. The axial CT views reveal intimate contact between the host bone and the metal. There is no lucent zone surrounding the implant to suggest failure of osseointegration. These images suggest that there is bone growing through the fenestrations in the implant. The excellent position of the implant with respect to the alveolar nerve is clearly demonstrated on the three-dimensional rendering.

The patient in Figures 6-16a and 6-16b also has a blade implant in place in the posterior portion of the mandible. There is, however, a wide zone of lucency surrounding the implant. There is no longer intimate contact between the bone and the blade. This appearance is characteristic of the failed or failing blade implant. Fibrous tissue, rather than bone, surrounds the implant. If there are symptoms related to the implant, it should be possible to remove this implant since it is not anchored in the bone. Removal will not add significantly to the amount of bone loss already obvious on the CT scan. Once there is bone healing around a blade, and especially if the blade osseointegrates into the bone, it becomes a challenge to remove the implant if there are problems with it.

Figures 6-17a and 6-17b present the scans of a patient who had a successful blade implant. The post supporting the prosthesis broke, and it was considered necessary to remove the blade. The scans demonstrate loss of the lingual surface of the bone where the excision was performed. The cortical bone along the buccal surface is missing.

Figs 6-15a to 6-15d *Well-positioned and well-integrated blade implant.*



Figs 6-15a to 6-15c Computerized tomography reformations reveal excellent contact between the blade and the bone. A small black band extends between the fenestrations in the blade because of beam-hardening artifact.

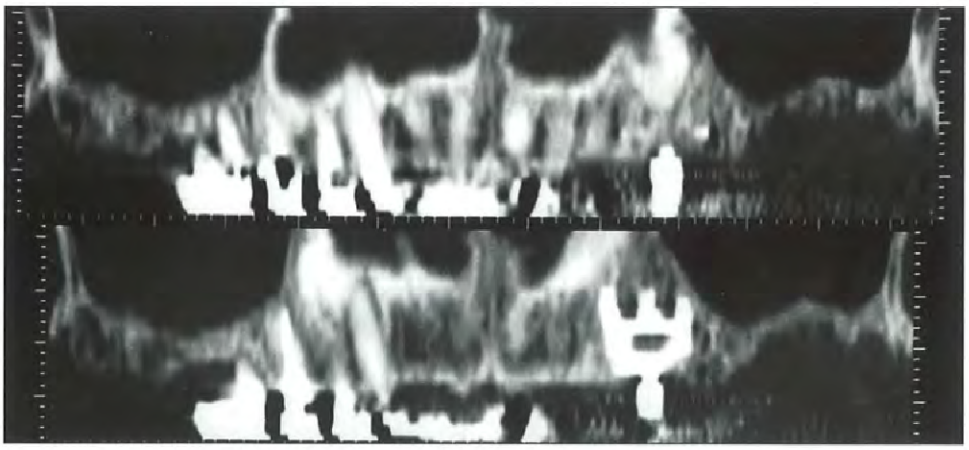


Fig 6-15b

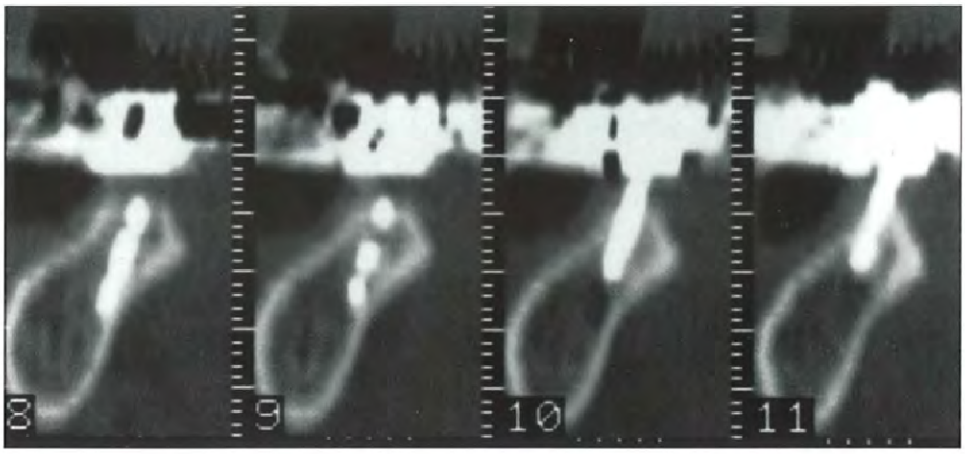


Fig 6-15c

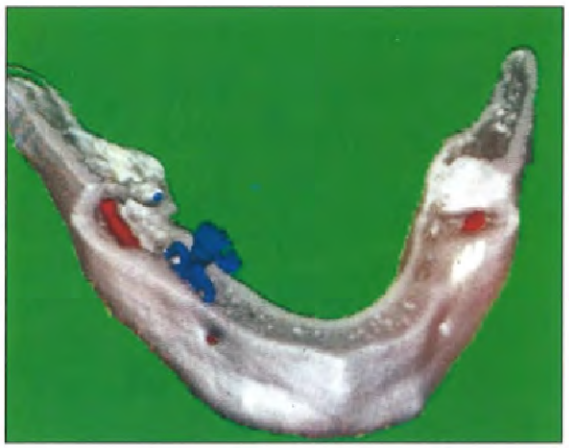


Fig 6-15d Three-dimensional reconstruction of the same case. Note the position of the implant *(blue)* buccal and rostral to the alveolar nerve *(red)*.





Figs 6-16a and 6-16b The failed blade implant. Three-dimensional reconstructions and CT reformations reveal lucency surrounding the implant.

Figs 6-17a and 6-17b *Mandible following blade removal. The apical portion of the mandible is thinned where an osteotomy was performed. A portion of the buccal cortical plate has been removed.*

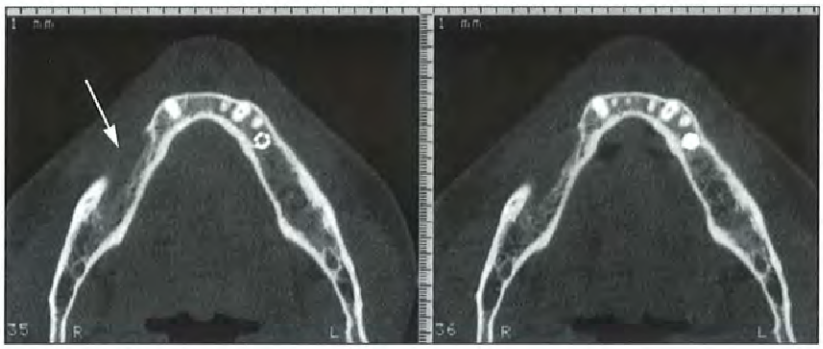


Fig 6-17a Axial reformations.

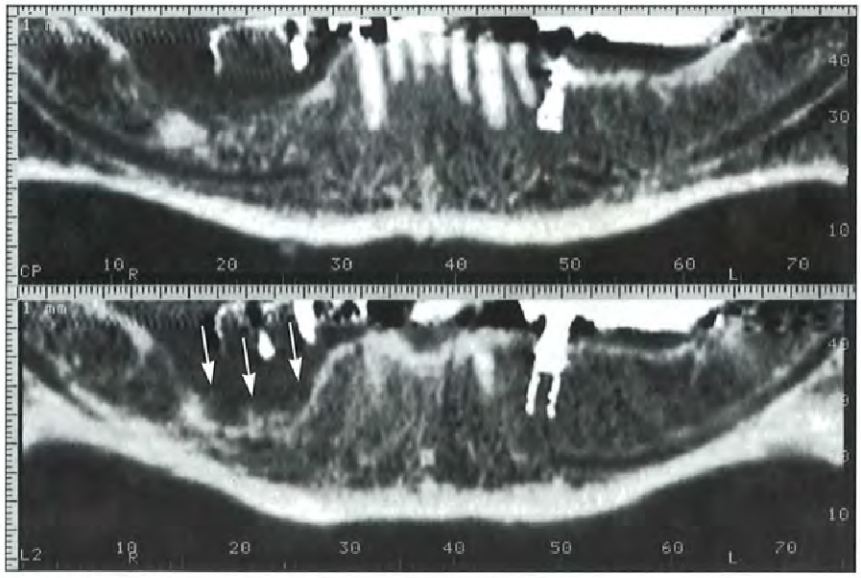


Fig 6-17b Panoramic reformations.

Evaluation of Subperiosteal Implants

Subperiosteal implants are metallic constructs made to fit over the mandible below the periosteum. They act as support for a removable prosthesis. These procedures are rarely done in recent years, since the popularization of root form osseointegrated implants. Various surgical techniques for subperiosteal implantation of mandibular prostheses have been available since the 1950s.

Most commonly, the fabrication and placement of a subperiosteal implant has required two surgical procedures. In the first operation, the mandible is exposed and an impression is made of the bone. The soft tissues are then closed and left to heal. A cast of the mandible is made from the impression, and the prosthesis is constructed on the cast. A second surgical procedure is required to implant the device about the mandible.

In recent years, the CT scanner has been used to create a true three-dimensional model of the mandible to be used instead of a cast derived from the first surgery. The patient undergoes a CT scan in a manner similar to that which has been previously described. The CT scan data are then sent to a model manufacturer, who generates a life-sized model using a computer and a computer-controlled milling machine (Figs 6-18a to 6-18c). The model is then used to fabricate the prosthesis. This eliminated the need for one operation. These models have been found to fit quite well.

Figs 6-18a to 6-18c *Subperiosteal implants.*



Fig 6-18a Computer-generated model of the mandible.



Fig 6-18b Second model with the finished subperiosteal implant that has been made for it.



Fig 6-18c Three-dimensional CT image from the front generated from a patient in whom a subperiosteal implant *(purple)* has been implanted. The upwardly projecting poles support the removable prosthesis, which was not in the patient's mouth during the CT scan. Note the remarkable atrophy of the mandible.

Evaluation of the Surgically Enhanced Jaw

In many patients, the alveolar process is so atrophic that it will not support an implant. Numerous surgical procedures have been described to enlarge the bone. The radiology of the enhanced jaw is the subject of Chapter 5. The appearance of successful and failed implants in the enhanced jaw is discussed at the end of that chapter.

Evaluation of Other Metallic Surgical Hardware

The metallic materials most commonly seen on CT scans of the jaw are silver amalgam restorations and gold crowns. These materials cause artifacts on the CT scan because of their ability to absorb nearly all of the x-ray striking them. The more metal within the scanned slice of tissue, the larger the artifact. It is possible, with strict attention to technical detail during the scan, to exclude restorations and crowns from the images. The artifacts then project away from the alveolar bone and do not interfere with the interpretation of the scans.

Stainless steel pins are used in endodontics as support for treated teeth. These pins traverse the root of the tooth and, therefore, must be present on the axial CT slices through the bone, regardless of the position of the patient. The artifact from a single pin does not degrade the image sufficiently to make the CT uninterpretable (Fig 6-19). The greater the number of pins, the more intrusive the artifact that will be present. The presence of more than three pins in the same arch will make the scans difficult, but not usually impossible, to interpret.

Surgical screws, wires, and plates made of metals other than titanium have been used throughout the years. These devices will produce artifacts that will degrade the images. Nevertheless, their presence does not absolutely contraindicate the use of CT.

Titanium is becoming the metal of choice for many intraoral appliances. The presence of these implants does not degrade the CT images. Several examples of titanium surgical appliances follow.

A lesion of the posterior mandible was removed from the patients shown in Figures 6-20a to 6-20c. A dowel-shaped prosthesis supported by a titanium mesh was placed in the bone. An increasing concavity began to form on the left side of the patient's face. Mastication was becoming difficult. A CT scan of the entire mandible was performed. The data were displayed three dimensionally for evaluation of the dowel and mesh. The images indicate that the dowel has broken near the center and has buckled medially. It is still contained within the titanium mesh. Appropriate surgical correction can be made based on the information on the images. There is no metallic artifact from the mesh or from the dowel graft.

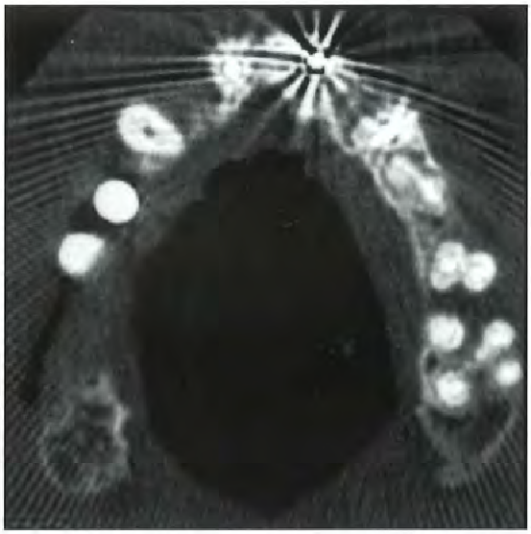
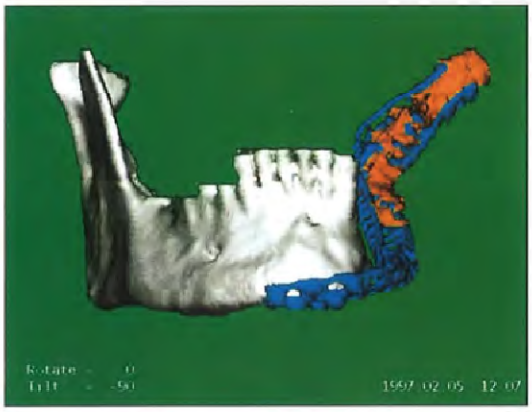


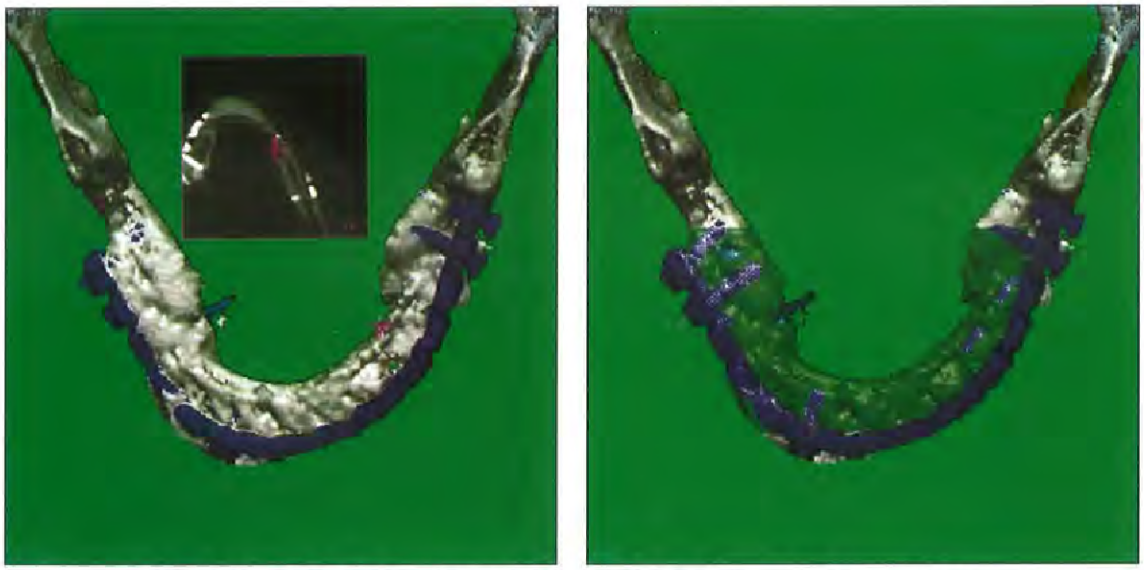
Fig 6-19 Artifact from interosseous pins. Axial CT scan showing streak artifacts emanating from a single pin implanted within a tooth.







Figs 6-20a to 6-20c Fractured dowel graft *(orange)* supported by titanium mesh *(blue)*. The graft has buckled inward, deforming the face.



Figs 6-21a and 6-21b Curved titanium plate *(purple)* attaching an iliac bone graft to the atrophic mandible. Multiple titanium screws fix the iliac graft to the posterior lingual side of the bone.

The patient in Figures 6-21a and 6-21b had a curved titanium support attached to the mandible with a series of screws placed at intervals around the jaw. An iliac bone graft has been placed along the lingual side of the bone on the right. This graft has successfully fused to the remainder of this very atrophic mandible. The posterior portion of the mandible has been expanded in such a way that it can now support an series of posterior implants.

A CT scan (Figs 6-22a to 6-22d) was performed prior to definitive therapy for a patient who presented at age 14 years with a history of having had an infection in the area of the temporomandibular joint as an infant. The joint underwent spontaneous ankylosis. The child had been unable to open her mouth for years. The CT images reveal total ankylosis of the right temporomandibular joint. The mandible, the zygoma, and the temporal bone are fused into a single bony unit. The left temporomandibular joint is present but atrophic. A CT scan at age 16 years, made following bilateral temporomandibular joint reconstruction, reveals successful bilateral titanium joint prostheses. The sagittal three-dimensional reformations show the articulation between the new titanium condyle and a crescentic plate of titanium forming the re-created articular fossa.

Figs 6-22a to 6-22d *Bilateral temporomandibular joint replacements.*

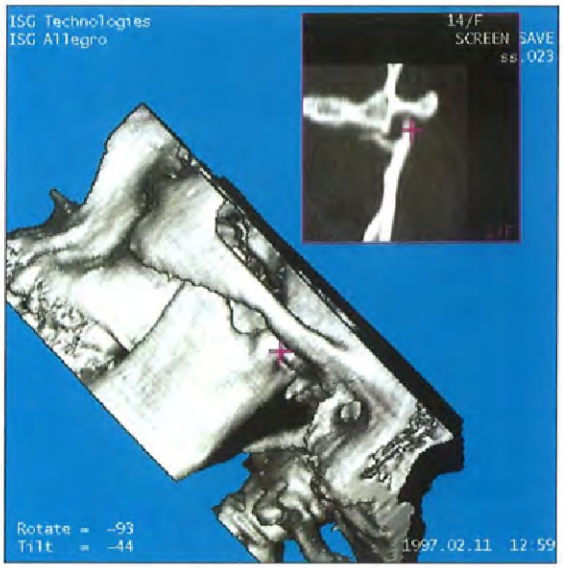


Fig 6-22a Right side of the face preoperatively. There is ankylosis of the mandible to the temporal bone.

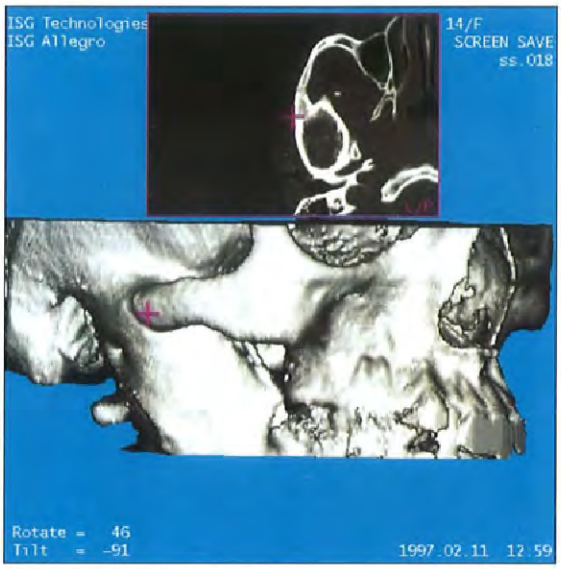
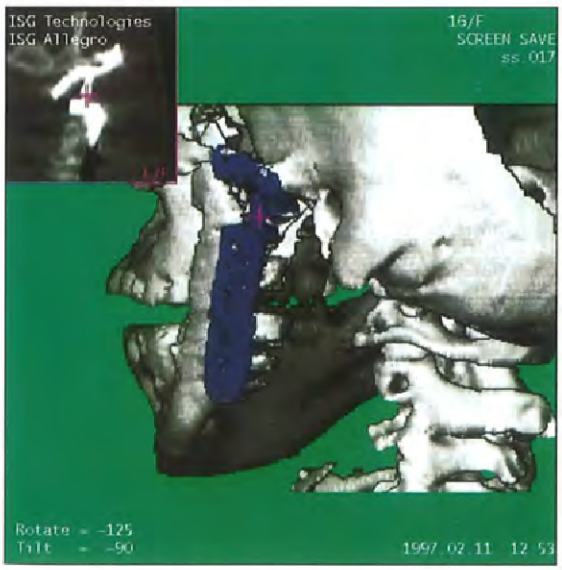


Fig 6-22b Left side of the face preoperatively. The temporomandibular joint is present but atrophic.





Figs 6-22c and **6-22d** Postoperative views of the joints, displaying the titanium prosthesis *(purple)*. Note the position of the new condyle in the reformed joint fossa.

Conclusion

Evaluation of most implant patients by the usual dental CT reformations does not prove to be difficult. Complex cases often require three-dimensional renderings to help define the anatomy. Although it is possible for some individuals who are very visually oriented to create a mental image of the anatomy from the planar reformations alone, most people are aided by the three-dimensional graphic displays.

For the most part, metallic materials in the mouth will not interfere with dental CT images. Nontitanium plates, wires, pins, and screws will produce some artifact on the scans but, in most cases, will not degrade the images sufficiently to preclude the use of diagnostic CT scanning.

References

1. Steinemann SA. The properties of titanium. In: Schroeder A, Sutter F, Krekeler G (eds): Oral Implantology. Stuttgart, Georg Thieme, 1991:37–58.
2. Mason M, Triplett R, VanSickles J, Parel S. Mandibular fractures through endosseous dental implants: report of cases and review. J Oral Maxillofac Surg 1990;18:311–317.
3. Tolman DE, Keller EE. Management of mandibular fractures in patients with endosseous implants. Int J Oral Maxillofac Implants 1991;6:427–436.
4. Rothman SLG, Schwarz MS. High resolution computerized tomography and nuclear bone scanning in the diagnosis of postoperative stress fracture of the mandible: a clinical report. Int J Oral Maxillofac Implants 1995;10:765–768.



Nonimplant Uses for Dental Computerized Tomography

James W. Borrow, MD / Justin P. Smith, MD

The inherent inaccuracy of using plain radiographs to evaluate the bony anatomy of the jaw is well established.[1,2] Technical factors contributing to this problem include varying degrees of distortion, blurring, and the overlap of other structures of the maxillofacial region and skullbase with dental anatomy on panoramic radiographs (panelipse). Dental multiplanar reformatted computerized tomography (CT) is recognized as the most accurate method of portraying the three-dimensional anatomy of the jaw[3-5] and has become an invaluable part of presurgical planning for the dental implant specialist.

The accuracy of dental CT in depicting mandibular and maxillary anatomy has prompted a number of authors to assess its utility in the evaluation of pathologic conditions affecting the mandible and maxilla. This chapter will review the nonimplant applications of dental CT in evaluating the following:

1. Impacted and unerupted teeth
2. Odontogenic cysts
3. Nonodontogenic cysts
4. Lingual mandibular bony defects
5. Mucoceles of the maxillary sinuses and large cystic lesions of the maxillary alveolar process that expand into the maxillary antrum
6. Fibrous dysplasia and ossifying fibroma affecting the jaw
7. Carcinomatous invasion of the mandible
8. Osteomyelitis affecting the jaw

The reader is referred to other sources for a general review of imaging methods other than dental CT as they apply to the wide spectrum of normal variants and pathologic processes that affect the jaw.[6-9]

Evaluation of Unerupted and Displaced Teeth

The longitudinal inclination of impacted and unerupted teeth and their relationship to adjacent structures are important factors for the oral surgeon and orthodontist to know when developing a treatment plan. Both conventional axial and reformatted dental CT are superior to panoramic radiography for visualizing the internal position and inclination of unerupted teeth, for the diagnosis of contact between teeth, and in cases of clearly visible or doubtful resorption of adjacent roots.

Figs 8-1a and 8-1b *Impacted mandibular left and right third molars in an adult male.*

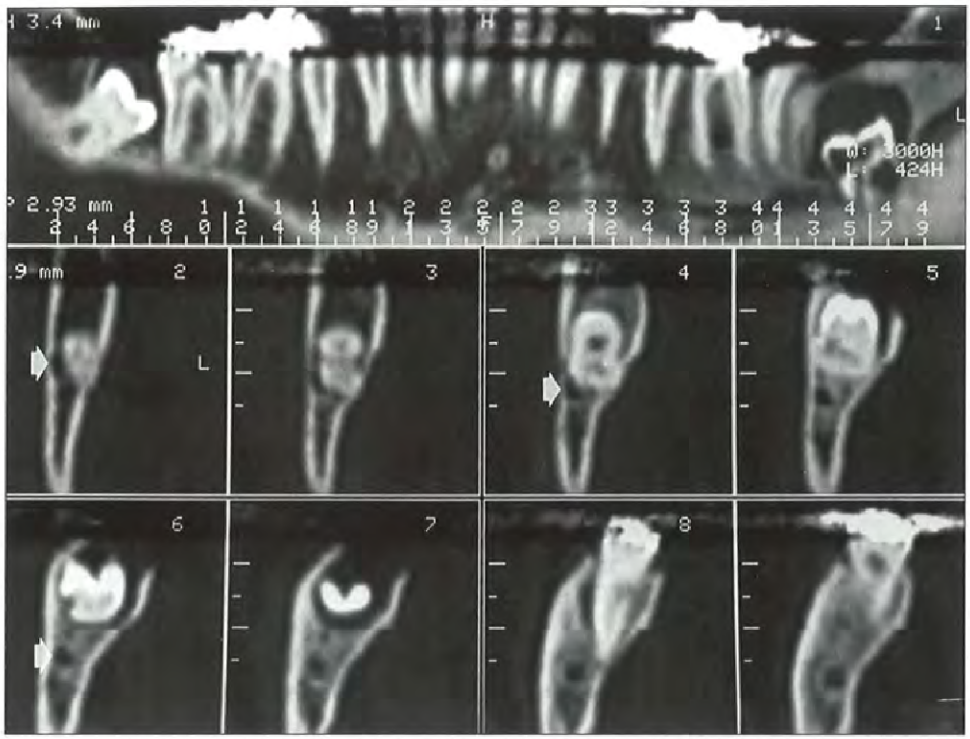


Fig 8-1a Cross-sectional dental CT images show the course of the mandibular canal *(arrows)* relative to the impacted right third molar.

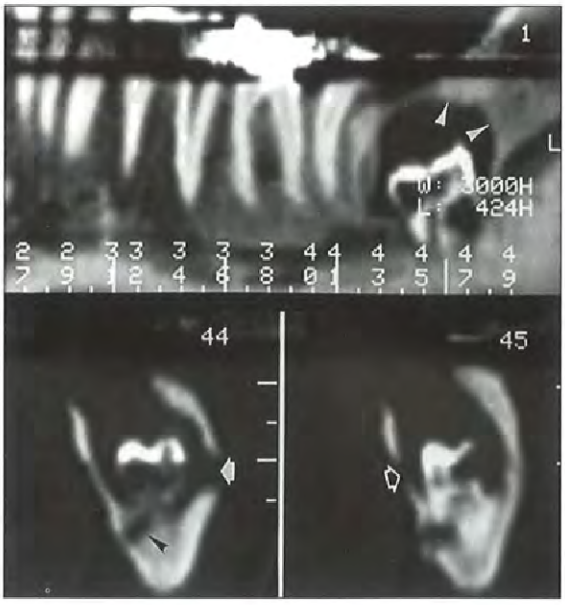


Fig 8-1b In an enlarged section of the curved coronal reformatted image in Fig 8-1a, reactive sclerosis is evident in medullary bone around the infected, impacted left third molar *(white arrowheads)*. A bone biopsy with culture would be needed to determine whether or not this is chronic osteomyelitis. Cross-sectional dental CT images show focal defects along the buccal *(solid arrow)* and lingual *(open arrow)* aspects of the alveolar process. This is particularly important information for the oral surgeon. The mandibular canal passes beneath the impacted tooth along the lingual aspect of the alveolar process *(black arrowhead, image 44)*.

Cross-sectional, life-sized images in particular show the surgeon the precise buccolingual and craniocaudal positions of involved teeth, the exact location of the mandibular canal, the amount of surrounding trabecular bone, and the exact relationship of affected teeth to adjacent structures[10] (Figs 8-1a and 8-1b). This information has therapeutic implications for both the oral surgeon and orthodontist. While panoramic radiography is still the imaging modality of choice for most patients with impacted or unerupted teeth, dental CT can be a valuable tool in complex cases, particularly if there is a question of resorption of neighboring roots.[10]

Evaluation of Cysts

Odontogenic cysts are lesions of the maxillary arch or mandible that develop from dental epithelium.[8] Dental CT has been used to evaluate the following types of odontogenic cysts:[7,8,11,12,16,17]

1. Radicular (periapical) cysts
2. Dentigerous cysts
3. Odontogenic keratocysts
4. Residual cysts

The radicular cyst (Figs 8-2a and 8-2b), the most common odontogenic cyst, originates from a periapical granuloma associated with the apex of a nonvital tooth.[7] Expansion of the cyst may be associated with displacement of tooth structures, and slight resorption of adjacent roots may occur. There is a continuum between periapical granulomas and radicular cysts; the former generally is smaller than 1.5 cm.[8]

The residual cyst is histologically the same as a radicular cyst but is not associated with a tooth. It may be a radicular cyst that was not removed when a nonvital tooth was extracted, or it may form from a bit of epithelial tissue that remained following an extraction.[7]

The dentigerous cyst (Fig 8-3) is the second most common of the odontogenic cysts[7] and is the most common developmental odontogenic cyst.[11] Most dentigerous cysts are located in the posterior mandible or maxillary canine area and form around the complete or partial crown of an unerupted tooth.[11] Their size varies greatly, and large cysts may cause marked expansion of the jaw and may expand into the maxillary sinus if located in the maxilla. They are most often unilocular, but can be multilocular, and may be associated with tooth displacement and apical root resorption.[8] Rarely, odontogenic tumors such as ameloblastoma may form along the walls of a dentigerous cyst (mural ameloblastoma). Cystic lesions that may have a similar appearance include mural ameloblastomas and odontogenic keratocysts associated with unerupted teeth.[7]

Radiographically, small unilocular dentigerous cysts may be difficult to distinguish from the normal follicle that surrounds the crown of an unerupted tooth. The feature that distinguishes the dentigerous cyst is the radiolucent space between the crown of the tooth and the margin of

Figs 8-2a and 8-2b *Radicular cyst.*

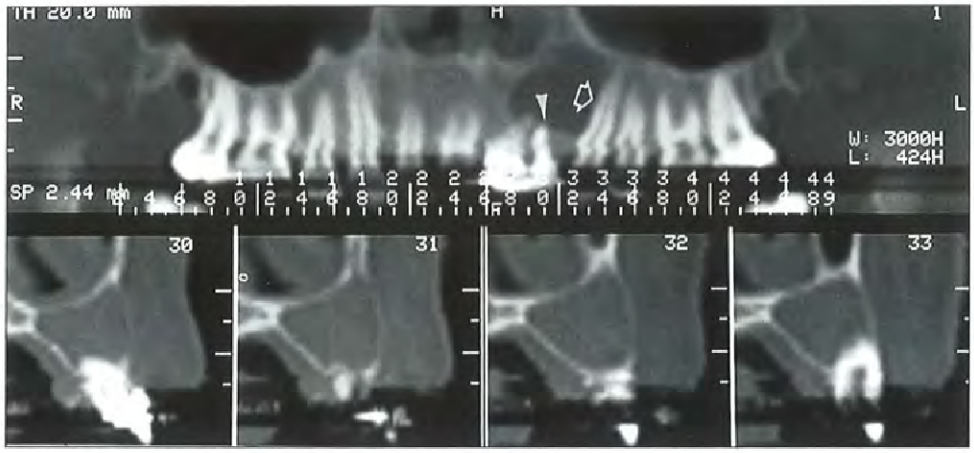


Fig 8-2a Curved coronal and cross-sectional reformatted dental CT images show a radicular cyst associated with a root canal at the left lateral incisor *(arrowhead)*. Expansion of the cyst has displaced the adjacent tooth *(open arrow)*. The labial and lingual cortices are intact on cross-sectional images *(lower row)*.

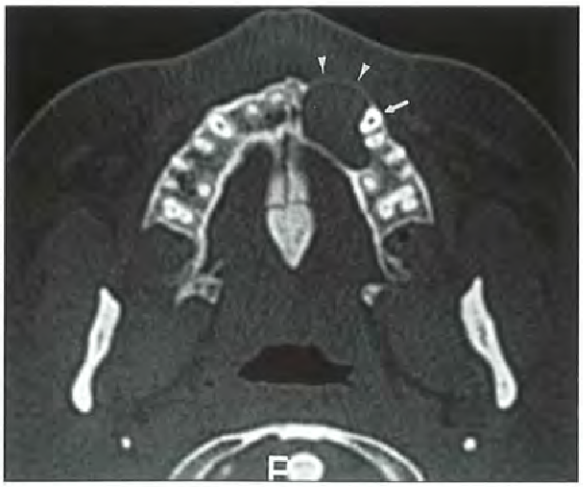


Fig 8-2b An axial 1-mm CT section shows the expanded, thinned labial cortex of the cyst *(arrowheads)*. Displaced tooth at the margin of the cyst is seen in cross section *(arrow)*.

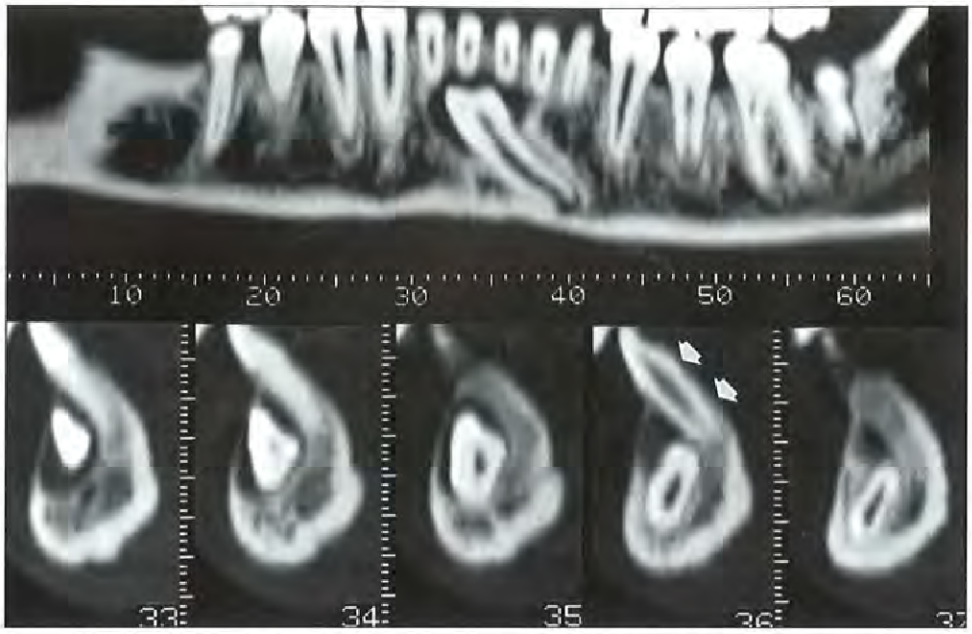


Fig 8-3 Dentigerous cyst. The curved coronal reformatted dental CT image shows a small, unilocular dentigerous cyst surrounding the crown of an impacted supernumerary tooth beneath the mandibular incisors. The apices of the incisors have not been resorbed, as suggested on the coronal image. Rather, this appearance is due to the thickness and position of the reformatted coronal image, which does not encompass the entire buccolingual/labiolingual dimension of the mandibular arch. Cross-sectional reformatted images show that the roots are intact and that the supernumerary tooth and cyst have rotated the long axis of the incisors in the labiolingual plane *(arrows)*. (Courtesy of Dr James Abrahams, Yale University School of Medicine.)

the cyst, which should not exceed 2.0 or 3.0 mm with the normal follicle.[9] Depending on its relationship with the erupting tooth, a dentigerous cyst may be classed as one of three variants: eruption cyst, circumferential dentigerous cyst, or lateral dentigerous cyst.[9]

The diagnosis of an odontogenic keratocyst is histologic. Odontogenic keratocysts associated with a tooth may be confused radiographically with dentigerous cysts, and otherwise odontogenic keratocysts may be confused with entities such as residual or fissural cysts, or with atypically located giant-cell granulomas or radicular cysts. The distinction is important because of the potential behavior of odontogenic keratocysts; recurrence rates of 20% to 60% have been reported after incomplete excision.[8]

Odontogenic keratocysts originate from rests of dental lamina and may be unilocular or multilocular; the latter have higher rates of recurrence. They are radiolucent, sharply marginated lesions that are commonly located in the body and ramus of the mandible and may be associated with marked cortical thinning and expansion as well as root resorption (Figs 8-4a and 8-4b). Multiple odontogenic keratocysts may be a part of the basal cell nevus syndrome.[8] Large odontogenic keratocysts in the maxilla may expand into the antrum and mimic a mucocele.[12]

Figs 8-4a and 8-4b *Odontogenic keratocyst.*

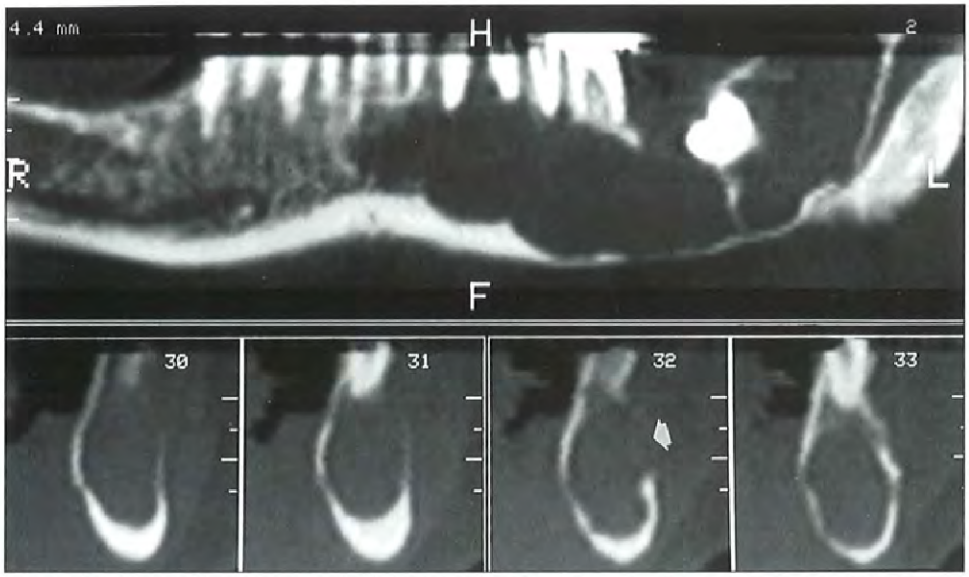


Fig 8-4a The preoperative dental CT (1990) displays extensive replacement of the medullary cavity of the body of the left hemimandible, with extension into the ramus. There is thinning of the cortex on both curved coronal and cross-sectional images, with disruption of the buccal cortex *(arrow)*.

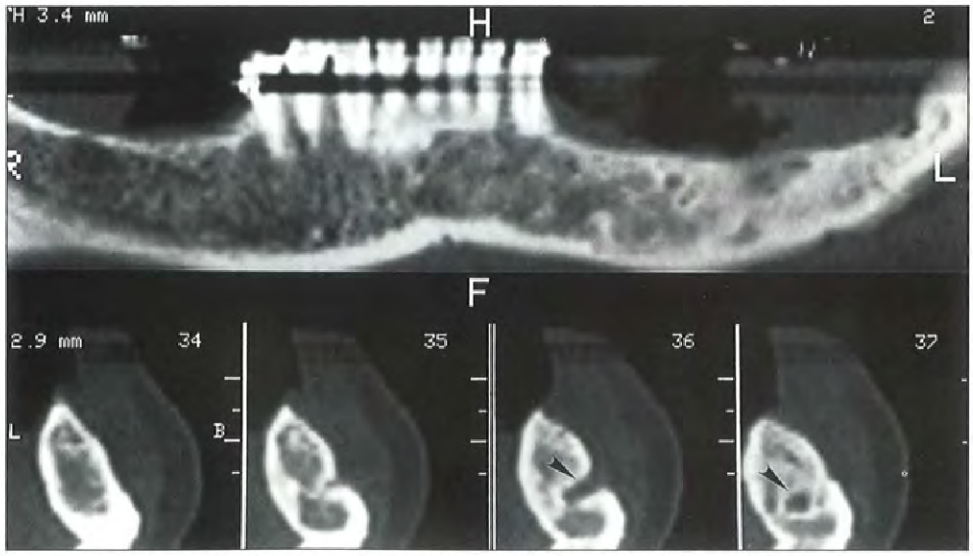


Fig 8-4b Dental CT 5 years after enucleation of odontogenic keratocyst (1995) shows extensive regeneration of medullary bone. The mandibular canal and the left mental foramen are visible on cross-sectional images 37 and 36, respectively *(arrowheads)*.

Evaluation of Nonodontogenic Cysts

The nonodontogenic cysts below have been evaluated with dental CT:[7,8,9]

1. Traumatic cysts
2. Nasopalatine cysts
3. Globomaxillary cysts
4. Giant-cell granulomas

The term *cyst* is a misnomer in the case of a traumatic cyst, because this lesion has no epithelial lining. It is a nonodontogenic cyst of uncertain origin, but it is believed to be the residue of an intramedullary hematoma.[8] These most often occur in the body of the mandible, are unilocular, and may be empty or filled with clear or serosanguineous fluid.[8] Computerized tomography may reveal scalloping, slight expansion of the medullary cavity with cortical thinning, and extension between the roots of the teeth without resorption (Figs 8-5a and 8-5b).[7]

Nasopalatine cysts (incisive canal cysts) are nonodontogenic cysts of the maxilla that originate as a proliferation of mucous or epithelial cells along the nasopalatine canal.[7] These small, paired canals, one on each side of the midline, carry the nasopalatine arteries and nerves and open immediately adjacent to the midanterior palate. Typically, nasopalatine cysts are asymptomatic and are found on routine dental radiographs. We have found that dental CT can be useful in delineating the three-dimensional anatomy of this lesion (Figs 8-6a and 8-6b).

Globomaxillary, or fissural, cysts are located along the incisive suture between the lateral incisors and the canines. They typically extend toward the alveolar ridge crest and may shift adjacent teeth. If a globomaxillary cyst extends over the root tip of an adjacent tooth or teeth, then the vitality of the involved tooth or teeth should be evaluated to distinguish the globomaxillary cyst from a radicular cyst.[8]

Central giant-cell granulomas typically occur in the mandible, usually anteriorly, and often cross the midline,[7] but one third of the cases reported in one study occurred in the maxilla.[9] Their imaging characteristics are nonspecific. The lesion shown in Figures 8-7a and 8-7b was somewhat atypical in location (right posterior mandible) but more typical in the age of the patient (mid-20s), because giant-cell granulomas are usually found in children and young adults.[7]

Histologically, central giant-cell granulomas (CGCG) are indistinguishable from giant-cell tumors (GCT) found elsewhere in the skeleton.[9] It has been suggested that there is a continuum between CGCG and GCT in the jaw, with CGCG representing less aggressive and GCT more aggressive forms of the same lesion.[9] Radiographic features of the more aggressive type include resorption of adjacent root tips, cortical perforation, and a diameter greater than 2 cm.[9] Aggressive lesions may also break through the cortex and expand into adjacent soft tissues. To add to the difficulty in diagnosing these lesions, brown tumors of hyperparathyroidism have an identical histology to CGCG and CGT, although they evolve as the manifestation of an entirely different condition.[9]

Figs 8-5a and 8-5b *Traumatic cyst.*



Fig 8-5a This unilocular lesion in the right hemimandible has displaced the mandibular canal inferiorly *(open arrows)*. The canal is better seen on cross-sectional dental CT images filmed at narrower settings than usual *(lower images)*, which show the canal more clearly, but factitiously increase the width of cortical bone ("bloom effect"). The upper row of cross-sectional images, filmed at normal settings, is shown for comparison. The distal and mesial roots of the mandibular right first and second molars *(arrowheads)* are surrounded by the cyst on the curved coronal reformatted image *(top)*, but are intact, which is typical of a traumatic cyst.

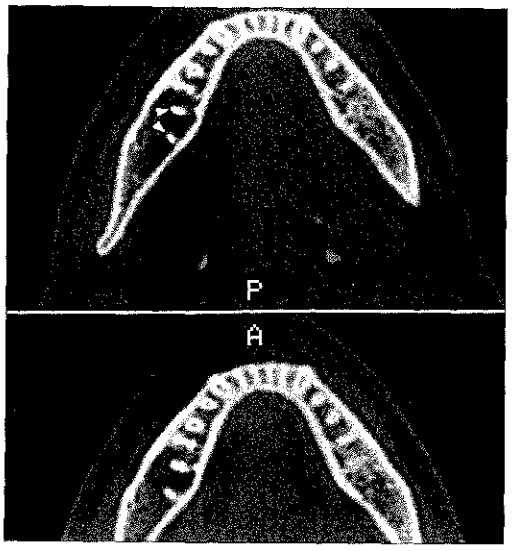


Fig 8-5b Axial 1-mm cross-sectional images from the dental CT show the rarefaction surrounding the distal root of the first molar and the mesial root of the second molar *(arrowheads)*.

Figs 8-6a and 8-6b *Nasopalatine cyst.*

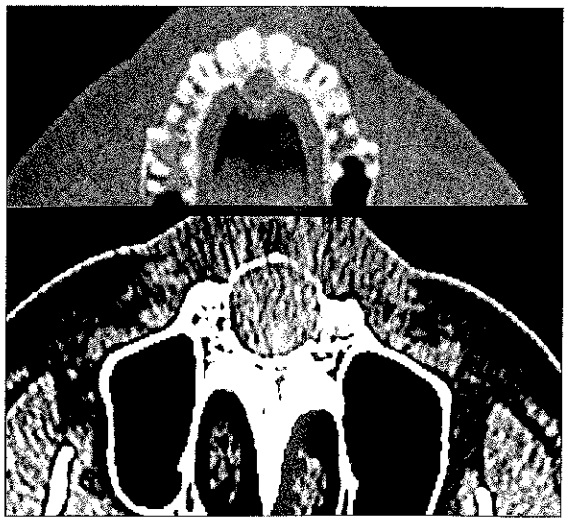


Fig 8-6a This expanded, cystic lesion, located directly behind the central incisors, is characteristic of a nasopalatine cyst *(top)*. Another axial 1.5-mm image, craniad to the first, above the roots of the incisors (enlarged and filmed at narrow settings), shows the expanded anterior maxillary cortex *(bottom)*.

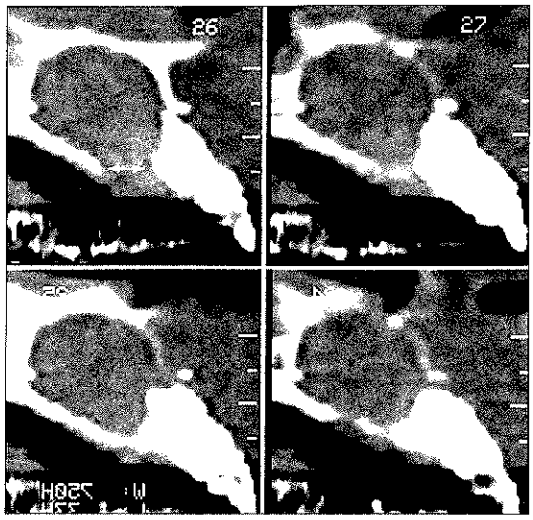


Fig 8-6b Cross-sectional dental CT images show the expanded nasopalatine foramina at the junction of the hard palate and maxillary alveolar process *(double arrow)*. The cyst lies craniad and posterior to the incisors. The orientation of the two bottom cross-sectional images has been reversed for continuity.

Figs 8-7a and 8-7b *Central giant-cell granuloma.*

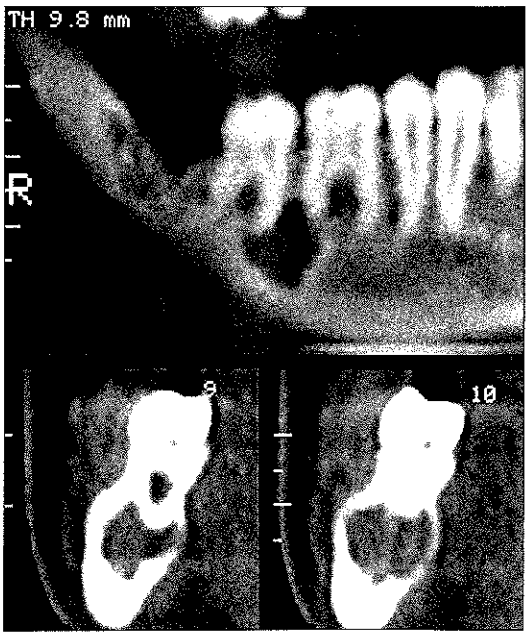


Fig 8-7a More typically a midline tumor of the mandible, the CT features of central giant-cell granuloma are nonspecific. Although the lingual cortex is thinned and expanded, it is intact. Resorption of root tips, cortical perforation, and a diameter greater than 2 cm are signs of the aggressive subtype of CGCG.

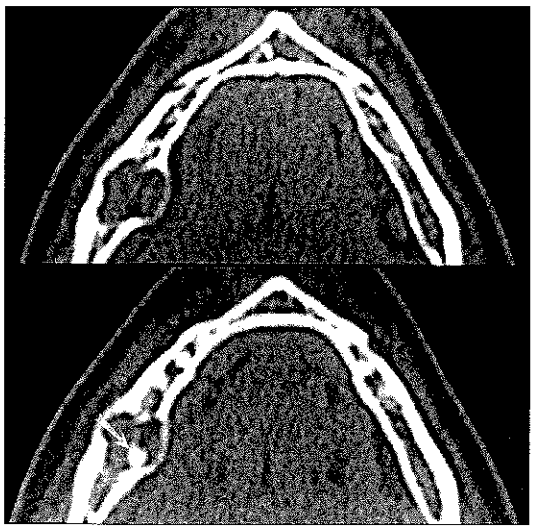


Fig 8-7b Axial 1.0-mm images show the mildly expansile cyst surrounding the mesial root of the right second molar *(arrow)*.

Evaluation of Lingual Mandibular Bony Defects

A lesion that may appear cystlike on plain radiographs is the misnamed Stafne cyst, which is, in fact, a corticated concavity along the lingual aspect of the jaw. On cross-sectional images, it is apparent that these are not true bone cysts. Rather, they are buccally oriented depressions along the lingual aspect of the posterior mandible that have no lingual cortex. First studied by Stafne in 1942, these are referred to by a number of different terms, including *Stafne cyst, Stafne's bone cavity, static bone defect,* and *submandibular salivary gland inclusion defect.* We prefer the more descriptive term, *lingual mandibular bony defect* (LMBD).[13] They occur predominantly in males (more than 80% of cases), are unilateral, and have an incidence of 0.1% to 0.48% in living series.[13]

Lingual mandibular cortical defects are clearly visible on conventional panoramic and reformatted coronal (panoramic) dental images, but, importantly, the defect in the lingual cortex that is the signature for their diagnosis can only be defined on the reformatted cross sections (Fig 8-8). They vary in size and shape, with most being oval, from 1 to 3 cm on their long axis, and have corticated margins. They are almost always located posteriorly, just anterior to the angle of the mandible. They are situated below the mandibular canal, which distinguishes them on panoramic radiographs from a traumatic cyst (which extends above the canal).[13] The size of the LMBD roughly correlates with its contents. Smaller, shallower defects contain fat, while larger defects (those that extend to the buccal cortex) typically contain salivary tissue that may or may not be a part of the submandibular ductal system.[14]



Fig 8-8 Lingual mandibular bone defect. An apparent cyst near the angle of the right hemimandible on the curved coronal reformatted dental CT image *(black arrow)* is shown to be a buccally oriented depression on the reformatted cross sections *(white arrow).* The concavity lies below the mandibular canal *(arrowheads)*, which is typical for an LMBD.

There is one report in the literature of another entity (osteomyelitis) masquerading as a posterior lingual mandibular bony defect on routine panoramic dental radiographs.[15] However, in that case, the patient noticed intermittent swelling near the angle of the jaw. Further evaluation with CT showed that the defect interrupted the inferior margin of the mandible and was associated with some adjacent sclerosis and an enlarged submandibular node. Because almost all lingual mandibular bony defects are asymptomatic (unless the contained salivary tissue is the source of pathosis), we believe that a symptomatic patient with what appears to be an LMBD on a conventional panoramic radiograph should be evaluated with CT. Oral carcinoma invading the mandible can also mimic the buccally oriented concavity of an LMBD, although there are important differentiating features (Fig 8-9).

Rarely, an LMBD may occur in the anterior mandible. The appearance of these lesions is more variable and may present a greater diagnostic challenge. Margins may be corticated or indistinct, and their location in the craniocaudal plane is variable. As with the posterior LMBD, the anterior variant occurs overwhelmingly (more than 85% of the time) in males.[13] Again, CT is critical in demonstrating the lack of cortical continuity along the lingual aspect. Lingual mandibular bony defects have also been rarely reported in the mandibular ramus.[13]

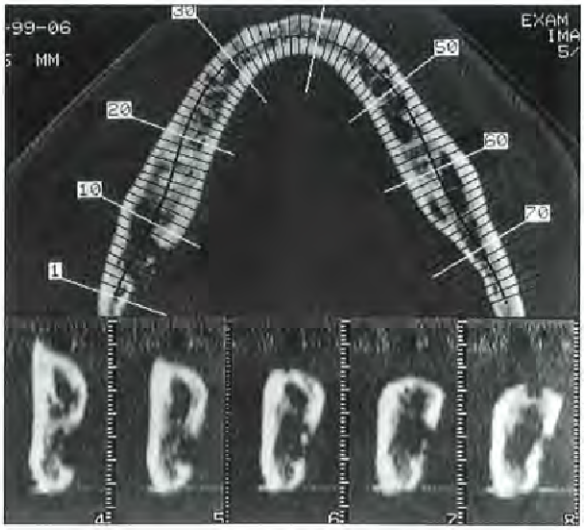


Fig 8-9 Carcinomatous invasion mimicking lingual mandibular bony defect. Local invasion of the lingual aspect of the distal right hemimandible is distinguished from an LMBD by lack of a corticated margin along the base of the buccally oriented concavity; irregular margins; and rarefaction extending into the medullary space with small isolated foci of bone. The numbers of cross sections along the bottom of the images correspond to the same-numbered location on the axial pilot image. (Courtesy of Dr James Abrahams, Yale University School of Medicine.)

Differentiation of Intra-antral and Extra-antral Cystic Masses of the Maxillary Sinus

Computerized tomography can be invaluable in determining whether large, cystic lesions of the maxillary sinus are intra-antral (eg, mucoceles) or extra-antral in origin (eg, nasopalatine cysts or odontogenic keratocysts).[12] The thin, expanded bony plate separating a lesion of extra-antral origin from the antral cavity will be visible on CT images (Fig 8-10). The caveat to this distinguishing feature will be those mucoceles that originate in septated or partially septated compartments of the maxillary sinus. The thin, bony walls of the septum may mimic the bony wall of a cyst that originates from the maxillary alveolar process.

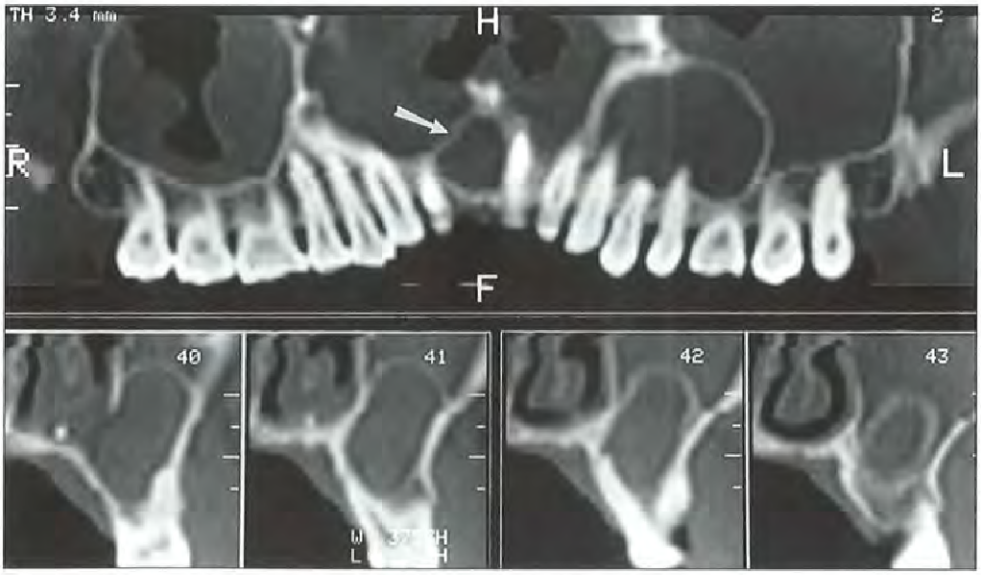


Fig 8-10 Left maxillary cyst. The thin, bony wall of the expansile cyst identifies its origin as the alveolar process rather than the mucosal lining of the sinus cavity. This patient also had severe sinus disease, indicated by prominent soft tissue thickening within the sinus cavity. Cross-sectional images 40 to 43 show the cyst in the buccolingual/labiolingual plane. A mesial extension of the cyst *(arrow)* is not completely seen on this thin-section coronal reformatted image.

It is apparent from the preceding examples that the detailed information derived from the three-dimensional images generated by a dental software program can be particularly valuable in evaluating cysts of the jaws, and cross-sectional reformatted CT images are especially useful.[16,17] The distance between the cyst and adjacent teeth, the mandibular canal, displacement of the neurovascular bundle, cortical involvement or erosion, and the relationship of expansile cystic masses of the maxilla to the nasal fossae or maxillary sinuses can be precisely defined on the reformatted cross-sectional and curved coronal images. Such information may help the surgeon minimize the risk of intraoperative hemorrhage and/or postoperative anesthesia by displaying the location of the neurovascular bundle. Identification of areas of thin or absent cortical bone allows the surgeon to assess the risk of intraoperative or postoperative fracture and whether bone grafts will be needed. When marsupialization of a large cyst is being considered prior to enucleation, identification of thinned or absent cortical bone may direct the surgical approach and prevent unnecessary bone loss. On occasion, the dental CT study may indicate the need for an extraoral rather than intraoral approach.[17] This is particularly relevant in regard to impacted teeth.[10]

Studies that have compared images generated by dental software packages with conventional dental radiographs of odontogenic cysts concluded that CT images significantly improve the identification of anatomy and lesions within the jaws. Dental CT imaging is essential at least in the evaluation of large cysts, where accurate three-dimensional information is imperative for surgical planning.[16,17]

Evaluation of Fibrous Dysplasia and Ossifying Fibroma

Fibrous dysplasia is classified as a hamartomatous, nonneoplastic developmental lesion of bone in which normal bone is replaced by fibro-osseous tissue.[9] There are two varieties, monostotic and polyostotic; the monostotic form is much more common than the polyostotic variety. The jaws are involved more frequently in the monostotic form, with the maxilla much more often affected than the mandible.[9]

Fibrous dysplasia has a wide spectrum of radiographic appearances, ranging from radiolucent to radiopaque to mixed, but mixed radiolucent-radiopaque lesions are the most frequent manifestation of fibrous dysplasia in the jaws[9] (Fig 8-11). Areas of radiolucency in a variety of shapes, with or without a variable, incomplete sclerotic margin, may be present, or the radiolucency may be multilocular. Radiolucent areas will be interspersed with sclerotic tissue, ranging from a ground glass to stippled to a dense, homogeneous appearance.[9] Computerized tomography may be particularly useful when fibrous dysplasia involves the maxilla. As with fibrous dysplasia elsewhere in the body, there is a risk of malignant transformation.[9]

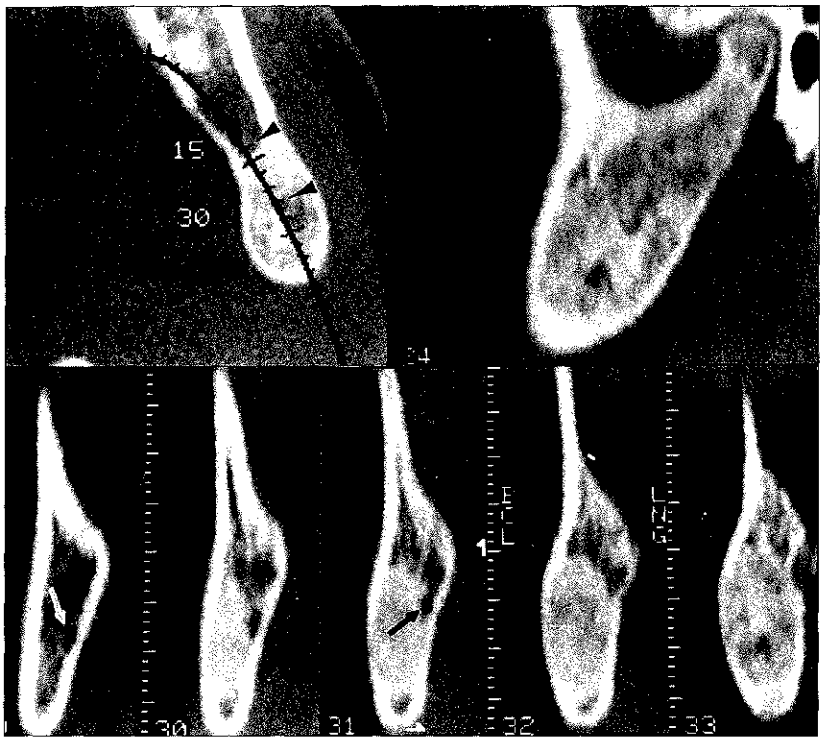


Fig 8-11 Fibrous dysplasia. A relatively dense form of fibrous dysplasia involves the left ramus of the mandible, including the head and neck of the condyle *(upper right)*. Cross sections along the bottom show the transition from involved to normal bone *(right to left)*. The mandibular canal is visible on some cross sections *(black and white arrows)*. The locations of the cross-sectional reformatted images are indicated by black arrowheads on the enlarged section of the axial CT image *(upper left)*.

Ossifying fibroma (Figs 8-12a and 8-12b) may present with a variety of appearances and may be confused with fibrous dysplasia. Ossifying fibroma occurs overwhelmingly in the mandible (70% to 89%).[9] The two most prevalent patterns are (1) a unilocular lucency with dense foci of calcification, ground glass opacification, or irregular opacification; and (2) a well-defined radiolucency without radiopaque foci, root displacement, or resorption. These two patterns accounted for 67% of cases studied in one series.[18] Less frequent appearances include massive, expansile lesions with well-defined margins containing ground glass or mottled radiopacities. These were classed as active or aggressive ossifying fibromas.[18] One primary difference between ossifying fibroma and fibrous dysplasia is the well-demarcated margin of the former and the lack of a well-defined margin with the latter.[9] In addition, ossifying fibroma tends to grow in a centrifugal or ball-like fashion, while fibrous dysplasia grows linearly.[9]

Figs 8-12a and 8-12b *Ossifying fibroma, left maxilla.*

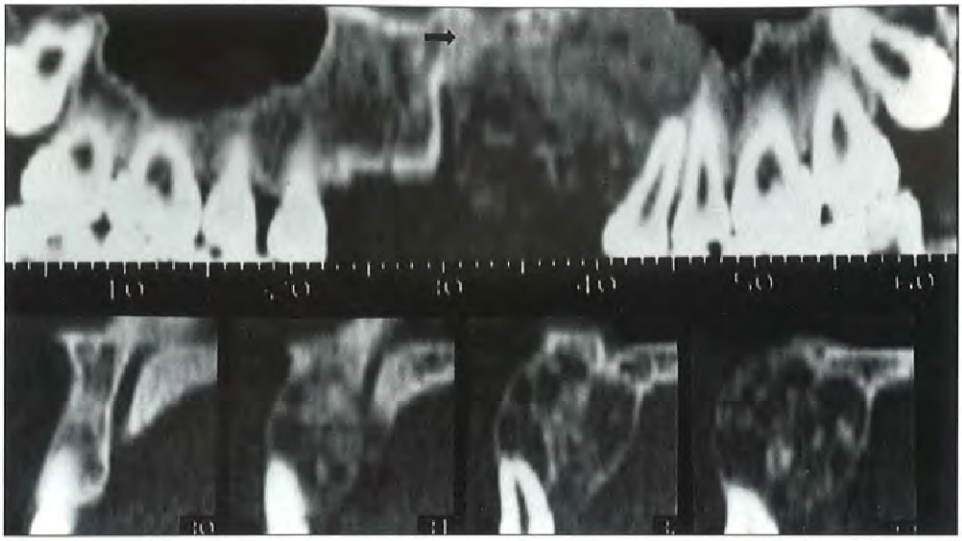


Fig 8-12a Although the majority of ossifying fibromas present in the mandible, this lesion was found in the maxilla. The lesion does not cross the intermaxillary suture *(arrow).* The expansile growth has displaced and angulated the adjacent tooth *(left first premolar)* laterally.

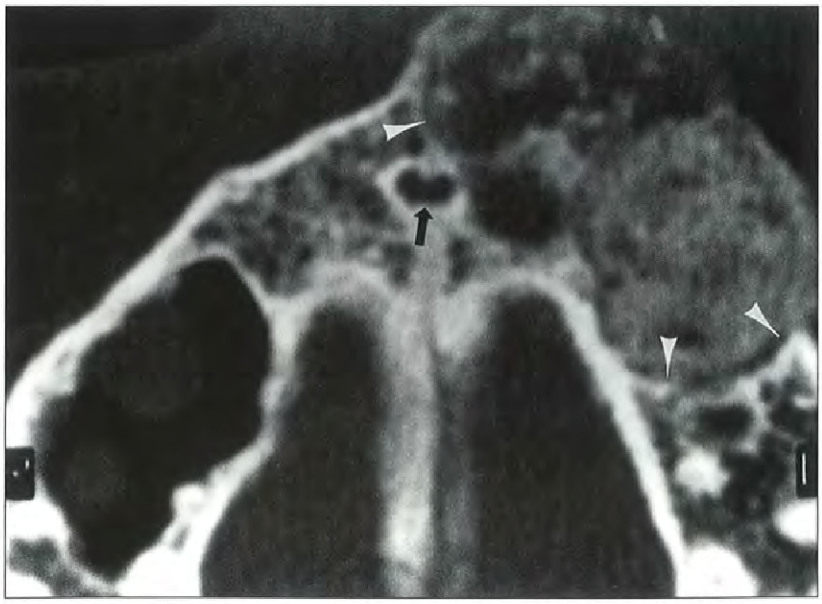


Fig 8-12b An axial 1.5-mm-thick image illustrates several features that help distinguish an ossifying fibroma from fibrous dysplasia: (1) clear demarcation between involved and uninvolved bone *(arrowheads);* and (2) centrifugal instead of linear growth with equal expansion in all directions. This ossifying fibroma exhibits two distinct types of calcification of the matrix. The paired nasopalatine canals are spared *(arrow).*

In one of our patients, regenerating bone at the site of an extirpated cyst mimicked fibrous dysplasia (Fig 8-13), while in another, ossification of a sinus lift and bone graft for implant placement looked much like an ossifying fibroma (Figs 8-14a and 8-14b). Both of these cases illustrate the importance of correlating clinical history with the dental CT.

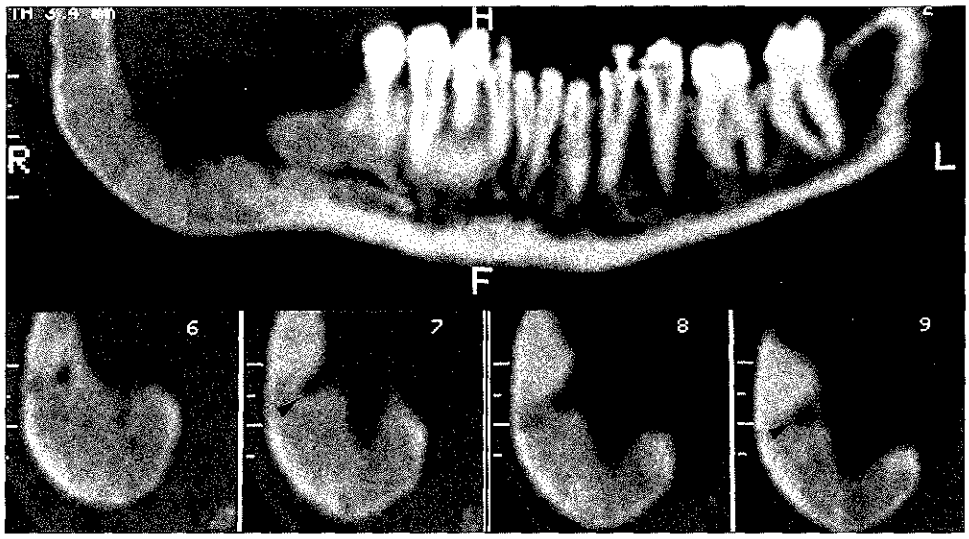
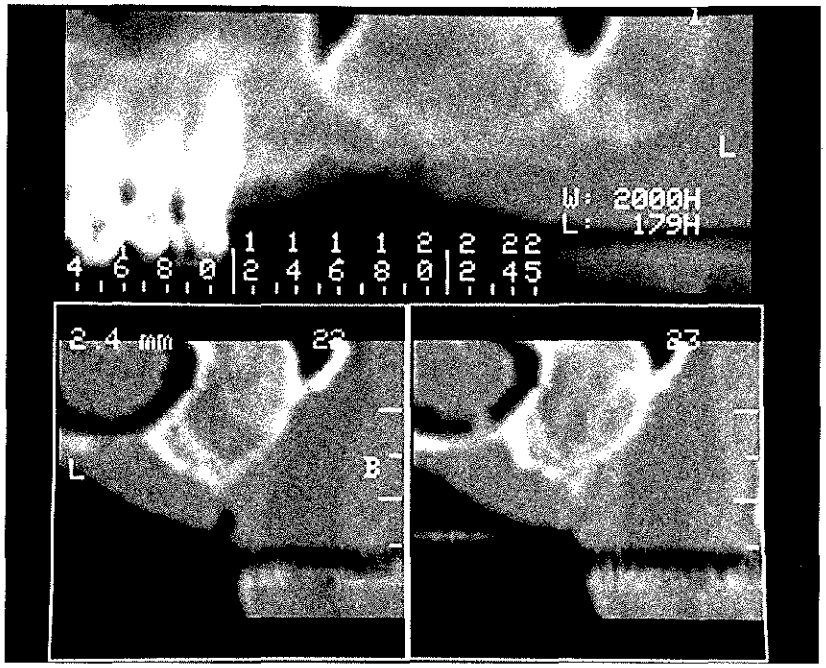


Fig 8-13 Regenerating bone mimicking fibrous dysplasia. Diffuse, sclerotic reparative bone fills the defect in the right hemimandible of an adult female after enucleation of a unilocular ameloblastoma. The mandibular canal *(arrowheads)* can be followed along the margin of new bone. This appearance might be mistaken for fibrous dysplasia. (Courtesy of Dr Philip Worthington, University of Washington.)



Figs 8-14a and 8-14b Sinus lift with autologous bone graft mimicking an ossifying fibroma. A key feature in this case is the linear, rather than centrifugal, pattern of the new bone. Ossifying fibromas tend to expand equally in all directions; thus the lesion should be spherical rather than elongated.



Evaluation of Carcinomas of the Mandible and Maxilla

Bony involvement of the mandible or maxilla by carcinoma of the oral cavity has grave implications for the surgeon and the patient; partial or complete resection of the mandible or maxilla can have profound functional and esthetic consequences, but failure to resect involved bone results in the progression of disease.[19] Because invasion of the mandible occurs by direct contact rather than by lymphatic spread,[20,21] tumor control without mandibular resection might be possible if it can be shown that bone is not involved.

A cooperative study published in 1994[19] made several important points. First, in their group of patients, CT findings of bony erosion were more accurate as a predictor of malignant involvement than was evidence of cortical erosion and/or marrow enhancement depicted on magnetic resonance imaging scans. Second, CT findings and primary tumor location considered sequentially (in a decision tree developed by the authors) yielded a 46% positive predictive value (PPV), compared to the 39% PPV of current standard staging practice, and, more importantly, had a 100% negative predictive value (NPV) when their criteria were used. Evaluation on the basis of CT results alone yielded a 73% PPV and a 69% NPV.

Tumor locations not associated with mandibular involvement corroborated by a CT scan that was negative for bone involvement included tumors of the tongue, buccal surface, and oropharynx. Tumor location that was associated with a significant chance of bony tumor involvement in spite of a negative CT scan included tumors of the alveolar gingiva, retromolar trigone, floor of mouth, labioalveolar/buccoalveolar sulcus, and tonsil. Because the CT scans used were standard, contrast-enhanced evaluations in the axial plane without the addition of a dental CT protocol, the addition of dental CT to their decision algorithm might have resulted in a higher degree of certainty as to the presence or absence of bony involvement.

Results of another study did imply that dental CT is helpful in determining maxillary or mandibular involvement in patients with oral carcinoma.[22] This may particularly be true in patients with subtle erosive changes. Our own experience suggests that dental CT may also be helpful in evaluating bony invasion in patients with recurrent tumor (Figs 8-15a and 8-15b). However, whether this will hold true for larger numbers of patients with recurrent tumor who have had surgery, chemotherapy or radiation therapy, or (as is often the case) combination therapy, is yet to be determined.

Figs 8-15a and 8-15b *Adult male with recurrent oral carcinoma.*

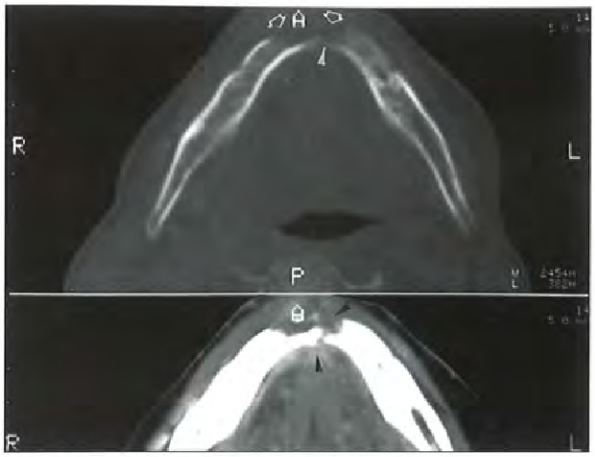


Fig 8-15a Axial 5-mm images display involvement of the anterior mandible. Bone and soft tissue settings highlight widespread erosion of the labial margin and focal erosion of the lingual margin *(open arrows and white arrowhead)* and the soft tissue component along the labial and lingual aspects of the anterior mandible *(black arrowheads)*.

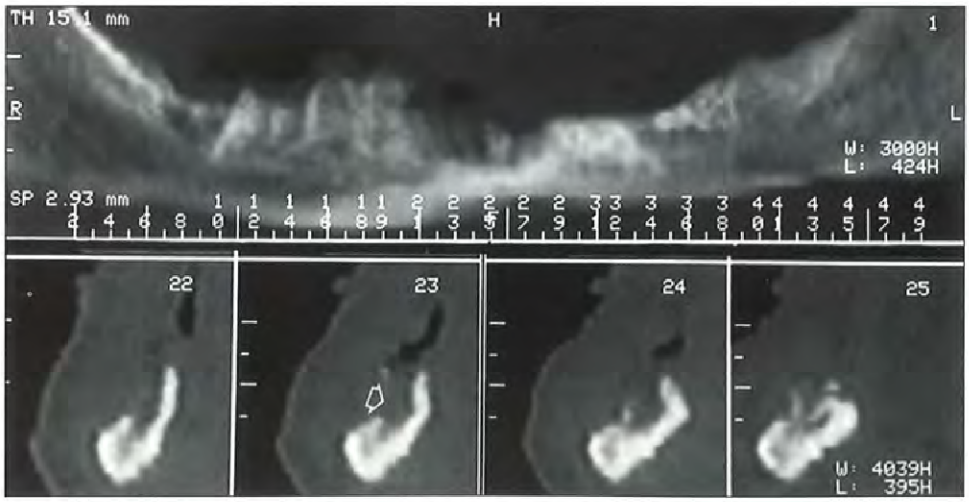


Fig 8-15b Cross-sectional images better show the extent of erosion along the labial aspect of the alveolar process *(open arrow)*. The focal erosion along the superior lingual margin visible on the axial image is evident on cross-sectional image 25.

Evaluation of Osteomyelitis

For a number of patients, we have also found dental CT to be a valuable addition to the assessment of osteomyelitis involving the jaws. Besides allowing precise determination of the extent and degree of bony erosion, the reformatted and curved coronal images display the relationship of the infection to vital structures such as the mandibular canal. This is particularly important in those patients with facial pain that is not clearly typical for inferior alveolar nerve involvement (Figs 8-16a to 8-16c).

Figs 8-16a to 8-16c *Adult female with a possible left submandibular mass or osteomyelitis. The patient had a history of endodontic procedure, periapical abscess, and subsequent extraction of the mandibular left second premolar.*

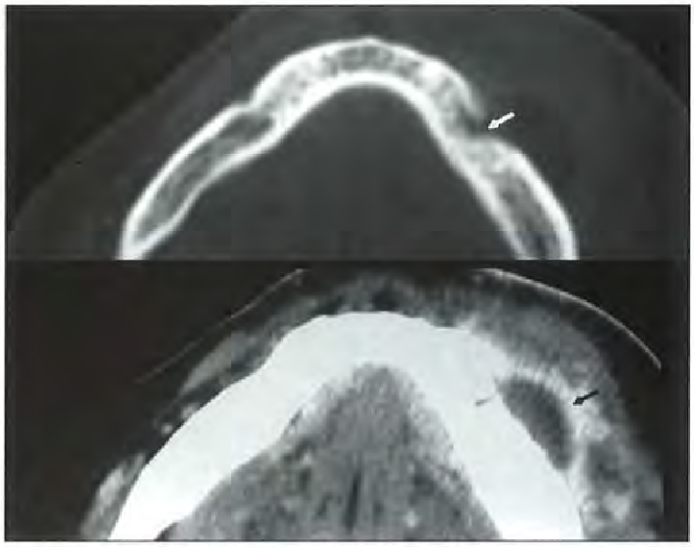


Fig 8-16a Routine axial 3.0-mm contrast-enhanced images show evidence of a soft tissue abscess *(black arrow)* along the inferior margin of the left hemimandible, with possible involvement of the left mental foramen *(white arrow)*.

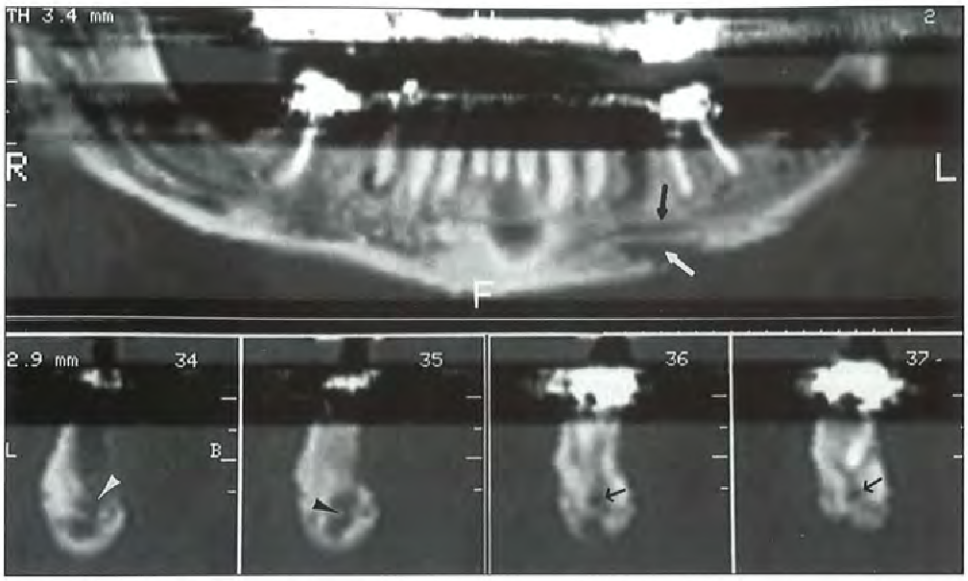


Fig 8-16b Reformatted curved coronal and cross-sectional dental CT images show erosion along the inferior margin of the left hemimandible *(white arrow)* below the mandibular canal *(black arrow)*. Communication with the mandibular canal (black arrowhead) near the mental foramen *(white arrowhead)* is clearly evident on the cross-sectional images. The mandibular canal *(thin black arrows)* is visible just distal to the mental foramen in cross sections 36 and 37.

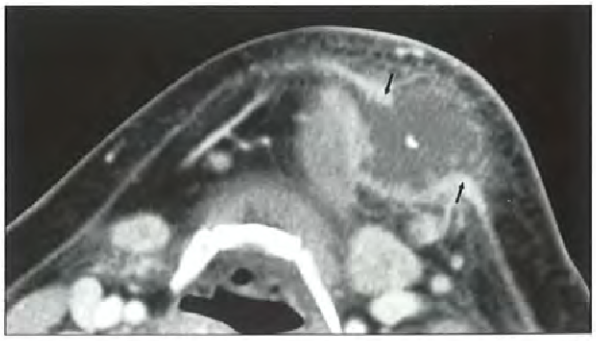


Fig 8-16c An axial 3.0-mm contrast-enhanced image below the mandible shows a soft tissue abscess containing a small spicule of bone or endodontic material. The platysma muscle *(arrows)* is thickened and disrupted by the abscess.

Conclusion

This chapter has reviewed the literature and our own experience in regard to the uses of dental CT as a diagnostic modality other than for the presurgical planning for implants. As documented in the literature, dental CT can be of value in evaluating a variety of lesions of the jaw when standard radiography and routine CT may not give adequate anatomic or diagnostic information. Our review has focused on those entities with which we have had personal experience and those that have been specifically evaluated with reformatted dental CT. However, we are certain that, in time, other studies will show dental CT to be useful in the characterization of, diagnosis of, and, where applicable, the surgical planning for other types of dental pathosis.

Reformatted dental CT is still a relatively new addition to the imaging armamentarium and is not yet widely used by the radiology community, but many CT scanners being sold today have dental imaging packages included with their software. Radiologists should be familiar with not only the application of dental CT to implant planning, but also the other uses to which this modality can be applied.

References

1. Petrikowski CG, Pharoah MJ, Schmitt A. Presurgical radiographic assessment for implants. J Prosthet Dentist 1989;61:59–64.
2. Sherman NJ. Pitfalls of panoramic radiology in implant surgery. Ann Dentist 1989;48:13–16.
3. Klinge B, Petersson A, Maly P. Location of the mandibular canal: comparison of macroscopic findings, conventional radiography, and computed tomography. Int J Oral Maxillofacial Implants 1989;4:327–332.
4. Rothman SLG, Chafetz N, Rhodes ML, et al. CT in the preoperative assessment of the mandible and maxilla for endosseous implant surgery. Radiology 1988;168: 171–175.
5. Schwartz MS, Rothman SLG, Chafetz N, et al. Computed tomography in dental implantation surgery. Dent Clin North Am 1989;33:555–597.
6. Abrahams JJ, Frisoli JK, Dembner J. Anatomy of the jaw, dentition, and related regions. Semin Ultrasound CT MR 1995;16;453–467.
7. DelBalso AM. Lesions of the jaws. Semin Ultrasound CT MR 1995;16:487–512.
8. Weber, AL. Imaging of cysts and odontogenic tumors of the jaw. Radiol Clin North Am 1993;31:101–120.
9. Langlais RP, Langland OE, Nortjé CJ. Diagnostic Imaging of the Jaws. Baltimore, MD: Williams & Wilkins, 1995.
10. Krennmair G, Lenglinger FX, Traxler M. Imaging of unerupted and displaced teeth by cross-sectional CT scans. Int J Oral Maxillofac Surg 1995;24:413–416.
11. Fagelman D, Huang AB. Prospective evaluation of lesions of the mandible and maxilla: findings on multiplanar and three-dimensional CT. AJR Am J Roentgenol 1994; 163:693–698.
12. Han HH, Chang KH, Lee CH, et al. Cystic expansile masses of the maxilla: differential diagnosis with CT and MR. AJNR Am J Neuroradiol 1995;16:333–338.
13. Slasky BS, Bar-Ziv J. Lingual mandibular bony defects: CT in the buccolingual plane. J Comput Assist Tomogr 1996;20:439–443.

14. Ariji E, Fujiwara N, Tabata O, et al. Stafne's bone cavity: classification based on outline and content determined by computed tomography. Oral Surg Oral Med Oral Pathol 1993;76:375–380.

15. Lam EWN, Dolan KD, Ruprecht A, Frank JA. Osteomyelitis of the mandible simulating a Stafne mandibular cortical defect. Ann Otol Rhinol Laryngol 1994;103:490–494.

16. Abrahams JJ, Oliverio PJ. Odontogenic cysts: improved imaging with a dental CT software program. AJNR Am J Neuroradiol 1993;14:367–374.

17. Bodner L, Bar-Ziv J, Kaffe I. CT of cystic jaw lesions. J Comput Assist Tomogr 1994;18:22–26.

18. Eversole LR, Merrell PW, Strub D. Radiographic characteristics of central ossifying fibroma. Oral Surg Oral Med Oral Pathol 1985;59:522.

19. Tsue TT, McCulloch TM, Girod DA, et al. Predictors of carcinomatous invasion of the mandible. Head Neck 1994;16:116–126.

20. Carter RL, Tanner NSB, Clifford P, Shaw HJ. Direct bone invasion in squamous carcinomas of the head and neck: pathological and clinical implications. Clin Otolaryngol 1980;5:107–116.

21. Carter RL, Tsao S, Burman JF, et al. Patterns and mechanisms of bone invasion by squamous carcinomas of the oral cavity and oropharynx. Head Neck Surg 1986; 8:247–256.

22. Bar-Ziv J, Eyal A, Talmi YP, et al. DentaCT for evaluating mandibular and maxillary invasion in cancer of the oral cavity. Ann Otol Rhinol Laryngol 1996; 105:431–437.